



This is to certify that the

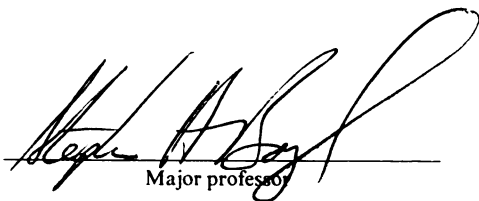
dissertation entitled

The Desorption Kinetics of Nonionic
Organic Compounds from Hexadecyltrimethylammonium-
Modified Soils and Clays
presented by

Thomas Reinhardt Benzing

has been accepted towards fulfillment
of the requirements for

Doctor of Philosophy degree in Crop and Soil Sciences



Major professor

Date June 30, 1993

**LIBRARY
Michigan State
University**

PLACE IN RETURN BOX to remove this checkout from your record.
TO AVOID FINES return on or before date due.

DATE DUE	DATE DUE	DATE DUE
<p>041203 FEB 23 2001</p> <p>1307 AUG 14 2000</p>		
_____	_____	_____
_____	_____	_____
_____	_____	_____
_____	_____	_____
_____	_____	_____
_____	_____	_____

MSU is An Affirmative Action/Equal Opportunity Institution

c:\circ\date.due.pm3-p.1



THE DESORPTION KINETICS OF NONIONIC
ORGANIC COMPOUNDS FROM HEXADECYLTRIMETHYLAMMONIUM-
MODIFIED SOILS AND CLAYS

By

Thomas Reinhardt Benzing

A DISSERTATION

Submitted to
Michigan State University
in partial fulfillment of the requirements
for the degree of

DOCTOR OF PHILOSOPHY

Department of Crop and Soil Sciences

1993

ABSTRACT

Desorption of alkylbenzenes from hexadecyltrimethylammonium (HDTMA)-modified soils and clays was studied using a gas purge system. Two soil A horizons were modified with HDTMA at 40% of their cation exchange capacities. Additionally, two homoionic HDTMA smectites were prepared, air-dried, ground and separated into two size fractions. Equilibrium distribution coefficients were measured for toluene, ethylbenzene, and n-propyl-benzene on these sorbents. The gas purge data were fit to a bicontinuum model to obtain kinetic information. Measured rate constants ranged from 0.011 to 0.183 min⁻¹. The modified soil A horizons exhibited higher desorption rate constants than the natural soils. For ethylbenzene and propylbenzene, the desorption rate constants from the modified soil were at least twice those from the natural soil. Toluene desorption rates from modified soils are rapid and exceed the sensitivity of the method. In these cases, the model collapses to an equilibrium model (desorption is not rate-limiting). The modified smectites exhibit faster desorption kinetics than the modified soils. Alkylbenzene desorption from an Arizona smectite is best fit by an equilibrium model for both size fractions. For a modified Wyoming bentonite, the rate constant for propylbenzene is 0.130 to 0.146 min⁻¹ on the small size fraction and 0.011 to 0.019 min⁻¹ on the large size fraction. The decrease in rate with increasing particle size is assumed to be a function of diffusion pathlength. Higher desorption rates for the Arizona smectite (relative to the Wyoming bentonite) may be related to a larger d_{001} spacing. These results suggest that transport and bioavailability of nonionic organic compounds are less likely to be influenced by desorption kinetics in systems containing modified versus natural soils and clays.

To my father, my first professor

TABLE OF CONTENTS

LIST OF TABLES	vii
LIST OF FIGURES	viii
Chapter 1: Literature Review and Research Objectives	1
The Concept of Dynamic Equilibrium	1
Sorption Kinetics of Organic Compounds in Soils	5
"Bound Residues"	6
Solute Transport in Aquifers	7
Biodegradation in Soils	9
Diffusion as the Rate-Limiting Step in Sorption	13
Basic Principles	13
Diffusion Models	13
Transfer Models	20
The Effect of Modification of Clays and Soils with Tetraalkylammonium Cations on the Sorption of Organic Contaminants	23
Research Objectives	25
Chapter 2: Construction and Behavior of the Gas Purge System	27
Introduction	27
Construction and Behavior	28
Construction	28
General Description of the MSU Gas Purge System	28
Reaction Flasks and Connections	31

The Photoionization Detector and Electrical	
Connections	33
Flow Control and Measurement	36
System Behavior and Modification	37
Detector Response Experiments	37
Determination of Henry's Law Constants	42
Conclusions	49
Chapter 3: HDTMA-modified Clays and Soils - Physical and Chemical	
Properties and Equilibrium Sorption of Alkylbenzenes	51
Introduction	51
Materials and Methods	52
Preparation Procedure - Modified Clay	53
Preparation Procedure - Modified Soils	54
Isolation of Organic Matter Size Fractions	55
Organic Carbon Content	55
Foaming Test	55
Equilibrium Isotherms	56
Results and Discussion	59
Conclusions	71
Endnotes - Chapters 1-3	73
Chapter 4: HDTMA-modified Clays and Soils - Kinetic Behavior in	
the Gas Purge System	79
Introduction	79
Materials and Methods	80
HDTMA-Clay Preparation	81
HDTMA-Soil Preparation	82
Organic Carbon Purification and Fractionation	82
Organic Carbon Determinations	83
Gas Purge Experimental Procedure	83
Sorption Isotherms	85

Data Analysis	87
Results and Discussion	94
Summary and Conclusions	119
Acknowledgements	123
REFERENCES	124

LIST OF TABLES

Table I: Nonionic Organic Compounds Found as Environmental Pollutants	8
Table II: Evaporation of Water from the Reaction Flask	39
Table III: Effect of Flow Rate on Detector Baseline	39
Table IV: Detector Linearity for Volatile Organic Solutes	43
Table V: System Volume Measurements	47
Table VI: Henry's Law Constants Obtained in Gas Purge System	49
Table VII: Properties of Soils and Clays	53
Table VIII: Organic Carbon Content of Modified Soils and Clays	59
Table IX: Foaming Test Results	61
Table X: Water Stability of Clay Aggregates	63
Table XI: Equilibrium Distribution Coefficients for Alkylbenzenes	64
Table XII: Distribution Coefficients Normalized for Carbon Content	64
Table XIII: Sorptive Strength of HDTMA Phase in Organoclay	70
Table XIV: Sorptive Strength of OM Fractions	70
Table XV: Sorptive Strength of Three Sorbent Types	71
Table XVI: Properties of Soils and Clays	80
Table XVII: Organic Carbon Content for Sorbents	94
Table XVIII: Distribution Coefficients for Soils and HDTMA-Soils	95
Table XIX: Distribution Coefficients for Organoclays	96
Table XX: Distribution Coefficients for OM Fractions	97
Table XXI: Fitted Parameters for Soils and Modified Soils	105
Table XXII: Fitted Parameters for Modified Clays	111
Table XXIII: Fitted Parameters for OM Fractions	119

LIST OF FIGURES

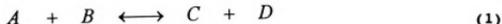
Figure 1: Energy Level Diagrams with Thermodynamic (a) and Kinetic (b) Parameters of Interest	2
Figure 2: Time Dependence of Retardation Factors in Solute Transport (Roberts et al, 1986)	10
Figure 3: Theoretical Effects of Sorption on Biodegradation Rates	12
Figure 4: Structural Characteristics of Soil Aggregates	18
Figure 5: The Bicontinuum Model	21
Figure 6: Inverse Relationship between Log K_d and Log k_d (Brusseau and Rao, 1989)	22
Figure 7: University of Florida Gas Purge System	29
Figure 8: Michigan State University Gas Purge System	30
Figure 9: Gas Flow Fitting for Reaction Flask	32
Figure 10: Cutaway View Of Photoionization Detector	34
Figure 11: Effect of Detector Temperature Control System on Response.	35
Figure 12: Detector Flow Configuration and Response to Ethylbenzene	41
Figure 13: Raw Data and Purge Curve for Ethylbenzene	45
Figure 14: Propylbenzene Isotherms on Natural and Modified Colwood A	65
Figure 15: HDTMA Exchange Reactions in Soil	67
Figure 16: Propylbenzene Isotherms on HDTMA-SAC Aggregates	69
Figure 17: The Bicontinuum Model	88
Figure 18: Submodels of the Bicontinuum Model	89
Figure 19: Raw Data and Purge Curve for Ethylbenzene	92
Figure 20: Purge Curves for Control Experiments	99
Figure 21: Purge Curves of Propylbenzene from Natural and Modified Colwood A Horizon	101
Figure 22: Model Fits for Propylbenzene/Colwood A Purge Curves	103
Figure 23: Purge Curves of Ethylbenzene from HDTMA-SAC	107
Figure 24: Model Fits for Ethylbenzene/HDTMA-SAC Purge Curves	109

Figure 25: Model Fits for Toluene/HDTMA-SAz-1 Purge Curves	112
Figure 26: Purge Curves of Toluene from OM Fractions	115
Figure 27: Model Fits for Toluene/OM Fraction Purge Curves	117
Figure 28: $\log(K_d)$ versus $\log(k_2)$ and Brusseau Line	121

Chapter 1: Literature Review and Research Objectives

I. The Concept of Dynamic Equilibrium

The concept of dynamic equilibrium is central to the science of chemistry. Consider the generic reaction of two starting materials, A



and B, to products, C and D (Equation (1)). An energy level diagram for the reaction can be drawn (Figure 1a). The combined free energies of A and B appear to be higher than the combined free energies of C and D. As a result, thermodynamics predict that the products will be more abundant than the reactants. And, this situation will be the case for the system at equilibrium. The equilibrium constant can be determined from the free energy difference between reactants and products (Equation (2)).

$$\Delta G = -RT \ln K_d$$

where ΔG = change in Gibb's free energy (2)

R = molar gas constant

T = temperature

K_d = equilibrium distribution coefficient

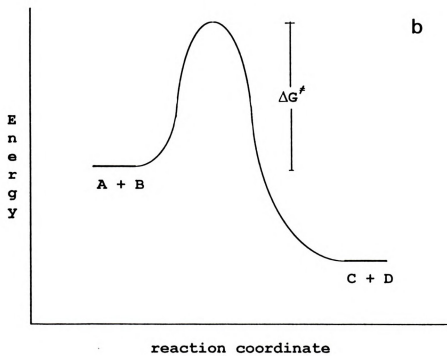
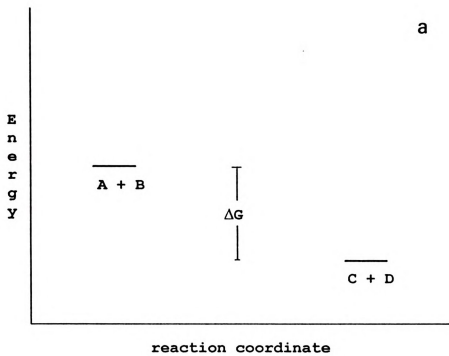
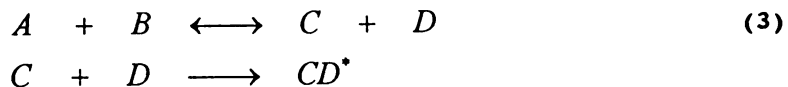


Figure 1: Energy Level Diagrams with Thermodynamic (a) and Kinetic (b) Parameters of Interest

Thus far, only the bulk properties of the system have been discussed. Now consider the same reaction at a molecular level. If this reaction is an elementary reaction and no intermediate steps are required, a molecule of A and one of B must undergo a collision to produce products. However, each collision will not necessarily lead to products. The collision must have sufficient energy to overcome an energy barrier that leads to the transition state. This activation energy can be placed on the energy level diagram as shown in Figure 1b.

Even when the system is at equilibrium, some collisions between A and B will lead to C and D. However, this rate of C and D formation will be balanced by a rate of C and D return to A and B. This concept of activity at the molecular level without changing the bulk properties of the system is the essence of dynamic equilibrium. The extent to which the equilibrium is dynamic will be related to the height of the activation barrier. High activation barriers will result in lower rates of interchange between the reactant and product pools at the molecular level.

Finally, consider a second reaction that affects C and D (Equation (3)). If CD' represents C and D that have been removed from the system, the rate of this reaction may affect the equilibrium expressed in the original reaction. According to Lechatelier's Principle, the removal of products will cause the reaction to respond by creating more products from A and B. If the rate of CD' formation is slow relative to the



dynamic equilibrium expressed in the original reaction, the state of equilibrium will be unaffected. However, if the rate of CD' formation is rapid, equilibrium in the original reaction will not be established. C and D will be formed from A and B, but will quickly react to form CD'. The original reaction becomes a rate-limiting step in the formation of

CD' from A and B. The rate of CD' formation is a function of the concentrations of A and B and these concentrations appear in the rate law (Equation (4)). The rate constant, k , is a function of the activation energy barrier and the frequency of successful collisions in the transition state as expressed in the Arrhenius Equation (Equation (5)).

$$\frac{d[CD^*]}{dt} = k[A]^m[B]^n$$

where k = rate constant

m, n = order of the reaction

(4)

Within any chemical system, an understanding of the state of equilibrium is central to predicting its behavior. In soil systems, sorption of chemical contaminants from water is often assumed to be under equilibrium conditions (1,2,3). A number of recent studies show that equilibrium parameters are not sufficient in predicting organic compound fate and transport in soils. These studies suggest that sorption kinetics must be considered.

$$k = Ae^{-\Delta G^*/RT}$$

where A = frequency factor

ΔG^* = activation energy

(5)

II. Sorption Kinetics of Organic Compounds in Soils

Three areas of research suggest that sorption kinetics must be

understood before predictions of organic compound fate can be made.

These three areas are:

1. the study of "bound residues"
2. the study of solute transport in aquifers
3. the study of biodegradation of organics in soils.

"Bound Residues":

The term "bound residues" appears most commonly in the pesticide and herbicide literature. Several studies have shown that upon incubation of soil with a pesticide, the pesticide becomes increasingly difficult to recover from the soil by extraction. These "bound residues" are believed to be responsible for the carryover of pesticides from one year to the next on cropped land. Ethylene dibromide (EDB), a relatively volatile soil fumigant, was shown to be retained by soils up to 19 years after its last known application (4). Simazine, a triazine herbicide, exhibits different herbicidal behavior as an aged residue in soil than when freshly applied (5).

However, "bound residue" behavior is not limited to pesticides. Nonionic organic compounds (NOCs) such as pyrene have also shown time-dependent, increasing resistance to extraction from soil (6). As a result of this behavior, isotherms of these compounds are often nonsingular. Nonsingularity (or hysteresis) describes the observation that the measured isotherm in the sorptive direction differs from one measured in the desorptive direction.

Hysteritic isotherms have several potential causes (7). Some isotherm studies may be plagued by method artifacts such as the effect of nonsettling particles on highly sorbed compounds (8). For compounds that contain reactive functional groups, covalent bonding to soil materials can cause irreversible sorption (9,10,11,12), which leads to hysteresis. However, this type of chemical bonding is distinctly different from nonsingularity that is caused by slow kinetics. Many isotherm nonsingularity observations can only be attributed to slow sorption kinetics (13,14).

Solute Transport in Aquifers:

Nonionic organic chemicals (NOCs), both as single compounds and as components in mixtures, represent a broad spectrum of materials (Table). Included in this class of compounds are gasoline, petroleum oils, pesticides, drycleaning solvents, degreasing solvents, and transformer oils. Also included are byproducts of combustion processes used in energy generation and mixed wastes from numerous chemical manufacturing processes. When NOCs are introduced into soils either intentionally as with pesticide application or accidentally as with chemical spills, they distribute themselves in the environment. A particularly important environmental compartment into which these compounds can migrate is groundwater. If NOCs reach elevated concentrations in groundwater, they often represent a threat to the environment and to human health. Groundwater is commonly used as a community drinking water supply and, therefore, represents a route of exposure for humans.

The threat posed by organic contaminants in groundwater is directly related to their ability to pass through soils on their way to an aquifer. An understanding of the processes involved in this passage is a central goal in studying organic contaminant transport.

Contaminant transport is governed by two phenomena. These two phenomena are the physical nature of water flow through porous media and the chemical properties of the NOCs including their interactions with soil solids. When under kinetic control, these two processes are called transport-related nonequilibrium (TNE) and sorption-related nonequilibrium (SNE), respectively. Transport-related nonequilibrium will not be reviewed here since excellent reviews of TNE have recently been written (15,16). However, it should be noted that TNE affects nonsorbing as well as sorbing solutes. This characteristic distinguishes TNE from SNE. Sorption-related nonequilibrium affects only sorbing solutes.

Sorption-related nonequilibrium with regard to contaminant

Table I: Nonionic Organic Compounds Found as Environmental Pollutants

<u>Products</u>	<u>NOC Components</u>
Gasoline	aromatic hydrocarbons (benzene, toluene, xylenes, etc.)
Fuel and Heating Oils	"
Pesticides	herbicides, insecticides, fungicides
Drycleaning Solvents	chlorinated ethenes (trichloroethene, tetrachloroethene, etc.)
Degreasing Solvents	"
Transformer Oils	polychlorinated biphenyls
Hydraulic Fluids	"
Combustion Products	polynuclear aromatic hydrocarbons (benzo-a-pyrene, dioxins, etc.)

transport arises from chemical nonequilibrium or rate-limited diffusive mass transfer. Chemical nonequilibrium results when the contaminant engages in a specific chemical reaction with a well-defined site on the sorbent (chemisorption) and this reaction is rate-limiting. For NOC transport, chemical nonequilibrium is not considered important since these nonionic and, generally, nonpolar compounds offer little in the way of reactivity (15,17). Chemical interactions of NOCs with soil solids, both mineral and organic, will be dominated by van der Waal's forces. These forces are significantly weaker than covalent or ionic bonds, less site-specific, and, therefore, do not represent interactions that typically lead to chemical nonequilibrium. The principle driving force in sorption of NOCs from water is the hydrophobic effect. Hydrophobic sorption results from entropy- rather than enthalpy-dominated thermodynamics.

The driving force in hydrophobic sorption is the increase in entropy of water (18,19,20). Water, as a solvent, is structured around the solubilized NOC. Upon removal of the NOC by sorption, the water loses its imposed structure, often referred to as a "solvent cage", and thereby experiences an increase in entropy. This process has a low activation energy barrier and is, therefore, rapid. Because this process is rapid, chemical nonequilibrium is not expected to contribute to SNE for NOC sorption in soils.

The second type of SNE derives from rate-limited diffusive mass

transfer; specifically, processes involving diffusion within soil particles. Recall that sorption-related nonequilibrium based on diffusion as the rate-limiting step must involve a mechanism exclusively affecting sorbing solutes. Two mechanisms have been proposed in the literature. A review of these mechanisms will be presented in detail following some literature examples of nonequilibrium in solute transport and biodegradation.

Solute transport of several halogenated solvents (carbon tetrachloride (CTET), bromoform (BROM), tetrachloroethene (PCE), 1,2-dichlorobenzene (DCB), hexachloroethane (HCE)) in the Borden aquifer exhibited nonequilibrium behavior (21). Retardation factors calculated using equilibrium distribution coefficients and aquifer material properties (Equation (6)) failed to predict the movement of the organic solutes. Instead, the observed retardation factors showed a time

$$R = 1 + \frac{\rho K_d}{\theta}$$

(6)

where ρ = bulk density of the medium
 θ = volumetric water content

dependence indicating the influence of kinetics on NOC transport (Figure 2, adapted from 21).

In the common practice of pump-and-treat remediation of contaminated aquifers, the influence of kinetics may be even more important since water flow rates are greater than under natural conditions (15). Slow release kinetics often require multiple efforts to remediate these aquifers.

Biodegradation in Soils:

An important component of the fate of organic contaminants in the

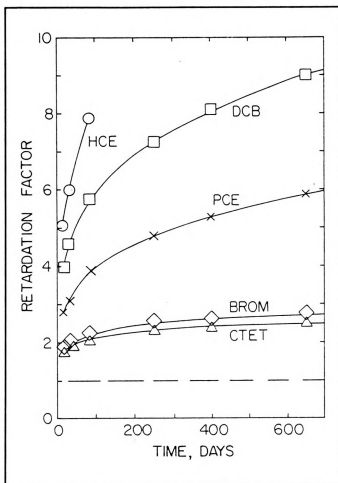


Figure 2: Time Dependence of Retardation Factors in Solute Transport (Roberts et al, 1986)

irreversible process for most compounds, this process could potentially affect sorption equilibrium.

environment is their susceptibility to microbial degradation. Soil microbes perform a vital function in degrading organic materials in soil. Although there is still some disagreement in the literature, many researchers believe that NOCs are only susceptible to microbial attack when they are in solution (22,23,24), and hence, sorption of NOCs by soil solids decreases their bioavailability. Other studies suggest that microorganisms can release bound residues from soils (25). Clearly, the process of NOC degradation is coupled to NOC desorption (Equation (7)). And, since microbial degradation is an



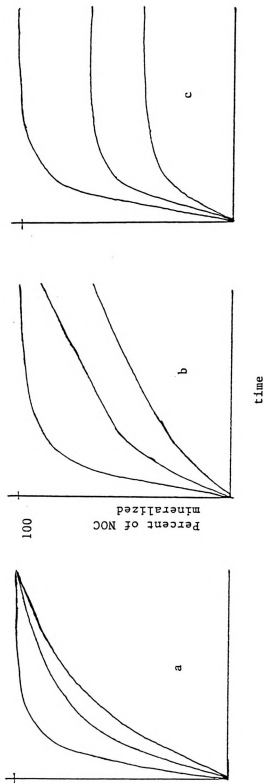
As in the generic discussion of kinetics presented earlier, the significance of degradation on the state of sorption equilibrium will be dependent on its rate and the degree to which the sorption equilibrium

is dynamic.

In a closed system, where sorption equilibrium has been established and microbes are introduced at time zero, three scenarios are possible (Figure 3). If the degradation rate is slow relative to the sorption process, the equilibrium of the sorption reaction will be maintained and increasing sorbent concentration will not affect the extent of mineralization although it will diminish the rates of mineralization (Figure 3a). However, if the degradation rate is much faster than the desorption rate, sorption equilibrium will not exist as the microbes only consume the NOC present in the water. Mineralization of the NOC will be incomplete since a significant portion will remain sorbed and, therefore, not bioavailable (Figure 3c). The intermediate situation, where the degradation rate and sorption rate are similar, leads to more complex behavior. In this case, the NOC will be degraded from solution and the rate-limiting step in its degradation becomes the desorption reaction. Sorption will not be in equilibrium and serves to extend the time required for complete mineralization of the substrate (Figure 3b). In a practical sense, these scenarios may lead to profoundly different results in bioremediation of contaminated soils or aquifers.

Studies of the dependence of degradation rates on desorption kinetics have been limited to the laboratory. Naphthalene degradation rates are organism-specific in soil-containing systems (26). A *Pseudomonas* strain exhibits mineralization curves that suggest access to a portion of the sorbed naphthalene. In contrast, another bacterial strain exhibits mineralization curves indicating that only solution phase naphthalene is available and that the degradation rate exceeds the desorption rate. These differences appear to be related to properties of the bacteria since the desorption rates in sterile soils should be identical.

Taken together, the evidence from "bound residue" research, NOC solute transport in aquifers and biodegradation of NOCs point to the importance of NOC sorption kinetics in soils. Now, a review of



- a. The rate of nonionic organic compound (NOC) degradation is much less than the rate of NOC desorption.
- b. The rate of NOC degradation and the rate of NOC desorption are similar.
- c. The rate of NOC degradation is much greater than the rate of NOC desorption.

The presence of soil in the system is indicated by the Roman numerals:

- I. No soil or a small amount of soil present,
- II. A moderate amount of soil present, and
- III. A large amount of soil present.

Figure 3: Theoretical Effects of Sorption on Biodegradation Rates

mechanisms that use diffusion to explain slow sorption kinetics will be presented.

III. Diffusion as the Rate-Limiting Step in Sorption

Basic Principles:

Adolph Fick first presented his theory of diffusion by analogy to Fourier's theory of heat transfer. Fick's First Law says that the flux (Q) of solute mass through a unit area per unit time is proportional to the concentration gradient (dC/dx) along a distance normal to that area (Equation (8)). The proportionality constant, D , is the diffusion coefficient.

Fick's Second Law states that the rate of change in concentration is proportional to the slope of the concentration gradient (Equation (9)). Again, the diffusion coefficient is the proportionality constant.

$$Q = -D \left(\frac{dC}{dx} \right) \quad (8)$$

Solutions to Fick's First and Second Laws have been used to describe a broad range of diffusion processes and as models for the process of hydrodynamic dispersion (27).

$$\frac{dC}{dt} = -D \left(\frac{d^2C}{dx^2} \right) \quad (9)$$

Diffusion Models:

Two mechanisms have been proposed in the literature to explain

sorption-related nonequilibrium based on diffusion as the rate-limiting step. These mechanisms will be referred to as retarded intraparticle diffusion and intraorganic matter diffusion. In describing these mechanisms, an understanding of the underlying physical and chemical picture of soil associated with each mechanism is necessary. Also, some introductory discussion of the models associated with each mechanism will be presented.

The mechanism known as retarded intraparticle diffusion emphasizes the microporous nature of soil particles. Soil particles are viewed as agglomerations of smaller pieces of mineral and organic matter (Figure 4b). Diffusion of a solute through the soil particle occurs along tortuous micropore channels. The tortuosity of this diffusional process results in a slow rate of mass transport between the interior of the particle and the bulk solution. At this point, the mechanism does not distinguish between sorbing and nonsorbing solutes.

To explain the difference between the behavior of these solutes, a retardation step is invoked. Along the microporous channels through which the solute must diffuse, organic matter is present. This coating of organic matter on the mineral surface slows the migration of NOCs through the channel by sorbing them. Repetitive sorption and desorption steps as the NOC passes through the channel serve to reduce the amount of time spent in solution and therefore lower the rate of the diffusional process. It should be pointed out that local equilibrium between micropore fluid and the organic matter is assumed. So, the diffusional process becomes retarded for NOCs and the mechanism presents a picture of a diffusional process dependent upon the sorption coefficient of organic matter for the NOC. While the retarded intraparticle diffusion mechanism generally assumes a linear sorption isotherm for the retardation process, the nature of the sorption (adsorption or partitioning) is not a matter of great concern with this mechanism. The slow diffusion rate is explained solely by virtue of the path tortuosity and the fact that sorption necessitates that some time is spent by the solute in an immobilized state.

Retarded intraparticle diffusion has been used to explain the kinetic behavior of pesticides (4,28) and NOCs (29,30) in soils and sediments. Diffusion coefficients have been extracted from kinetic data by using models that make a variety of assumptions about the physical structure of the soil particles. Because of these assumptions and because of their dependence upon the sorption equilibrium constant (through the retardation step), fitted parameters from these models are referred to as effective (or apparent) diffusion coefficients, D_{eff} s (or D_s s).

Both sorption and desorption of several chlorobenzene congeners from river sediments and a soil were interpreted using Equation (10) (29). The fitted D_{eff} s ranged from 1.0×10^{-9} to 8.3×10^{-12} cm²/sec. The

$$\frac{dS(r)}{dt} = D_{eff} \left[\frac{d^2 S(r)}{dr^2} + \frac{2}{r} \frac{dS(r)}{dr} \right] \quad (10)$$

where $S(r)$ = local total volumetric concentration
 r = radial distance

effective diffusion coefficient was defined by Equation (11) (29) and the path length is assumed to be one half the particle diameter. Using the same model, 1,2-dibromoethane (EDB) release from two soils exhibited D_{eff} s of 2×10^{-17} and 8×10^{-17} cm²/sec (4). Since pore fluid diffusivities of about 10^{-7} cm²/sec are expected for NOCs in water, the governing variables in this retarded intraparticle diffusion model are the tortuosity of the diffusion path and the equilibrium partition coefficient. Together these factors are used to explain a nine order of magnitude difference between diffusivities in water and within soil particles. Since measured K_s s ranged from 1.5 to 300 for EDB depending on whether the isotherm was generated from sorption or desorption

direction, the retarded intraparticle diffusion model relies on the tortuosity to explain at least a seven order of magnitude reduction in diffusivity.

$$D_{eff} = \frac{D_m n f(n, \tau)}{(1-n)\rho_s K_d + n}$$

where D_m = pore fluid diffusivity (11)

n = porosity

ρ_s = specific gravity of sorbent

$f(n, \tau)$ = "a correction factor which is a function of intraaggregate porosity and tortuosity, τ " (Wu and Gschwend, 1986)

The question of choosing a single representative particle diameter was avoided in a study of the sorptive uptake of tetrachloroethene (PCE) and 1,2,4,5-tetrachlorobenzene (TeCB) by a sandy aquifer material (30). A single fitting parameter, D_a/a^2 , includes both the apparent diffusion coefficient and the particle radius, a . D_a/a^2 is called the diffusion rate constant. Again, the definition of D_a includes the equilibrium distribution coefficient and physical characteristics of the particle (Equation (12)).

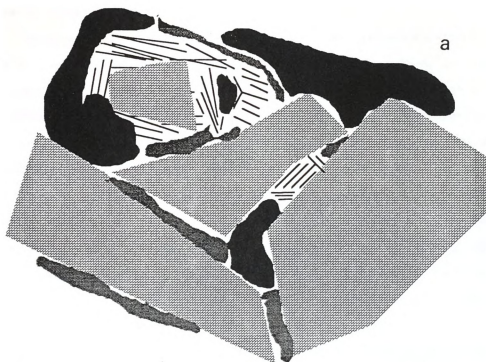
$$D_a = \frac{D_m}{\left[1 + \left(\frac{\rho_s}{n} \right) K_d \right]} \quad (12)$$

The fitted diffusion rate constant for PCE sorption on the bulk aquifer solids was $2.8 \times 10^{-7} \text{ sec}^{-1}$. Size fractions of the aquifer material exhibited PCE diffusion rate constants of 1.7×10^{-6} to $3.1 \times 10^{-8} \text{ sec}^{-1}$, with the smaller sizes exhibiting faster rates. Diffusion rate constants for TeCB were less and the difference could be explained by a difference in K_d .

Models based on the mechanism of retarded intraparticle diffusion rely heavily on the microporous structure of soil particles. Because of the retarded intraparticle diffusion model's heavy reliance on the tortuosity of micropores and retardation factors related to pore wall sorption, some researchers have sought to develop an alternative model. This model invokes diffusion through soil organic matter as the rate-limiting step in sorption.

To understand the basis for considering intraorganic matter diffusion (IOMD) as the rate-limiting step in sorption of NOCs, a picture of organic matter's chemical and physical nature is necessary. Soil humus has been described as having an aromatic backbone similar to lignin which has been amended by incorporation of peptides and sugars. Humus is viewed as heterogeneous in nature, being composed of a mixture of operationally defined fractions such as humic acids, fulvic acids and humin (known collectively as humic substances) and various known classes of biochemicals such as amino acids, carbohydrates, fats, waxes, resins, and organic acids (known collectively as nonhumic substances). These compounds are combined in such a manner as to make them resistant to degradation. From this description, it is clear that soil humus is chemically complex in nature and not easily characterized with regard to its reactivity. Soil humus should be viewed as having a range of acidity, molecular weight, and polarity. With regard to its physical appearance, Brusseau and Rao envision soil organic matter as "a three dimensional network of randomly oriented polymer chains and as having a relatively open, flexible structure perforated with voids" (17) (Figure 4a). It is through this chemically heterogeneous, "flexible mesh" structure that NOCs are pictured to diffuse.

A solvent's ability to extract "bound residues" of di(2-ethylhexyl)phthalate has been related to its swelling of a sediment organic matter matrix (31), suggesting that diffusion of the solute is enhanced by expanding the SOM polymer structure. To date, direct observation of diffusion of NOCs through soil humus has not been made.



-  = mineral
-  = oxides
-  = organic matter
-  = clay minerals

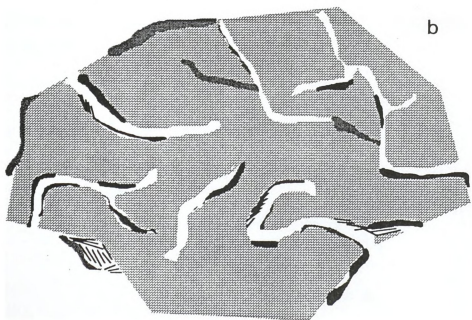


Figure 4: Structural Characteristics of Soil Aggregates



Transfer Models:

Brusseau and Rao have shown that natural sorbents behave according to a bicontinuum model (Figure 5) in which organic matter is composed of a region, S_1 , in rapid equilibrium with the soil solution and a region, S_2 , governed by slow kinetics. Equilibrium is established between solution phase concentration (C_s) and the concentration in the rapidly equilibrating domain (C_{s1}). This equilibrium is governed by the distribution coefficient, K_d . The kinetically controlled process, mass transfer between S_1 and S_2 , is described by a forward rate constant, k_1 , and a reverse rate constant, k_2 . The region of slow kinetics has been postulated to be organic matter that is not in direct contact with the soil solution. This organic matter region may be deeper within the soil aggregate (32). Brusseau and Rao believe that diffusion within this region is slow due to the fact that the "pores" through which molecules must diffuse are nearly the same size as the molecules themselves.

Experimental determination of rate constants for the bicontinuum model is accomplished through curve-fitting either miscible displacement (column) data or gas purge system data. Brusseau and Rao have shown that literature data and their own experimental data describe an inverse relationship between the partition coefficient for a given NOC and its rate constant for desorption (Figure 6, adapted from 33). The reverse rate constant is related to the polymer diffusion coefficient by Equation (13) (15).

$$k_2 = \frac{\alpha}{1-F}$$

$$\text{where } \alpha = \frac{cD_{py}}{\ell^2} \quad (13)$$

ℓ = characteristic diffusion length

D_{py} = polymer diffusion coefficient

c = shape factor

F = fraction of NOC in S_1 domain

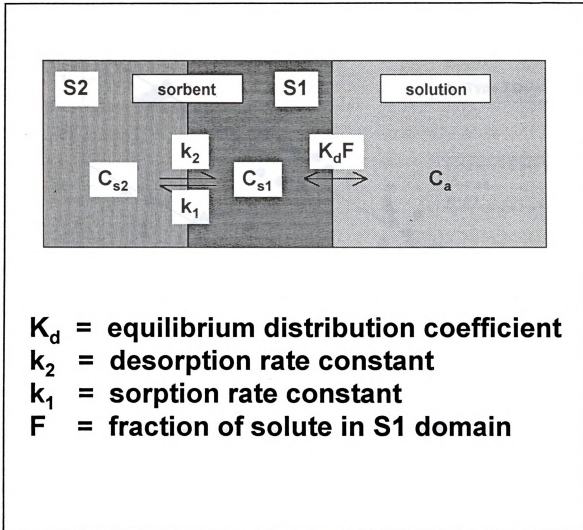


Figure 5: The Bicontinuum Model

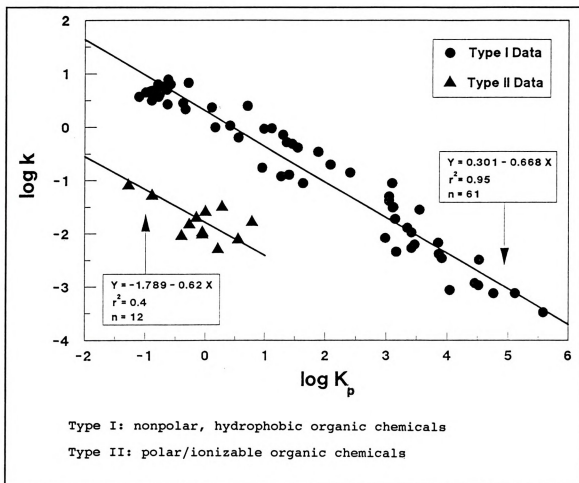


Figure 6: Inverse Relationship between $\log K_p$ and $\log k$ (Brusseau and Rao, 1989)



IV. The Effect of Modification of Clays and Soils with Tetraalkylammonium Cations on the Sorption of Organic Contaminants

The sorption of NOCs to soils has been shown to depend most strongly upon soil organic matter (SOM) content (34,35,36). Soil organic matter or humus can be viewed as an organic phase into which an NOC can dissolve (37). The dissolution of an NOC from water into SOM is analogous to dissolution from water into an organic solvent and is referred to as partitioning. In fact, the distribution coefficient for an NOC between octanol and water, K_{ow} , has been shown to be a good indicator for the strength of NOC sorption to soils (38,39,40).

To increase the degree of NOC sorption, native inorganic cations in soils can be exchanged with organic cations to increase the organic matter content (41). Various quaternary alkylammonium cations (QUATs) have been used to enhance sorption of NOCs by soils (41,42) and pure clays (43,44,45,46,47,48,49,50). Equilibrium sorption of chlorophenol to a modified Wyoming bentonite depends on the nature of the organic cation and the solute hydrophobicity (43). For cations with large alkyl substituents such as hexadecyltrimethylammonium (HDTMA) and dioctadecyldimethyl-ammonium (DODMA), the cation exchange reaction transforms the interlamellar region of Wyoming bentonite into a partitioning medium for pentachlorophenol (44). The effectiveness of HDTMA-Wyoming bentonite at partitioning NOCs from water is closely related to K_{ow} (45,49).

The same clays exchanged with smaller organic cations such as tetramethylammonium (TMA) and trimethylphenylammonium (TMPA) exhibited lower uptake of pentachlorophenol (44). The operative mechanism in sorption of NOCs by TMA-clays is surface adsorption rather than partitioning. Benzene was selectively adsorbed by TMA-Wyoming bentonite in preference to compounds with lower water solubility (46). The Langmuir-type adsorption isotherms of benzene on two TMA-smectites support surface adsorption as the principle mechanism in these clays (46,48). Trimethylphenylammonium exchange of smectites exposes the



siloxane surfaces which interact strongly with planar aromatic hydrocarbons (47), indicating the hydrophobic nature of these surfaces (50).

Partitioning of a series of alkylbenzenes, naphthalene and biphenyl onto HDTMA-modified smectites, illite, vermiculite and kaolinite demonstrated the importance of clay mineral type (49). The structure of the interlayer region varies with the charge density of the clay. Arrangement of HDTMA molecules in the interlayer ranged from bilayers up to paraffin complexes, where the hexadecyl groups form a more contiguous medium, with increasing charge density. Among the smectites, the effectiveness of the sorptive medium was higher in paraffin complexes than in bilayers.

Hexadecyltrimethylammonium-exchange of the A and Bt horizons of Marlette soil resulted in substantial increases in the equilibrium distribution coefficients for benzene, tetrachloroethene, and 1,2-dichlorobenzene (41). The added organic matter was 10-30 times more effective than SOM at sorbing the organic solutes. The increase in sorption was attributed to the formation of a partitioning medium upon HDTMA exchange of the natural soil clays. An expanded study involving seven NOCs, two additional organic cations (nonyltrimethylammonium and dodecyltrimethylammonium), and three soils from different textural classes confirmed the broad applicability of this technology to the stabilization of contaminated soils (42).

The in situ modification of soils and aquifer materials, coupled with biodegradation, has been suggested as a remediation technology for contaminated hazardous waste sites (51). Modified pure clays may be used to enhance the effectiveness of landfill liners by increasing the time required for breakthrough of NOC contaminants. A laboratory study of naphthalene transport through an aquifer material showed that in situ HDTMA-modification of the material reduced the extent of the contaminant plume (52). As discussed earlier, solute transport and solute bioavailability may be controlled by the kinetics of sorption under these conditions. Although extensive research into NOC sorption



equilibria in modified clays and soils has been conducted, little information on the dynamic behavior of sorption on QUAT-modified soil materials is available.

V. Research Objectives

Research Objective #1: Sorption Kinetics of Organic Compounds in Organoclays

The dynamic behavior of the sorption process of alkylbenzenes to tetraalkylammonium-exchanged clays will be investigated. The hexadecyltrimethylammonium cation will be used to prepare organophilic clays. Aggregates of the prepared clays will be used to study the effect of particle size on the kinetics of sorption. Rate constants for the sorption process will be obtained by fitting the bicontinuum model to the data.

Research Objective #2: Sorption Kinetics of Organic Compounds in Modified Soils

The effects of modifying surface soil horizons with a tetraalkylammonium cation on the sorption kinetics will be investigated. The hexadecyltrimethylammonium cation will be used to prepare the modified soils. A series of alkylbenzenes represent nonionic organic compounds to be used as model compounds. Rate constants for the sorption process will be obtained by fitting the bicontinuum model to the data.

Research Objective #3: The Gas Purge System as a Method for Studying Sorption Kinetics

A gas purge system for measuring sorption kinetics of volatile organic compounds in sorbent-containing aqueous systems will be

constructed. Experiments to evaluate system behavior and to determine optimal conditions for measuring sorption kinetics using the system will be performed. Necessary modifications to current system designs will be made based on system performance. In addition, the necessary models and curve-fitting routines will be assembled for interpreting desorption experiments run on the system.



Chapter 2: Construction and Behavior of the Gas Purge System

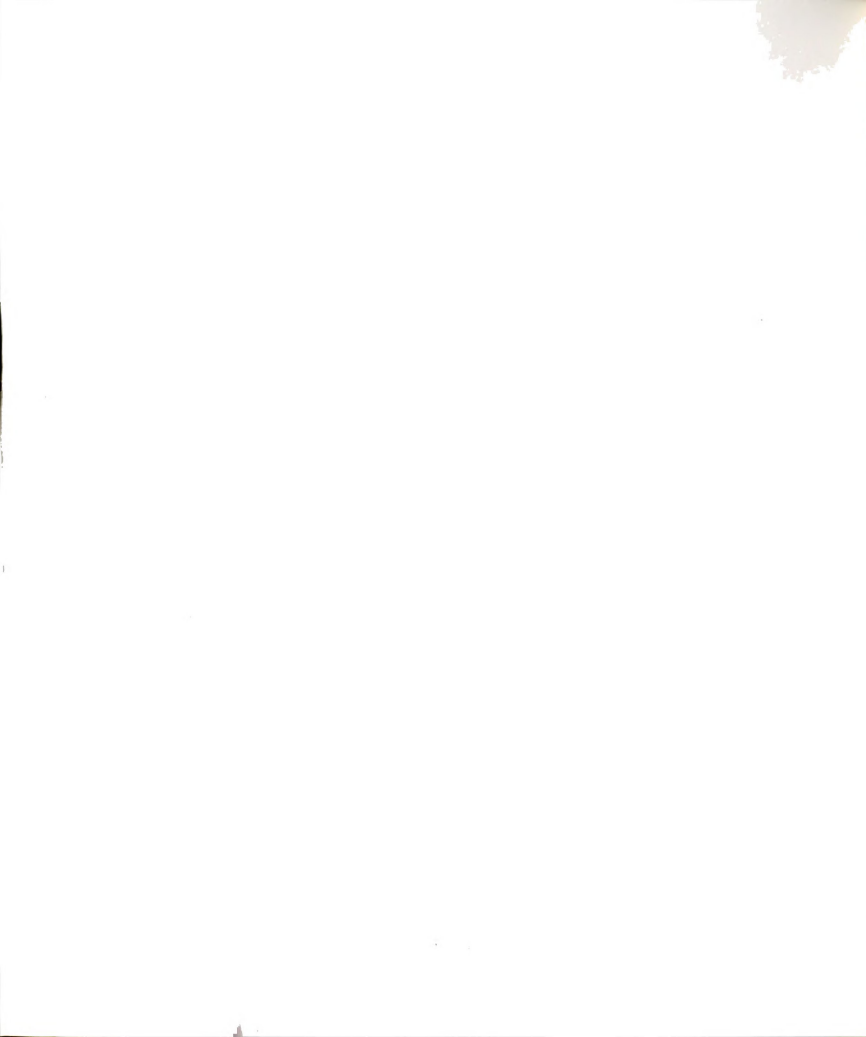
Introduction

Several methods have been used to perform laboratory studies of the sorption kinetics of organic chemicals to soils. These methods include batch experiments (53,54,55), column experiments (56,57,58,59) and gas purge experiments (29,60,61,62,63,64). Their relative advantages and disadvantages have been reviewed (64).

Batch experiments are unable to capture the initial rapid uptake or release kinetics of sorbed material because only discrete sampling intervals are possible. To overcome this problem, continuous monitoring of solute concentration is usually incorporated into either column or gas purge methods. When solute sorption coefficients are high, column experiments require long elution times or mixed solvents (65,66). Gas purge experiments are most appropriate when sorption coefficients are large and when volatile compounds are being studied.

This chapter describes the construction and behavior of a gas purge system (MSU Gas Purge System). Physical characteristics of the system are detailed. To validate our understanding of the system, the dynamic behavior of several volatile organic compounds was evaluated. In the absence of any sorbent, the distribution of volatile organic compounds between their gas and water concentrations, C_g and C_w , is controlled by Henry's Law (Equation (14)). Literature values for Henry's Law constants, K_{Hs} , are abundant (67,68). In addition, K_H can be approximated by dividing the vapor pressure by the solubility (69).

Sorbent studies using this system will be described in future publications.



$$C_g = K_H * C_w \quad (14)$$

Construction and Behavior

I. Construction

A gas purge system (MSU Gas Purge System) was constructed using the University of Florida system (UF Gas Purge System, Figure 7) (64) as a model. The purpose of this chapter is to record specifics about materials used in its construction and to explain necessary modifications to the UF Gas Purge System that were employed. First, a general description of the gas purge system is given. The general description is followed by a detailed description of the MSU Gas Purge System's component parts.

General Description of the MSU Gas Purge System:

Figure 8 shows the MSU Gas Purge System. The heart of the system is a reaction flask which contains the sorbent, a matrix solution and the solute. Other major system components include an air pump and the photoionization detector. These components are connected by 1/8" stainless steel carrier tubing. Arrows indicate the direction of flow at various points in the system. Air enters through a filter, passes through the pump and into the flask through a fritted glass bubbler. This bubbler is designed to disperse the air through the stirring suspension in the reaction flask. Air flow continues from the flask to the detector. The photoionization detector responds to gas-phase solute concentration and this response is registered on the chart recorder. Flow exits the system through a flowmeter.

The preceding description of flow summarizes the purge or open mode of system operation. The purge mode represents only one of two

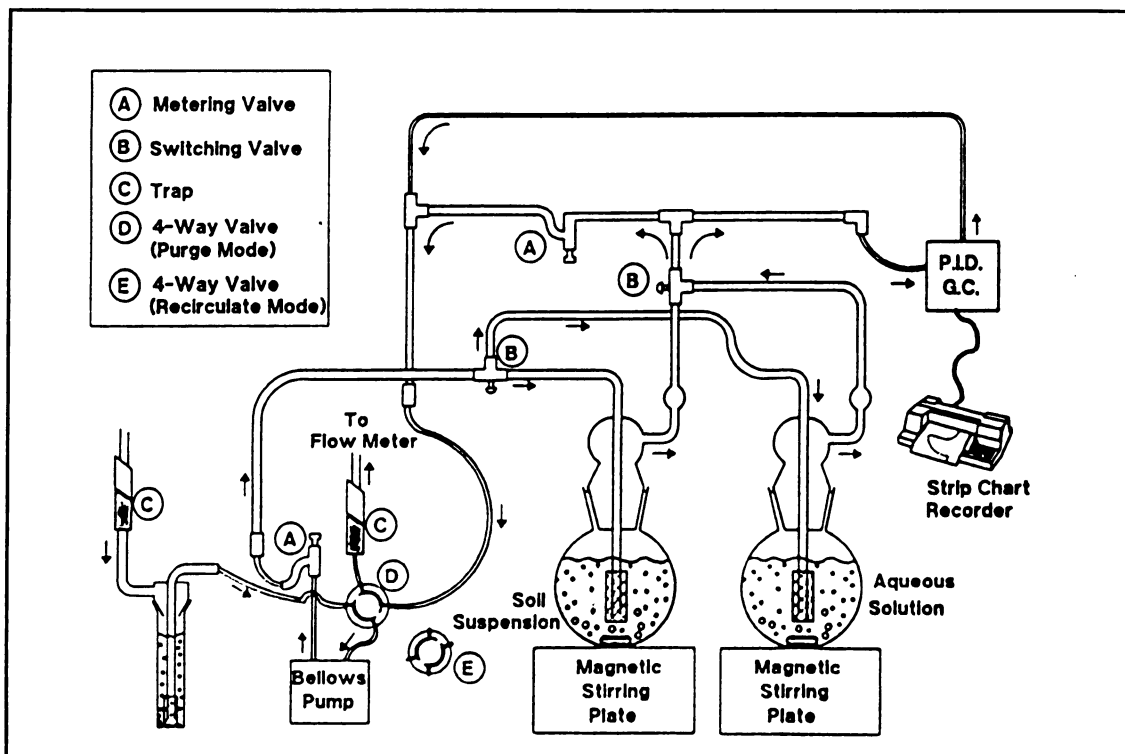


Figure 7: University of Florida Gas Purge System



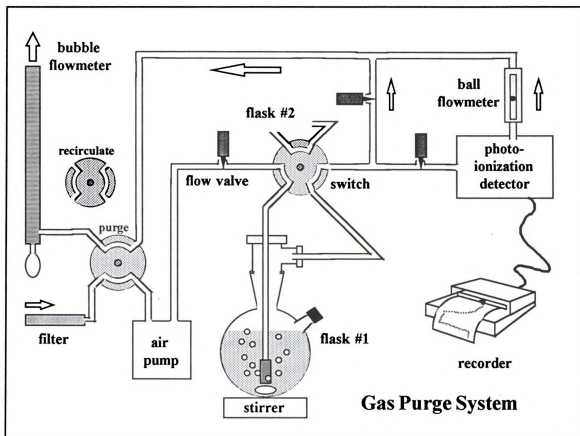


Figure 8: Michigan State University Gas Purge System



possible flow configurations for the MSU Gas Purge System. The other flow configuration is the recirculate or closed mode. In this mode, the exit gas from the detector is returned through the pump to the flask. Selection between the two possible flow configurations is made using the four-way switching valve.

Another valve in the system, the six-way switching valve, chooses between two identically constructed reaction flasks. For purposes of clarity, Figure 8 only shows one of these flasks.

The flow control and measurement components of the system include the switching valves, three needle valves, the air pump and two flow meters. Control of flow will be described in more detail in the components section of this chapter.

Reaction Flasks and Connections:

A 250-mL roundbottom flask is the reaction flask in the MSU Gas Purge System. On the shoulder of the reaction flask, an injection port (Ace Glass 7609-07) is installed. This port accepts a 15 mm Teflon-lined septum (Ace Glass 11710-15) held in place with a screw cap (Ace Glass 9590-47). The injection port allows access to the flask through a gas-tight syringe without opening the flask.

Connected to the top of the reaction flask through a 24/40 ground glass joint is the gas flow fitting (Figure 9). This fitting is composed of two Ace-Thred connectors (Ace Glass 7644-15 and 5027-05). These connectors are Teflon compression fittings. Air flowing from the pump enters the gas flow fitting through a 1/8" x 1/4" reducing union (Supelco 2-2031M). The reducing union connects to a 1/4" metal-glass joint which is connected to the fritted glass bubbler (Fisher Scientific 11-138B). An airtight seal to the bubbler tube is accomplished using a Teflon reducing ferrule (Ace Glass 11710-15) in the larger connector.

Gas exits the gas flow fitting through the smaller connector. A Swagelock adaptor (Ace Glass 5844-58) converts the exit connection back to the stainless steel carrier tubing.

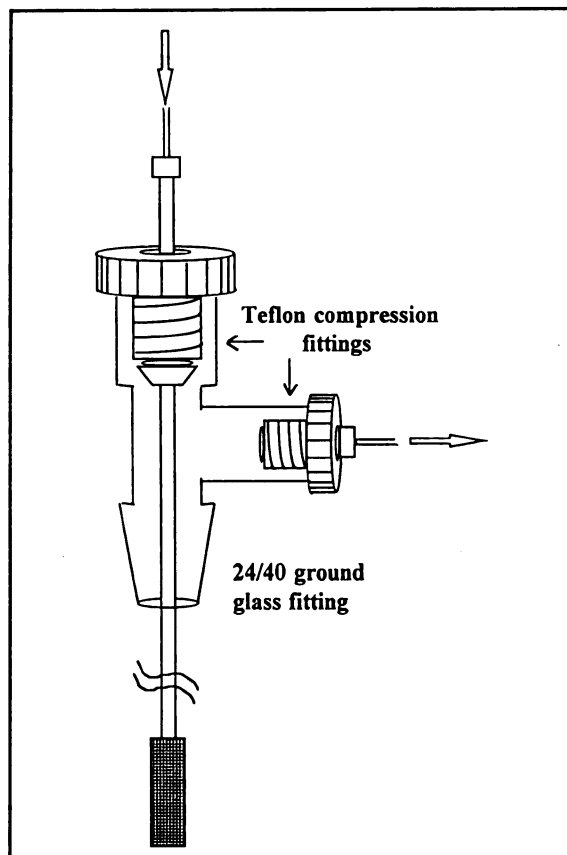


Figure 9: Gas Flow Fitting for Reaction Flask

Gas flowing through the reaction flask and its connections to the system contacts only stainless steel, glass and Teflon surfaces.

The Photoionization Detector and Electrical Connections:

A photoionization detector (OI Analytical Model 4430) (PID) is used to monitor gas phase concentration of the solute. A 1/8" x 1/16" reducing union (Supelco 2-2042M) connects the PID inlet to the carrier tubing. The gas passes into the ionization chamber, past the 10.0 electron volt ultraviolet lamp (OI Analytical 181180 or equivalent), and returns to the system through a 1/16" outlet tube (Figure 10). The outlet tube is connected to the carrier tubing using another 1/8" x 1/16" reducing union. To maintain the closed character of the MSU Gas Purge System, the sweep gas and vent ports of the PID were sealed.

The PID is electrically connected to a lamp power supply, a temperature control circuit and a series of signal processing equipment. The lamp power supply (OI Analytical 181727) and the dual channel electrometer (OI Analytical 194910) are connected according to the manufacturer's instructions. The electrometer amplifies the PID signal. The amplified signal is sent to a flatbed chart recorder (Fisher Scientific 13-939-85A), which attenuates the signal and continuously records it on graph paper. In addition to adjusting signal attenuation, the chart recorder sets a baseline and the graph paper speed.

The PID is designed by the manufacturer for use in a gas chromatograph. Its use outside of a gas chromatograph requires a unique insulation and temperature control system specifically suited to the MSU Gas Purge System. At the University of Florida, Brusseau and Rao (64) wrapped a heat rope around the PID. During my experience on the UF Gas Purge System, I found that this temperature control system contributed to regular fluctuations in the signal (Figure 11). The fluctuation in signal is due to electrical noise arising from the on-off cycles of the heat rope. The MSU Gas Purge System uses the proportional temperature

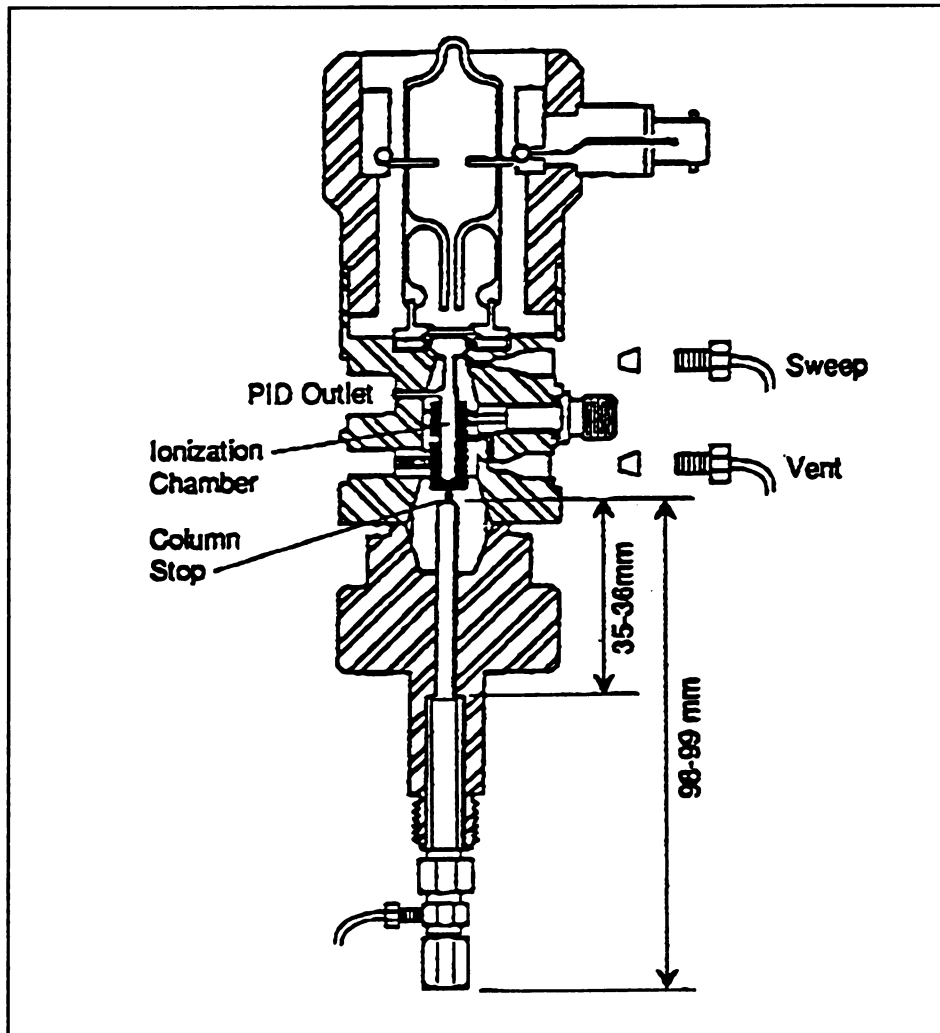


Figure 10: Cutaway View Of Photoionization Detector

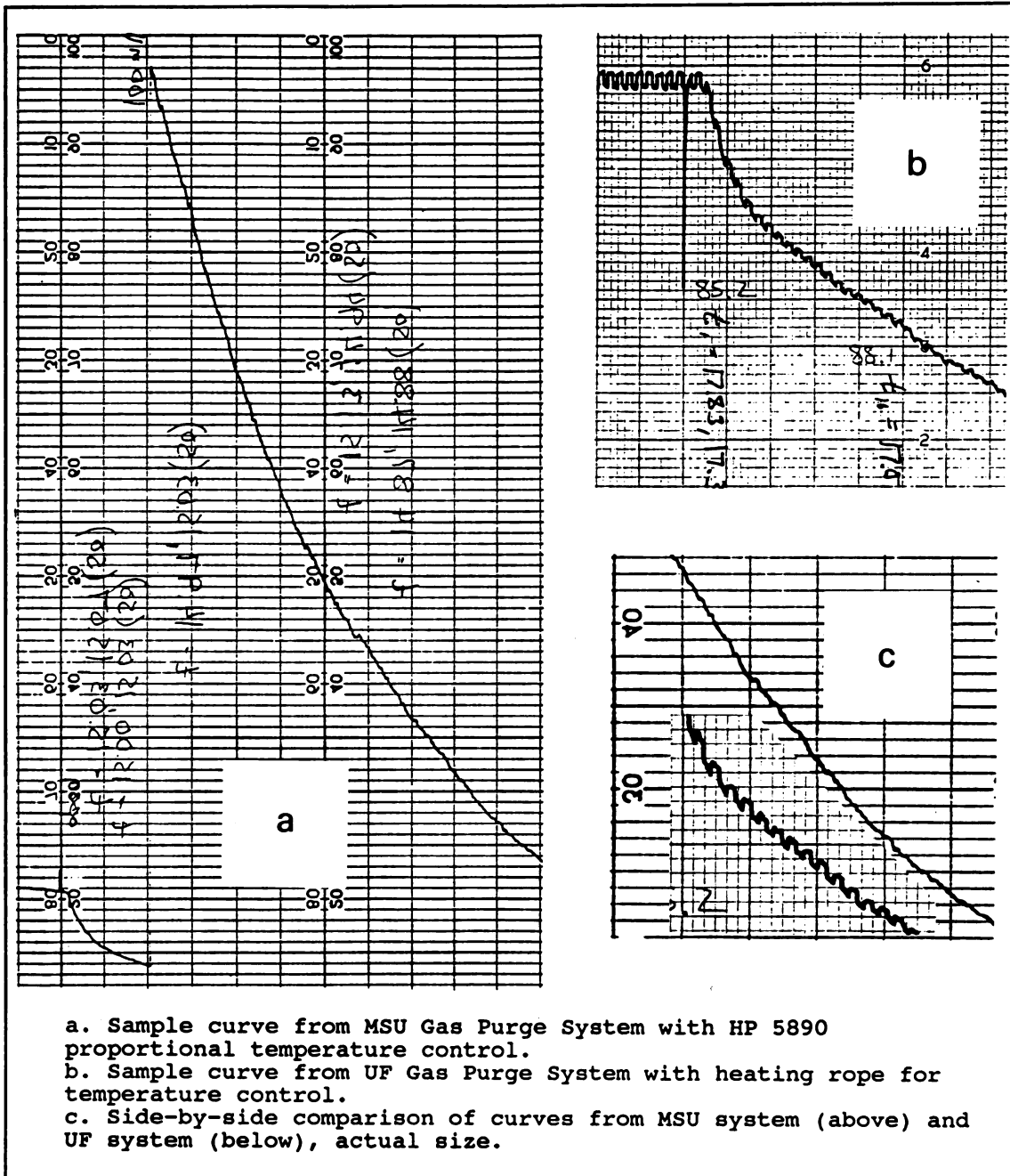


Figure 11: Effect of Detector Temperature Control System on Response.

controller found aboard a Hewlett-Packard 5890 Gas Chromatograph (HP 5890). The proportional temperature controller uses a resistance heater and an internal heat sensor to carefully monitor and adjust the detector temperature. To reduce heat losses, urethane foam insulation (1" Thermax) was cut to fit snugly around the heated block of the PID (lower half of Figure 10). The insulation and temperature control system for the MSU Gas Purge System reduces the PID signal noise (Figure 11) and allows digital selection and readout of detector temperature through the HP 5890's electronics.

Flow Control and Measurement - Air Pump, Valves, Switches and Meters:

A Metal Bellows MB-21 air pump drives the flow through the MSU Gas Purge System. The magnitude of the air flow is controlled by three 1/8" stainless steel metering valves (Supelco 2-2117M) and is monitored with two flow meters.

The first metering valve following the pump provides a coarse adjustment of overall flow. This valve is upstream from the reaction flask and provides the most resistance to flow in the system. Downstream from the flask, air flow is split between the detector loop and a shunt tube which bypasses the detector. This configuration allows detector flow to be adjusted independently of overall flow through the system. The fraction of the overall flow that goes to the detector is controlled using the two remaining metering valves in the system. In tandem, these valves also provide a fine adjustment of overall flow.

While in the purge mode, a bubble flow meter measures overall flow through the system. This flowmeter is constructed from a sidearm 100-mL buret supported by buret clips and a ring stand. Flow enters the sidearm and passes up the buret. A rubber pipet bulb is fixed to the bottom of the buret and contains a soap solution. The flow rate is measured by introducing a soap bubble into the flow stream. The bubble travel time in the buret is converted to flow rate.

To measure the detector flow rate, a floating ball meter (Gilmont

F2160) is installed in the detector loop. This meter continuously monitors that portion of the overall flow that goes to the detector. Detector flow is measured in both the recirculate and purge modes for the MSU Gas Purge System.

Two Valco switching valves (Supelco 2-2975M and 2-2977M) are used to select from various flow configurations of the MSU Gas Purge System. As outlined in the general description, a 4-way valve selects between the purge (open) and recirculate (closed) modes. Its four ports are connected to the exit flow from the detector (and shunt tube), the bubble flow meter, the filtering system, and the air pump. In the purge mode, this switch connects the detector exit flow to the bubble flowmeter and the filtering system to the air pump. In the recirculate mode, this switch connects the detector exit flow to the air pump. The bubble flow meter and filtering system are not used in the recirculate mode.

A 6-way valve switches between two identical reaction flask loops. Its six ports are connected to the air pump exit flow, the gas fitting inlet for reaction flask 1, the gas fitting inlet for reaction flask 2, the exit flow from flask 1, the exit flow from flask 2, and the detector inlet (and shunt tube). This switch connects the air pump exit flow to one flask inlet and the flask exit flow to the detector inlet. The other flask is in a closed loop; its inlet and outlet are connected. In this way, the six-way switch allows replacement of flasks without interrupting the flow to other parts of the system. This switch performs the same function as the two switches labelled "B" in the UF Gas Purge System (Figure 7).

II. System Behavior and Modification

Detector Response Experiments:

Procedure:

This section describes experiments that characterize the behavior

of the detector in the MSU Gas Purge System. The results of some of these experiments led to modifications of the system configuration. These modifications distinguish the MSU Gas Purge System from the UF Gas Purge System (after which the system was initially modelled). Both baseline behavior and detector response linearity were evaluated.

The effect of flow rate and various gas treatment systems on the detector baseline were evaluated. The gas treatment system is attached to the pump inlet in the purge flow configuration. The MSU Gas Purge System draws air from its surroundings. Since the quality of the ambient air is variable, the treatment system filters and purifies the incoming air of any contaminants.

The UF Gas Purge System passes the incoming air through a gas washing bottle. The gas washing bottle serves as a filter for particulates. Also, the gas washing bottle saturates the incoming air with moisture. Saturating the air reduces the potential for evaporating water from the reaction flask during the purge experiments.

In the MSU Gas Purge System, a gas washing bottle was initially used. However, the washing bottle was observed to effect gas flow rates. Moisture collected in the air pump after a few hours of operation in the purge mode. This moisture resulted from droplets of water carried with the air flow from the washing bottle to the pump. Because of the moisture, the pump was unable to maintain a constant flow. Since constant flow rates are essential to future experiments, the effect of removing the washing bottle from the system was studied. Specifically, measurements of the amount of water evaporated from the reaction flask were made under typical run conditions. In order to filter the incoming air of particulates and contaminants, solid filters and sorbents were used. A tube packed with cotton, glass wool and activated carbon proved to be the most practical gas treatment system.

The water volume in the reaction flask was measured before and after operating the system for one and a half and 22 hours in the purge mode without the washing bottle (Table II). Even after the longer run time, the amount of water lost from the system due to evaporation was



negligible. Since evaporation is not a problem and since the ability of the pump to maintain a consistent flow rate is affected, the washing bottle was eliminated from the MSU Gas Purge System. Consistent baselines and flow rates were observed using the activated carbon tube as the sole purifying agent in the gas treatment system.

Table II: Evaporation of Water from the Reaction Flask

<u>Initial Mass</u> <u>(grams)</u>	<u>Final Mass</u> <u>(grams)</u>	<u>Run Time</u> <u>(hours)</u>	<u>Water Evaporated</u> <u>(% of total)</u>
200.01	198.86	22	0.57
205.26	205.21	1.5	0.02

To observe the effect of overall flow rate on the detector baseline response, the response was monitored while the metering valve upstream from the detector was adjusted. The effect of overall flow rate through the system was observed to have a negligible effect on the baseline (Table III).

Table III: Effect of Flow Rate on Detector Baseline

<u>"Upstream" Valve Setting</u>	<u>Flow Rate (mL/min)</u>	<u>Baseline Reading</u>
1.0	69.6	6.2
2.0	119.2	6.2
3.0	158.2	6.1
4.0	174.6	6.1
5.0	190.5	6.1

To evaluate detector response linearity, several experiments were conducted on the system in the recirculate mode. When the system is operated in the recirculate mode, no solute mass is lost from the system. A volatile solute distributes itself throughout the system. Its distribution is controlled by a gas-solution distribution coefficient known as the Henry's Law constant, K_H (Equation (14)).

Since Equation (14) is a linear relationship, linear increases in

overall solute mass in the system give linear increases in gas phase concentration. By linearly increasing gas phase concentration and monitoring the detector response, a determination of detector linearity was made. Measurements of detector response linearity to a number of alkylbenzenes, two chlorinated ethenes and naphthalene were taken.

The neat organic liquids and Millipore water were allowed to equilibrate in 500-mL amber glass bottles. The resulting aqueous solutions saturated in organic solute were used as stock solutions.

For the detector linearity experiments, reaction flask 1 contained 200 mL of Millipore water. Reaction flask baselines at several attenuation settings were established in the recirculate mode. Flow was switched to the flask 2 loop to isolate flask 1 from the system. Solute stock solution from below the organic layer in the amber bottle was withdrawn using a Gastight syringe (Hamilton Series 1000) and introduced into flask 1 through the injection port. After two minutes, flask 1 was switched back into the system and the detector signal was allowed to stabilize. Several minutes of constant detector response were recorded on the chart paper. The closed system response to the solute was recorded at several concentrations by repeatedly isolating flask 1, introducing more solute, returning flask 1 to the system, and recording the detector response.

Results:

The linearity of the detector was tested for the system in two flow configurations. Initially, the system was configured like the UF Gas Purge System; no valve or meter was present within the detector loop. Detector response is not linear with the system in the initial configuration (Figure 12). The nonlinear response is believed to be related to detector flow rate. When the flow rate through the detector exceeds the ability of the detector to ionize the incoming analyte, the ionization is incomplete. Incomplete ionization of the analyte reduces the response and leads to a deviation from Beer's Law, the linear relationship relating response to concentration.



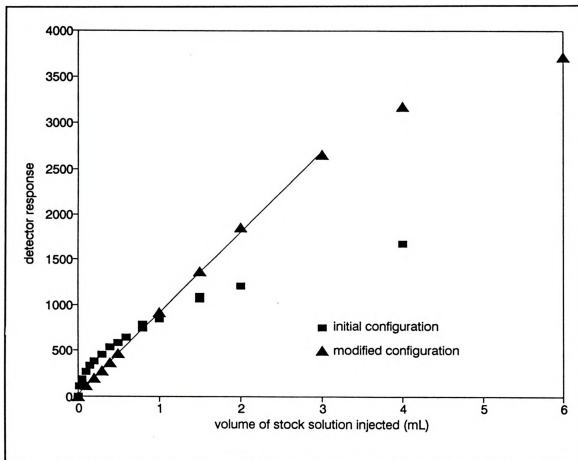


Figure 12: Detector Flow Configuration and Response to Ethylbenzene

To achieve linearity in response, the initial configuration was modified to improve control and measurement of detector flow rate. A valve and flowmeter were inserted within the detector loop. The modified configuration allowed the flow rate to be set at 40 to 50 mL/min. In the modified configuration, the detector responds linearly up to 3.0 mL of ethylbenzene stock solution introduced (Figure 12). Even in the modified configuration, higher concentrations (>3 mL) fall below the linear relationship because ionizing efficiency suffers.

Knowing the K_H and water solubility of the solute, it is possible to calculate the gas phase concentration of the solute. Using ethylbenzene as an example, a saturated water concentration of 152 mg/L (70), a K_H of 0.345 (71), and 3.0 mL of stock solution in flask 1 represents a gas phase concentration of 0.68 mg/L. The results for detector linearity experiments using other organic solutes appear in Table IV. For the alkylbenzenes, the detector responds linearly to concentration the gas phase concentration of the solute does not exceed about 1 mg/L. Solute concentrations were kept in the linear response range in all subsequent experiments performed on the system.

Determination of Henry's Law Constants in the MSU Gas Purge System:

Procedure:

200 mL of Millipore water were weighed into a dry 250 mL reaction flask. The injection port of the flask is fitted with a Teflon-lined septum and a cap with a hole. A glass stirbar (Fischer Scientific 09-311-7) is placed in the bottom of the flask. The flask was connected to a gas fitting and placed in the flask 1 loop of the MSU Gas Purge System. To buffer fluctuations in ambient temperature, the reaction flask is immersed in a water bath. The water bath sits atop a magnetic stir plate (Corning PC-161).

With the system in the purge mode, baselines for flask 1 were established at several attenuations. A coarse adjustment of flow was made using the metering valve upstream from the flask. Fine adjustment

Table IV: Detector Linearity for Volatile Organic Solutes

<u>Compound</u>	<u>Response Factor[†]</u>	<u>r²</u>	<u>Maximum Volume (uL)</u>	<u>Solubility (mg/L)</u>	<u>K_w</u>	<u>Gas Concentration (mg/L)</u>
toluene	13.43	0.977	1500	515	0.272	0.94
ethylbenzene	4.52	0.999	3000	152	0.345	0.68
propylbenzene	1.78	0.996	10000	60	0.283	0.76
naphthalene	13.2	0.999	750 [*]	30	0.0197	0.29
TCE	6.72	0.996	2000	1100	0.371	3.53
PCE	8.73	0.995	2500	150	0.833	1.16

[†] Response factors are reported for system in modified flow configuration with a detector flow rate of 50 mL/min.

^{*} Because of naphthalene's low solubility, a stock solution in methanol rather than water was prepared. The concentration of stock was 3950 mg/L.

TCE = trichloroethene, PCE = tetrachloroethene.

and detector flow were controlled using the two downstream metering valves.

Flask 1 was isolated from the system (by diverting flow through the flask 2 loop), injected with a known volume of solute-saturated Millipore water and allowed to stir for several minutes. With the appropriate chart recorder speed and attenuation/range setting, the system was switched to the recirculate mode and the flask selection switch returned to flask 1. Approximately 10 minutes of constant detector signal was recorded to ensure that the system was free of leaks.

To initiate the purge portion of the experiment, the system was switched into the purge mode. Readings of flow, attenuation/range settings and chart speed were written directly on the chart. Overall flow was calculated using measurements of bubble travel time between the 0 to 25 mL buret readings. Detector flow was read directly from the ball flowmeter. The water bath temperature was also recorded



periodically.

Attenuation/range settings were adjusted to keep the signal on scale. Toward the end of the run, chart speed was reduced to conserve paper. When the signal had decayed to the baseline, the run was ended. Another set of baseline readings were recorded to determine if any baseline drift had occurred during the experiment. All detector response readings were corrected for baseline response.

Between purge runs, the system was dried by running the incoming air through a Drierite drying tube. Fresh activated carbon was placed in the gas treatment system.

Results:

Figure 13a shows an example of the raw data obtained during a purge of ethylbenzene from water. The detector signal decreases curvilinearly with time as ethylbenzene is purged from the reaction flask. Since the detector is responding linearly to concentration in the gas phase, the area under the curve is proportional to the mass removed from the system.

In order to facilitate the comparison of different purge experiments, the area at selected time points is normalized to total area. The ratio of the area at a given time to the total area is a measure of the relative mass purged (RMP). Using Figure 13a as an example, RMP at ten minutes is the area to the left of the dotted line divided by the total area. In this case, RMP equals 0.67. The plot of RMP versus time will be referred to as a purge curve (Figure 13b).

The shape of the purge curve is determined by several factors. These factors include the volumes of gas and solution in the system, the K_H for the solute, and the gas flow rate. The system volumes and gas flow rate are measured directly. The Henry's Law constant is determined using a fitting program. A description of experiments to determine system volume will be followed by an explanation of the fitting procedure used to determine K_H .

The total volume of the system can be measured by weighing it both

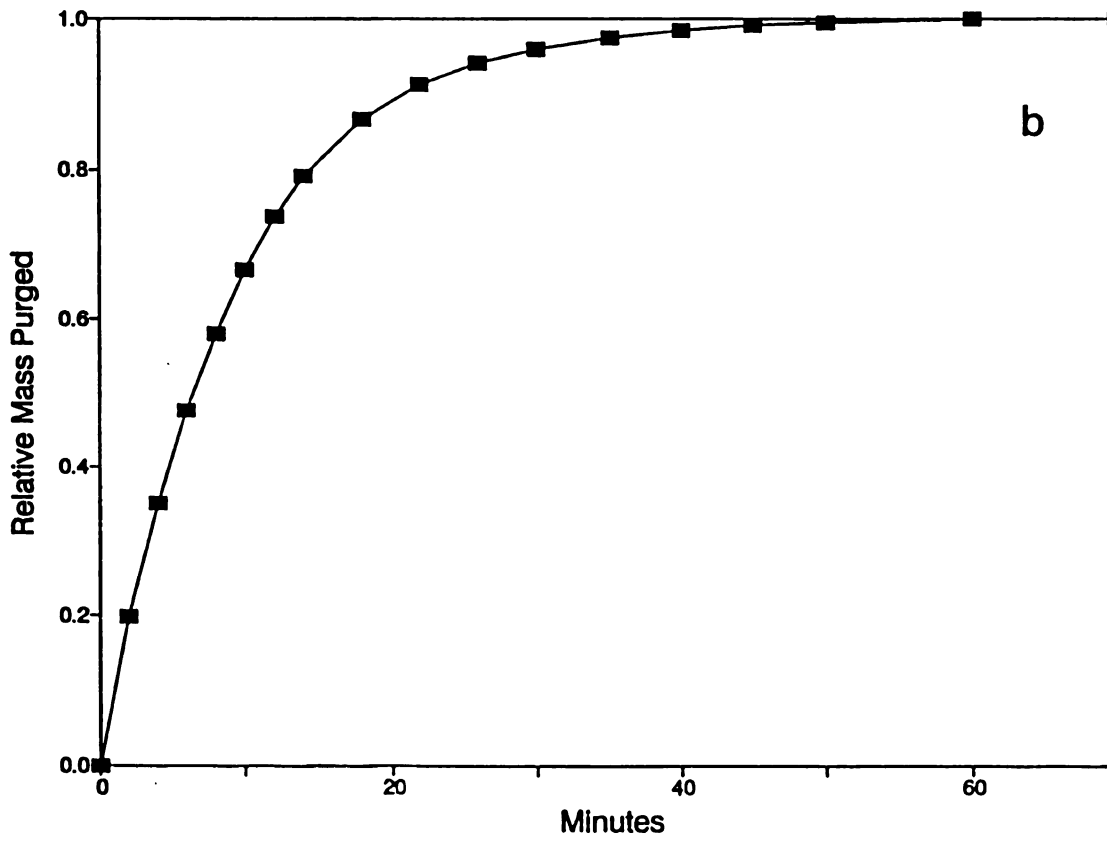
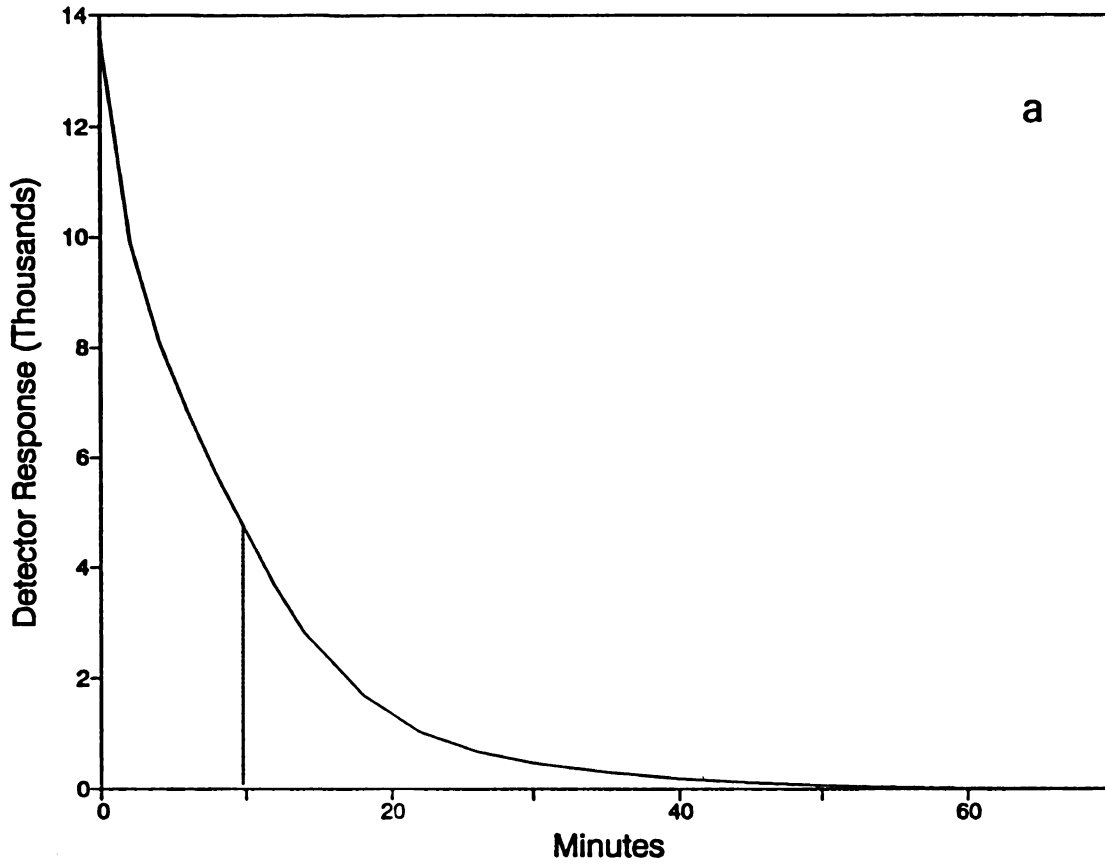
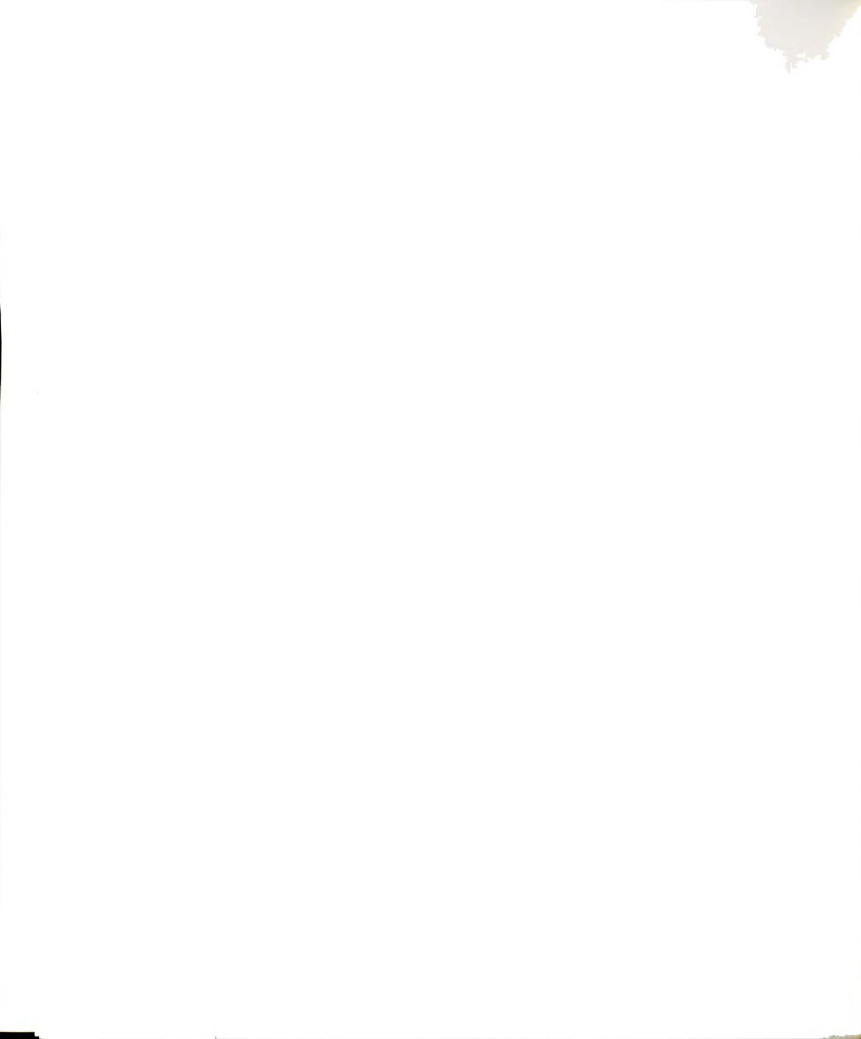




Figure 13: Raw Data and Purge Curve for Ethylbenzene



empty and full of water. Since water has unit density, the difference in mass is equivalent to the volume. Results of this type of measurement appear in Table V. Since several gas flow fittings and reaction flasks were made, the system volume varies slightly depending on the combination of flask and fitting used. However, this volume difference had little effect on later modelling results. Knowing the total system volume and the water volume for a given purge experiment, the volume of gas is simply calculated by difference.

Table V: System Volume Measurements

Mass of Glassware (grams)		Volume of Glassware (mL)
<u>Full of Water</u>	<u>Empty</u>	
547.36	258.12	289.24
574.13	301.49	272.64
average volume:		281 mL

The general shape of the purge curve for organic solutes is an exponential decay curve. The curve can be fit to an exponential expression (Equation (15)). The first order purge constant, k_p , is determined by a curve-fitting routine. The rate of distribution of solute between the gas and aqueous phases is assumed to be rapid relative to the gas flow rate. The distribution is described by the Henry's Law constant (Equation (14)). In this case, the purge rate constant is defined by Equation (16).

$$RMP(t) = 1 - e^{-k_p t} \quad (15)$$



$$k_p = \frac{q}{(V_w / K_H) + V_g}$$

where q = gas flow rate (mL / min) (16)

V_w = volume of aqueous phase (mL)

V_g = volume of gaseous phase (mL)

Therefore,

$$RMP(t) = 1 - \exp\left[\frac{-qt}{(V_w / K_H) + V_g}\right] \quad (17)$$

SIGMAPLOT, a nonlinear curve-fitting program was used. This program uses the Marquardt-Levenberg algorithm to minimize the sum of the squares of the differences between the equation values and the data values. K_H is independently determined since it is the only remaining unknown in Equation (17) and, therefore, the SIGMAPLOT fits for K_H exhibit no codependency.

The fitted Henry's Law constants for a series of alkylbenzenes, trichloroethene, tetrachloroethene, and naphthalene appear in Table VI. For propylbenzene, the results of 19 separate experiments were averaged to give 0.323. The standard deviation is about 12% of this average value. For each individual experiment, the standard deviation is roughly 1% of the determined K_H . The larger standard deviation in the population reflects the fact that the experiments were conducted on different days over the course of a year. On a given day, the ambient temperature and variations in system volume depending on glassware used probably account for the variation.

The purge runs for the alkylbenzenes and chlorinated ethenes lasted about two hours. Naphthalene, the compound with the lowest K_H ,



Table VI: Henry's Law Constants Obtained in Gas Purge System

<u>Compound</u>	<u>Average K_H</u>	<u>Standard Deviation</u>		<u>No.</u>	<u>Literature Values</u>	
		<u>pop.</u>	<u>sample ave.</u>			
toluene	0.225	0.021	0.002	7	0.205 ^a	0.272 ^b
ethylbenzene	0.250	0.044	0.002	16	0.239 ^a	0.345 ^b
propylbenzene	0.323	0.039	0.003	19	0.348 ^a	0.283 ^b
TCE	0.281	0.028	0.002	5	0.354 ^c	0.371 ^b
PCE	0.372	0.032	0.006	4	1.107 ^c	0.833 ^b
naphthalene	0.0154	0.0008	0.0001	3	0.045 ^c	0.0197 ^b

^aPerliger et al, 1993. ^bMackay and Shiu, 1981. ^cHwang et al, 1992.

required a purge time of 22 hours. During the naphthalene purge runs, the air pump had difficulty maintaining a constant flow rate over this extended period. For this reason, naphthalene represents a lower limit for compounds whose K_H can be determined in this system. Also, compounds with K_H s lower than naphthalene become more difficult to detect continuously since their vapor phase concentrations approach PID detection limits. In these cases, a trap and analysis setup (61) is more appropriate.

Literature values for K_H (67,68,72) appear in the last two columns of Table VI. For propylbenzene, the value determined in the MSU system falls between the two literature values. In general, the fitted values do not differ from the literature values more than these values differ from one another. In most cases, the K_H determined in the gas purge system is lower than the literature values. The measured K_H in a similar dynamic system was shown to be a function of the liquid depth (67).

Conclusions:

The MSU Gas Purge System has been constructed to operate in both recirculate and purge modes. Modification of the initial detector temperature control and gas filtering systems improved the baseline behavior. A modified flow configuration which contained an additional

flow valve and meter within the detector loop resulted in a detector response which was linear with concentration. K_H values determined in the system are relatively consistent and generally agree with literature values.

For the MSU Gas Purge System, naphthalene represents a lower limit with respect to volatility. Compounds with K_H s less than naphthalene require long run times and raise a problem with maintaining constant flow and with vapor phase concentrations that approach PID detection limits.



Chapter 3: HDTMA-modified Clays and Soils - Physical and Chemical Properties and Equilibrium Sorption of Alkylbenzenes

I. Introduction

The sorption of nonionic organic compounds (NOCs) to soils has been shown to depend most strongly upon soil organic matter (SOM) content (34,35,36). Nonionic organic compounds such as alkylbenzenes exhibit linear sorption isotherms on soils with greater than 0.1% organic carbon (2) or when clay mineral content is less than 30 times organic matter content (20). The extent of sorption has been found to be related to the compound's solubility and the soil organic matter content (19). In fact, equilibrium distribution coefficients (K_d s) determined in soil systems are often normalized for organic matter content (Equation (18)). These normalized K_d s are known as K_{om} s. K_{om} is relatively constant for a given compound across a wide range of soils and has been correlated with the octanol-water partition coefficient (K_{ow}) (Equation (19),39). Regression equations of this type allow the K_d on a given soil to be predicted using K_{om} s or K_{ow} s found in the literature.

To increase the degree of NOC sorption, native inorganic cations in soils can be exchanged with organic cations to increase the organic matter content (41). Various quaternary alkylammonium cations (QUATs)

$$K_d = f_{om} * K_{om} \quad (18)$$



$$\log K_{om} = 0.904 \log K_{ow} - 0.779 \quad (19)$$

have been used to enhance sorption of NOCs by soils (41,42) and pure clays (43,44,45,46,47,48,49,50). For cations with large alkyl substituents such as hexadecyltrimethylammonium (HDTMA) and dioctadecyldimethylammonium (DODMA), the cation exchange reaction transforms the interlamellar region of clays into a partitioning medium for NOCs.

Partitioning of a series of alkylbenzenes, naphthalene and biphenyl into HDTMA-modified smectites, illite, vermiculite and kaolinite demonstrated the importance of clay mineral type (49). Hexadecyltrimethylammonium-exchange of the A and Bt horizons of Marlette soil resulted in substantial increases in the equilibrium distribution coefficients for benzene, tetrachloroethene, and 1,2-dichlorobenzene (41). The added organic matter was 10-30 times more effective than SOM at sorbing the organic solutes. The increase in sorption was attributed to the formation of a partitioning medium upon HDTMA exchange of the natural soil clays. An expanded study involving seven NOCs, two additional QUATs (nonyltrimethylammonium and dodecyltrimethylammonium), and three soils from different textural classes confirmed the broad applicability of this technology (42).

The sorptive properties of the modified soils and clays prepared in this study will be evaluated under equilibrium (Chapter 3) and nonequilibrium (Chapter 4) conditions.

II. Materials and Methods

The properties of the soils and clays used in this study are summarized in Table VII. The Colwood soil is a fine-loamy, mixed, mesic Typic Haplaquoll. The Capac soil is a fine-loamy, mixed, mesic Aeric Ochraqulf. Both soils were collected in Michigan.



Table VII: Properties of Soils and Clays

<u>Property</u>	<u>Capac A horizon</u>	<u>Colwood A horizon</u>	<u>SAC</u>	<u>SAz-1</u>
% org. C	3.46	5.36	-	-
CEC (meq/100g)	12.2	21.6	88	130
% sand	44	41	-	-
% silt	36	35	-	-
% clay	20	24	100	100
clay mineralogy:				
smectite	--	ND	low charge	high charge
chlorite	\	ND	montmorillonite	smectite
vermiculite	XXXX	ND		
mica	XX\	ND		
kaolinite	XX\	ND		
quartz	\	ND		
source	Ingham Co., MI	Ingham Co., MI	American Colloid	Clay Mineral Society
\ = approximately 5% of clay fraction (<2 um) X = approximately 10% of clay fraction Clay mineralogy from Haile-Miriam, S. 1990. PhD thesis. ND = not determined				

Preparation Procedure - Modified Clay:

A Wyoming bentonite (SAC) was obtained from American Colloid. An Arizona smectite (SAz-1) was obtained from the Source Clay Repository (Clay Mineral Society, Columbia, MO). The SAz-1 sample was Na-saturated using 1 M NaCl, acidified to pH 4 to remove carbonates. The SAC sample was used without further modification.

A suspension of 40 grams of the clay in 4 liters of deionized water was prepared in an amber glass bottle. Large impurities were removed by allowing the suspension to settle overnight. The clay size fraction (<2um) was transferred to a fresh bottle. The solids content of the purified suspension was determined gravimetrically by evaporating a 30-40 mL subsample to dryness.

1000 mL of the suspension were transferred into a 2L Erlenmeyer flask containing a magnetic stirbar. Based on the suspension concentration, sufficient HDTMA bromide to satisfy one equivalent of the

clay's cation exchange capacity (CEC) was dissolved in a minimum volume of deionized water (roughly 700 mL). The HDTMA solution was poured into the stirring clay suspension. The mixture was allowed to stir for 2 hours.

The flocculated HDTMA-clay was allowed to settle and the supernatant was decanted. The remaining slurry was split between 2 1L polyethylene bottles. About 500 mL of deionized water were added to each bottle. The bottles were capped, shaken and centrifuged at 500 rpm for 20 minutes. After centrifuging, the wash water was replaced with fresh deionized water. The shaking and centrifuging step was repeated. The washed clay was stored in a 1L polyethylene bottle. Several batches of modified clay were combined at this point.

To remove the majority of the water, the clay slurry was poured onto a sheet of filter paper (Whatman #1) which sat on top of several paper towels. This dewatering step produced a thick paste which was transferred to watch glasses and dried in the oven at 100 degrees Centigrade. Upon drying, the clays cracked into thick flakes.

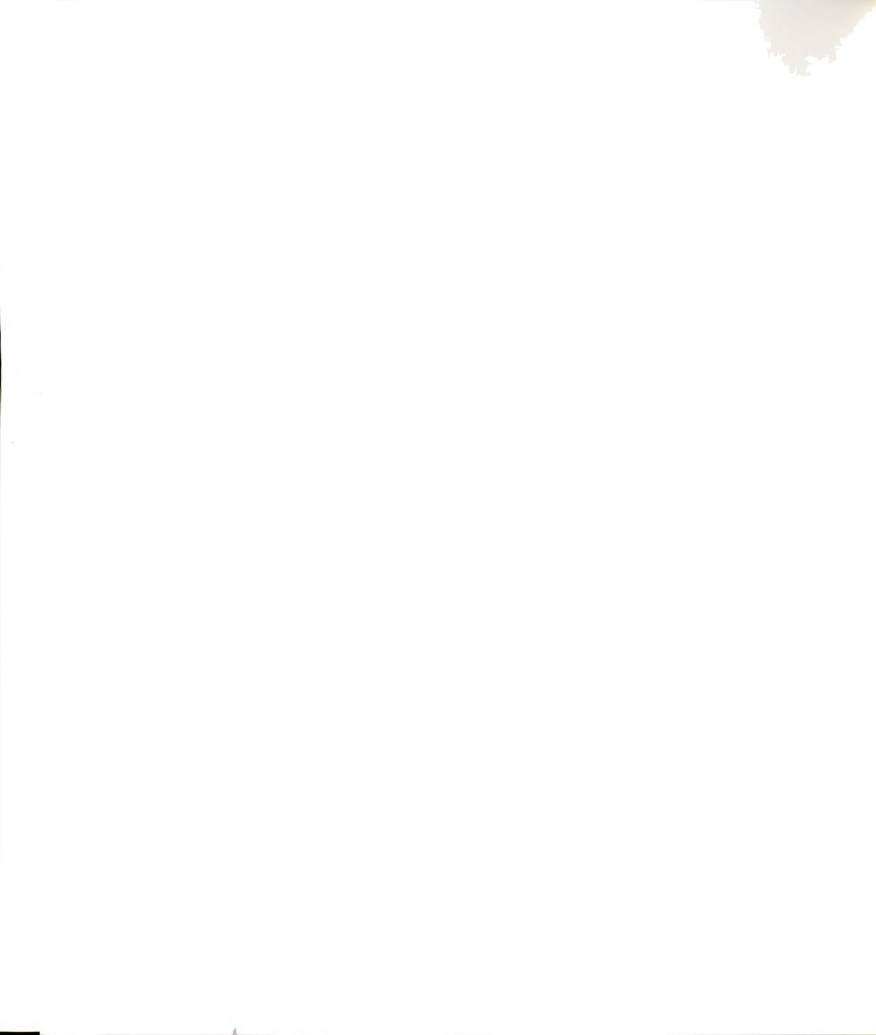
The air-dried clays were ground in a mortar and pestle. The ground clay was passed through nested sieves (10, 18, and 60 mesh) to separate three size fractions; 1.0 - 2.0 mm, 0.25 - 1.0 mm, and <0.25 mm. The dried modified clays were stored in amber glass jars.

Preparation Procedure - Modified Soils:

The A horizons from both Colwood and Capac soil were collected and air-dried. 50 grams Colwood A (or 80 grams Capac A) horizon were weighed into a 1000 mL Erlenmeyer flask. 500 mL of deionized water were added to the flask. A glass stirbar was used to mix the soil and water.

Sufficient HDTMA bromide to satisfy the desired percentage of the soil CEC was dissolved in another 500 mL of deionized water. The HDTMA solution was added to the flask and mixed with the soil for one hour.

The mixture was vacuum filtered (Whatman #1, 12 cm). Complete transfer of the solids to the filter was accomplished with a minimal



amount of water (<100mL). The filter cake was placed on paper towels and allowed to air dry for several days. A spatula was used to break apart the soil during drying. Several batches of the dried soil were combined and stored in a glass jar.

Isolation of Organic Matter Size Fractions:

A purification and separation of organic matter from Colwood A horizon was performed (73). Air-dried Colwood A horizon (200 g) was added to a sealable 1 L polypropylene bottle. The bottle was filled with a 5% solution of sodium hexametaphosphate in deionized water (Millipore MilliQ). The bottle was sealed and placed on a rotary shaker for 24 hours.

After shaking, the mixture was transferred to a continuous flow separation system. A density separation was performed by vortexing the solution in a column. The lightest material passed through the column into a series of sieves. The sieve trays (500 um, 250 um, 125 um, and 53 um) collected various sizes of the soil solids.

The size fractions were harvested from the trays and centrifuged to remove excess solution. The solids were freeze dried and stored in polypropylene bottles.

Organic Carbon Content:

Organic carbon content was determined using a Dohrmann DC190 with 183 Boat Sampling Module. This instrument combusts the sample in a platinum boat and measures the liberated carbon dioxide with an IR detector. A 3% sucrose solution was used to standardize the instrument.

Foaming Test:

To evaluate the potential for the HDTMA-modified soils to cause foaming, a foaming test procedure was developed. This procedure is

quite simple yet it accurately simulates the environment of the gas purge system.

One gram of HDTMA-modified soil and 15 mL 0.01N CaCl_2 solution were placed in a 25 mL glass vial. After 30 minutes, air was blown into the solution through a disposable pipet tip at a rate of approximately 100 mL per minute. If the slurry developed sufficient foam to crest the lip of the vial, the test was considered positive.

Equilibrium Isotherms:

Isotherms of several alkylbenzenes were measured on the soils and the modified soils and clays.

Stock solutions of toluene, ethylbenzene and propylbenzene were prepared by equilibrating the neat alkylbenzene with Millipore water in a 500 mL amber glass bottle for several days. Whenever the alkylbenzene-saturated aqueous solution was withdrawn from the flask, a Gastight syringe (Hamilton Series 1000) was used to penetrate the overlying organic phase. With the needle below the interface, a few bubbles of air were expelled from the syringe to clear the needle. The syringe was filled beyond the necessary volume, removed from the bottle, the needle wiped clean, and the excess liquid exhausted to bring the syringe to the appropriate volume. These precautions were taken to avoid capturing any neat organic liquid in the syringe.

In order to determine the mass of soil to use for a given isotherm, an approximate K_d is necessary. For soils, K_d was estimated from K_{om} (Equation (18)) using the fraction of organic matter, f_{om} . For the modified soils and clays, a range-finding experiment was performed. The approximate K_d is used to calculate the mass of sorbent, m , necessary to reduce the aqueous phase concentration by some fraction, x , relative to the initial concentration (Equation (20)). Since sorbed concentrations will be determined by difference, a reduction in aqueous concentration of 50% ($x=0.5$) minimizes error in the determination of sorbed concentration and in the K_d from the isotherm. The volume of

aqueous phase, V , is the volume of matrix solution plus the volume of alkylbenzene stock solution injected.

$$m = \frac{xV}{K_d(1-x)} \quad (20)$$

Range-finding experiments were performed to get a rough estimate of K_d for the HDTMA-modified soils and clays. Different amounts of the sorbent were weighed into three centrifuge tubes (25 mL Corning Corex). 25 mL of matrix solution were pipetted into each tube. At the same time, an additional tube was filled with 25 mL of the matrix solution. The matrix solution for isotherms and range-finding experiments of the soils and modified soils was 0.01N CaCl_2 with 0.5% HgCl_2 as a bioinhibitor. The matrix solution for the modified clays was Millipore water. All four tubes were fitted with Teflon-lined septa (Thomas Scientific 9711D45) and caps with a 5/16" hole. A syringe was used to introduce the same volume of alkylbenzene stock solution into each tube. The tubes were placed on a shaker for 24 hours.

After the equilibration period, the tubes were centrifuged (Sorvall RC5C with Model SS34 rotor) at 8000 rpm for 20 minutes. Five scintillation vials (Research Products International 121000) containing 10 mL carbon disulfide were chilled in a freezer for several hours. A Gastight syringe was used to withdraw 10.0 mL of the supernatant from the centrifuge tube. The supernatant was injected into the chilled CS_2 for extraction. Each scintillation vial was quickly recapped to minimize volatilization losses. The extraction vials were allowed to warm to room temperature and shaken occasionally to promote the extraction of the alkylbenzene.

Two crimp seal vials (Supelco 3-3123) were filled with the CS_2 extract from each scintillation vial. The fifth scintillation vial provided a blank. The vials were analyzed by gas chromatography (GC) for the alkylbenzene used. A one-point determination of the K_d for each

tube can be made by using a ratio of the soil-containing and soil-free GC responses. This ratio is equivalent to the alkylbenzene concentration ratio and can be substituted for the quantity, $1-x$, in Equation (20).

With an approximate K_d in hand, an accurate isotherm experiment can now be performed. Twelve clean, dry centrifuge tubes were placed in a tube rack. An amount of sorbent necessary to reduce the aqueous phase concentration by 50% (as calculated using Equation (20)) was weighed into six of these tubes. 25.0 mL of the matrix solution was pipetted into all twelve of the tubes. The tubes were fitted with septa and capped as above. Each tube was inverted several times to insure that the sorbent was fully wetted.

Each sorbent-containing tube was paired with a sorbent-free tube. Each tube pair represents one point on the isotherm. Different initial concentrations were produced in each tube pair by varying the amount of stock solution injected. For example, toluene isotherms were set up with 50, 100, 200, 300, 400, and 500 μL of stock solution. The initial concentrations ranged over an order of magnitude and encompassed the initial concentration to be used in the gas purge experiments.

The tubes were placed on a rotary shaker for 24 hours, centrifuged, extracted and analyzed for final aqueous alkylbenzene concentrations as explained earlier.

The aqueous solubility (70) was used to calculate initial concentrations of the alkylbenzenes in each tube. Using these calculated concentrations, a standard curve for the GC was generated using the sorbent-free tubes. The equilibrium concentration, C_e , in the sorbent-containing tubes was calculated from the standard curve and used together with the initial concentration, C_i , in Equation (21) to

$$m_{\text{sorbed}} = V(C_i - C_e) \quad (21)$$

calculate the mass sorbed. The mass sorbed was normalized to the

measured sorbent mass to yield the sorbed concentration, x/m .

The isotherms were fit to a linear equation (Equation (22)).

$$\frac{x}{m} = K_d * C_e \quad (22)$$

III. Results and Discussion

Organic carbon contents for the soils, modified soils, modified clay aggregates, and the isolated SOM fractions appear in Table VIII.

Table VIII: Organic Carbon Content of Modified Soils and Clays

<u>Sample</u>	<u>%CEC Exchanged with HDTMA</u>	<u>OC Content (%)</u>	
		<u>calculated</u>	<u>measured</u>
Capac A	0	---	3.32(0.06)
	20	3.85	3.60(0.21)
	40	4.38	4.03(0.17)
	60	4.90	5.01(0.42)
	80	5.41	5.86(0.24)
	100	5.92	6.11(0.72)
Colwood A	0	---	5.19(0.13)
	40	7.00	7.41(0.36)
SAC			
<0.25 mm	100	16.3	16.0(0.8)
0.25-1.0 mm	100	16.3	16.2(0.1)
SAz-1			
<0.25 mm	100	22.1	20.7(0.5)
0.25-1.0 mm	100	22.1	21.0(1.0)
OM Fractions			
53-125 um	0	---	23.3(0.6)
125-250 um	0	---	24.8(1.0)
250-500 um	0	---	26.1(0.9)

Numbers in parentheses represent the standard deviation.

Knowing the native organic carbon content and the CEC, a prediction of the carbon content after modification can be made. Consider the Capac A horizon modified at 40% of its CEC. The final



carbon content will be the sum of the native carbon and the carbon derived from the HDTMA. The native carbon was measured at 3.32%. The mass of HDTMA carbon added is simply the product of 0.4 times the CEC and the mass of carbon in one milliequivalent of HDTMA, 228.21 mg C/meq HDTMA. The predicted carbon content is 4.38%. The results of this type of calculation also appear in Table VIII.

The measured carbon contents agree fairly well with predictions. The high standard deviations (up to 12%) in some of the measured values reflect the variability associated with subsampling a soil. The soil subsamples were 5-10 milligrams. At this scale, soil properties such as organic carbon content are variable. This variability can also explain the differences between measured and predicted values.

The organic carbon analyses of the organoclay aggregates agree with predicted organic carbon contents. For both modified clays, the two aggregate size fractions have the same organic carbon content. This result is expected since they are ground and separated from the same source material.

The organic matter fractions that were isolated from Colwood A horizon range from 23.3 to 26.1% organic carbon. To express these values in terms of organic matter, the carbon content of organic matter is needed. Soil humic and fulvic acids range from 41 to 59% carbon (74). Therefore, these fractions still contain 36 to 60% mineral matter. The separation and isolation procedure resulted in a 4- to 5-fold purification of the organic matter.

A gas purge system will be used to evaluate the dynamic sorption behavior of the modified soils and clays. In this system, the modified materials must be water stable. If the clay aggregates are not stable, kinetic interpretations based on particle size will be difficult. If either the clays or soils release HDTMA to the aqueous solution, this surfactant will cause foaming during gas purge experiments and will foul the gas purge system.

The results of foaming tests for the modified soils appear in Table IX. At loadings greater than 60% of the CEC, both soils release



enough HDTMA into solution to cause foaming in both the preparation procedure filtrate and the slurried soil. Some evidence of foaming was observed in the filtrate from the preparation procedure of the 40% CEC Colwood A sample. Foaming in the preparation procedure filtrate suggests that the HDTMA is not completely exchanged onto the soil. Foaming in the soil slurry suggests that washing and drying the soil does not eliminate free HDTMA or that HDTMA is being released from the exchange sites. No foaming was observed for any of the modified clays.

Table IX: Foaming Test Results

<u>Sample</u>	<u>HDTMA Treatment</u>	<u>Foaming Test Result</u>	
		<u>Filtrate</u>	<u>Slurry</u>
Colwood A	20% CEC	-	-
	40% CEC	+/-	-
	60% CEC	+	+
	80% CEC	+	+
	100% CEC	+	+
	60% CEC, 2 wks aged		-
	80% CEC, 2 wks aged		+
	60% CEC, slow add'n	+	-
	80% CEC, slow add'n	+	+
	Capac A	20% CEC	-
40% CEC		-	-
60% CEC		+	+
80% CEC		+	+
100% CEC		+	+

+ = foam present, - = foam absent, +/- = foam took several minutes to fill vial to the top

The foaming test method was calibrated using standard solutions of HDTMA bromide. The standard solutions with a concentration greater than 35 uM gave a positive foaming test. Assuming that the foaming point is the same in the soil slurries, a positive foaming test would be obtained in the 60% CEC samples with roughly 0.5% of the total HDTMA being released from the soil to solution.

A positive foaming test was no longer obtained from the 60% CEC samples of both soils if the dried soil was allowed to age for two weeks or if the period of time over which the HDTMA was added was extended.

The "slow addition" modification of the procedure involved adding the HDTMA solution dropwise from a buret over a four and a half hour period. However, even "aged" or "slow addition" samples foamed at 80% CEC.

Although no previous studies on the effect of aging exist, the results of foaming tests on these soils are consistent with a study of HDTMA modification of a B horizon. A semilog linear relationship between the concentration of free HDTMA and the loading level (as a fraction of the soil CEC) was found for the Bt horizon of Oshtemo soil (75). Up to a loading level of 75% CEC, the solution concentration of HDTMA, C_{HDTMA} , can be calculated from Equation (23). At the foaming point of HDTMA, 3.5×10^{-5} M, the loading level on the Oshtemo Bt horizon would be 73% CEC. At higher loadings, this modified Bt horizon would be expected to foam.

$$\text{HDTMA loading} = 1.91 + 0.211 \log C_{HDTMA} \quad (23)$$

Alkylammonium cations can slowly replace fixed potassium cations in the interlayer of micas (76,77). Perhaps, this slow exchange reaction is able to fix some of the free HDTMA if given sufficient time in either the preparation or upon storage. In any event, the soils modified at any level greater than 60% will foam in the gas purge system. For preparing the large amounts necessary to carry out further experiments, a CEC loading of 40% was used. Since the effect of slow addition was minimal, the original procedure was used to prepare soils for the remainder of the experiments.

The stability of the modified clay aggregates was evaluated in aqueous solutions under shaking and stirring conditions. Measurements of the recovered clay aggregates indicate that these aggregates are stable in water (Table X). The first treatment simulates conditions found inside a gas purge reaction flask. The second treatment tests the stability over a longer term and in the presence of methanol. These

results suggest that simply shaking the aggregates in water or water/methanol is not affecting their stability. The action of a stirbar may abrade the aggregates (they appeared somewhat more rounded) but for the 2-3 hour period of stirring that will be used in gas purge experiments, over 90% remain in the same size class.

Table X: Water Stability of Clay Aggregates

<u>Material</u>	<u>Size Fraction(mm)</u>	<u>Treatment</u>	<u>Recovery</u>
HDTMA-SAC	1.0-2.0	3 days shaking in H ₂ O + 2.5 hrs stirring in gas purge system	90% >1.0 95% all
HDTMA-SAC	0.25-1.0	17 days shaking in H ₂ O 17 days shaking in 50:50 MeOH:H ₂ O	96.8% (0.25-1.0) 94.6%

Toluene, ethylbenzene and propylbenzene isotherms were measured on the soils, modified soils and modified clays. The resultant K_d s and their associated standard deviations appear in Table XI.

All of the isotherms were linear in the concentration range tested (r^2 ranged from 0.97 to 1.0).

The K_d values determined on natural soils were converted to K_{om} and compared to K_{om} values predicted by Equation (19) and to literature values (78) (Table XII). The measured and predicted values are in close agreement. The K_{om} values determined for the Capac A horizon consistently fall below those determined for the Colwood A horizon. This result suggests that the organic matter found in the Colwood soil provides a slightly better solvating medium for the nonpolar alkylbenzenes. The organic matter in the Colwood soil may be more hydrophobic in character. This observation is consistent with characteristics of organic matter that might result from the soil's drainage conditions. In Capac soil, which developed under less poorly drained conditions, organic matter would be expected to be more oxidized. Oxidation of the organic matter results in carboxyl, carbonyl

Table XI: Equilibrium Distribution Coefficients for Alkylbenzenes

<u>Sorbent</u>	<u>Distribution Coefficients (K_d)</u>		
	<u>toluene</u>	<u>ethylbenzene</u>	<u>propylbenzene</u>
Capac A horizon	1.11(0.09)	2.78(0.08)	9.2(0.5)
40% HDTMA-Capac A	3.59(0.11)	6.25(0.33)	18.8(0.5)
Colwood A horizon	3.20(0.19)	7.24(0.32)	18.6(0.5)
40% HDTMA-Colwood A	6.62(0.20)	20.9 (1.0)	38.8(1.1)
<u>HDTMA-SAC</u>			
<0.25 mm	42.5 (2.7)	92.6 (2.8)	285 (12)
0.25-1.0 mm	41.3 (2.4)	97.1 (1.8)	287 (14)
<u>HDTMA-SAz-1</u>			
<0.25 mm	369 (20)	ND	2510 (400)
0.25-1.0 mm	549 (12)	ND	2860 (470)
<u>OM Fractions</u>			
53-125 um	16.6 (2.2)	ND	116 (11)
250-500 um	21.8 (1.1)	ND	146 (15)

ND = not determined
Numbers in parentheses represent the standard deviation.

and alcoholic moieties that increase the polar character of the organic matter and decrease its solvating power for the nonpolar alkylbenzenes.

Table XII: Distribution Coefficients Normalized for Carbon Content

<u>Compound literature*</u>	<u>Capac A</u>	<u>Colwood A</u>	<u>$\log K_{om}$ predicted'</u>	
toluene	1.29	1.55	1.69	1.94'
ethylbenzene	1.68	1.91	2.07	1.98
propylbenzene	2.20	2.32	2.56	--

' calculated using $\log K_{ow} - \log K_{om}$ regression equation
' Chiou, C.T. 1988. *E,S&T*. 22: 298-303.

The effect of modifying the soils with HDTMA is to greatly enhance their sorptive capability. Figure 14 shows the isotherm of propylbenzene on the natural and modified Colwood. The modification increases K_d by 109%. Clearly, exchanging 40% of the CEC of the Colwood A horizon with HDTMA is having a profound effect on sorption of

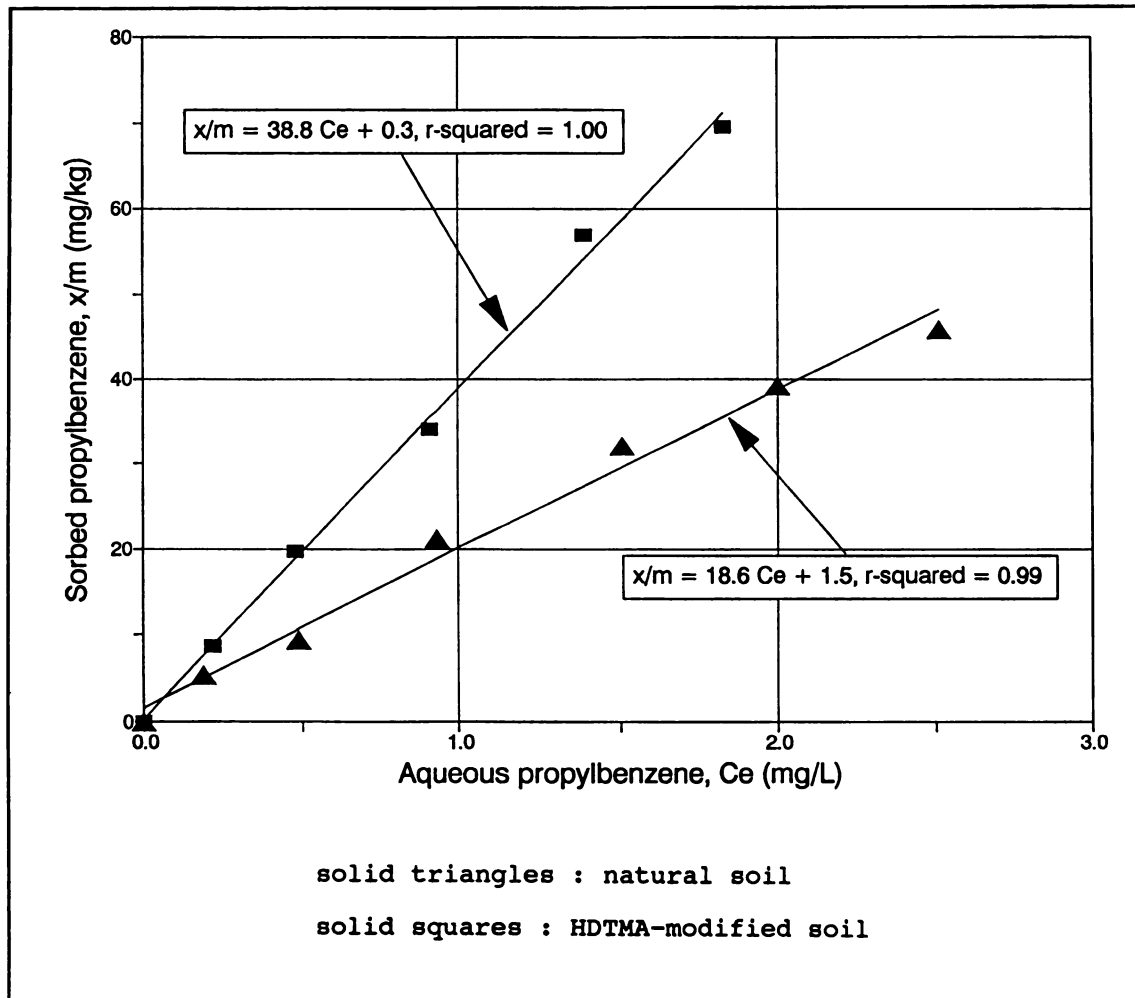


Figure 14: Propylbenzene Isotherms on Natural and Modified Colwood A

propylbenzene. Sorption of toluene and ethylbenzene is also enhanced on the modified Colwood. Similar enhancement of sorption is achieved by modifying the Capac A horizon (Table XI).

The cation exchange capacity of surface soils containing appreciable organic matter is derived from at least two main sources. The first class of exchange sites are associated with the natural clay minerals. The second class of sites are located in the organic matter. The contribution of organic matter to the exchange capacity of a surface soil can be from 25 to 90% (79). In modifying the Colwood soil, HDTMA exchanges for metal cations in both the clay minerals and the organic matter. The increase in sorptive capacity for alkylbenzenes reflects the combined effect of modifying both classes of sites.

To better understand how the modification is increasing sorptive capacity, the nature of the cation exchange sites was considered. Natural clay minerals carry permanent negative charge as a result of isomorphic substitution in their aluminosilicate lattice structure. In soils, this negative charge is satisfied by metal cations. The exchange reaction displaces these metal cations with HDTMA cations (Figure 15a) and creates an organic phase that acts as a partitioning medium for the alkylbenzene. This HDTMA-derived organic phase has a higher solvating power than natural organic matter for nonionic compounds (42,45).

Natural organic matter derives its cation exchange capacity from the carboxylate groups that reside within its structure. The charge on organic matter is not permanent and varies with pH. However, at the near-neutral pH of the Colwood and Capac soils, most of the carboxylate groups are deprotonated and interact with metal cations. An exchange of HDTMA for the metal cation (Figure 15b) is possible. The strength of the HDTMA-carboxylate complex is probably enhanced by van der Waals' interactions between hydrophobic regions in the organic matter and the long alkyl tail group of HDTMA. Exchange of HDTMA into natural organic matter increases the amount of organic material and the hydrophobicity in this sorptive phase.

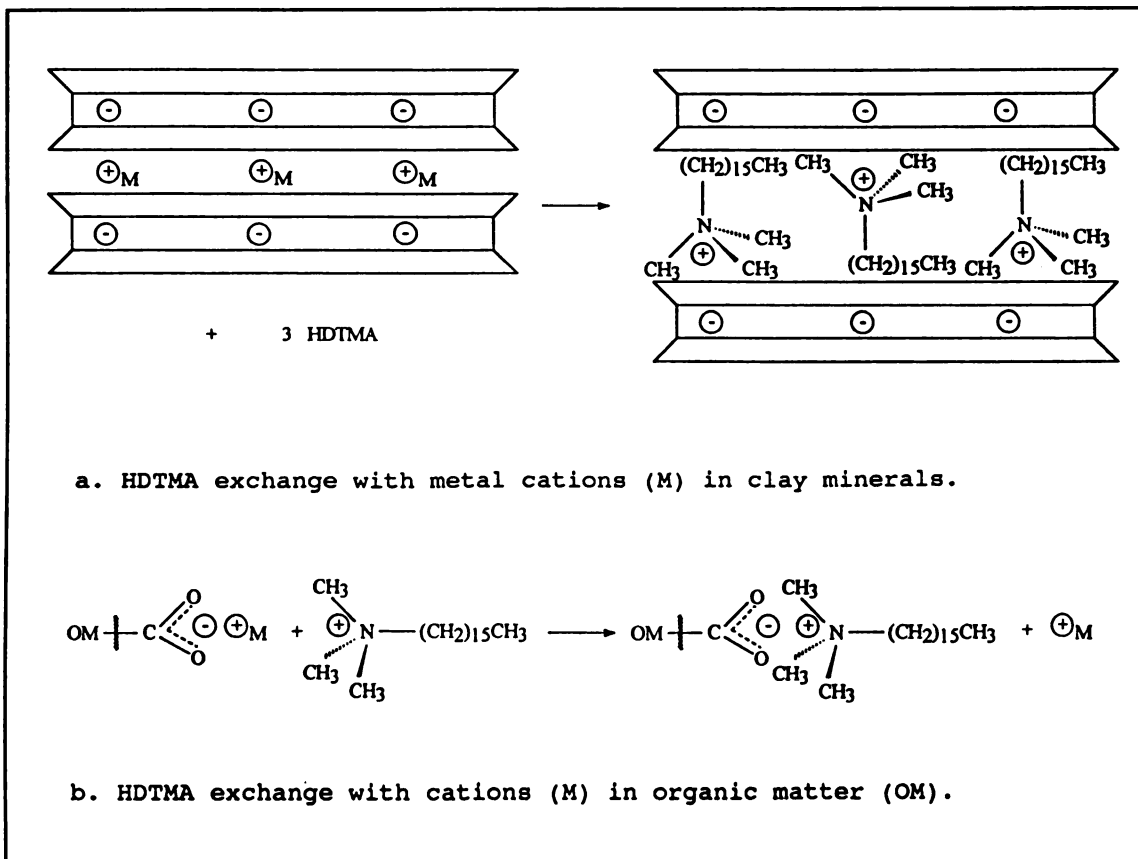


Figure 15: HDTMA Exchange Reactions in Soil

The exchange of HDTMA onto clay minerals and into natural organic matter both increase sorptive capacity. However, HDTMA exchanged onto clays represents addition of a new sorptive phase to the soil. Whereas, HDTMA exchanged into natural organic matter represents a modification of the existing sorptive phase in soil. These two processes may be intimately related in soils where clay minerals and organic matter are closely associated.

The equilibrium distribution coefficient for alkylbenzenes does not show any dependence on clay aggregate size (Table XI). The isotherms for propylbenzene on the two size fractions are coincident (Figure 16). The measured K_d s for toluene and ethylbenzene on the <0.25 mm and 0.25-1.0 mm fractions are also indistinguishable within the limits of experimental error. These results support the view that the sorption of nonionic organic compounds on these hydrophobic organoclays is a partitioning phenomenon (44,45). If the sorption were related to surface adsorption, the K_d should be higher on the small aggregates since they have a greater specific surface area. Since both aggregate size fractions have the same organic matter content (Table VIII), absorption or partitioning theory would predict the observed similarity in K_d . As expected, the K_d increases with decreasing water solubility of the alkylbenzene.

The organoclay distribution coefficients were normalized to organic matter content to yield K_{om} s (Table XIII). These K_{om} s allow evaluation of the effectiveness of the HDTMA-derived organic phase at solvating alkylbenzenes. The logarithm of K_{om} ($\log K_{om}$) for the organoclays derived from SAC falls between $\log K_{ow}$ (70) and $\log K_{om}$ for soils (78). The HDTMA-derived organic phase in SAC is better than soil organic matter at solvating alkylbenzenes but less effective than octanol. The $\log K_{om}$ s are close to those determined on a freeze-dried version of the same organoclay (49).

For the organoclays derived from SAz-1, the $\log K_{om}$ is greater than the $\log K_{ow}$, implying that this partitioning phase is stronger than octanol. The increase in $\log K_{om}$ between SAC and SAz-1 is related to



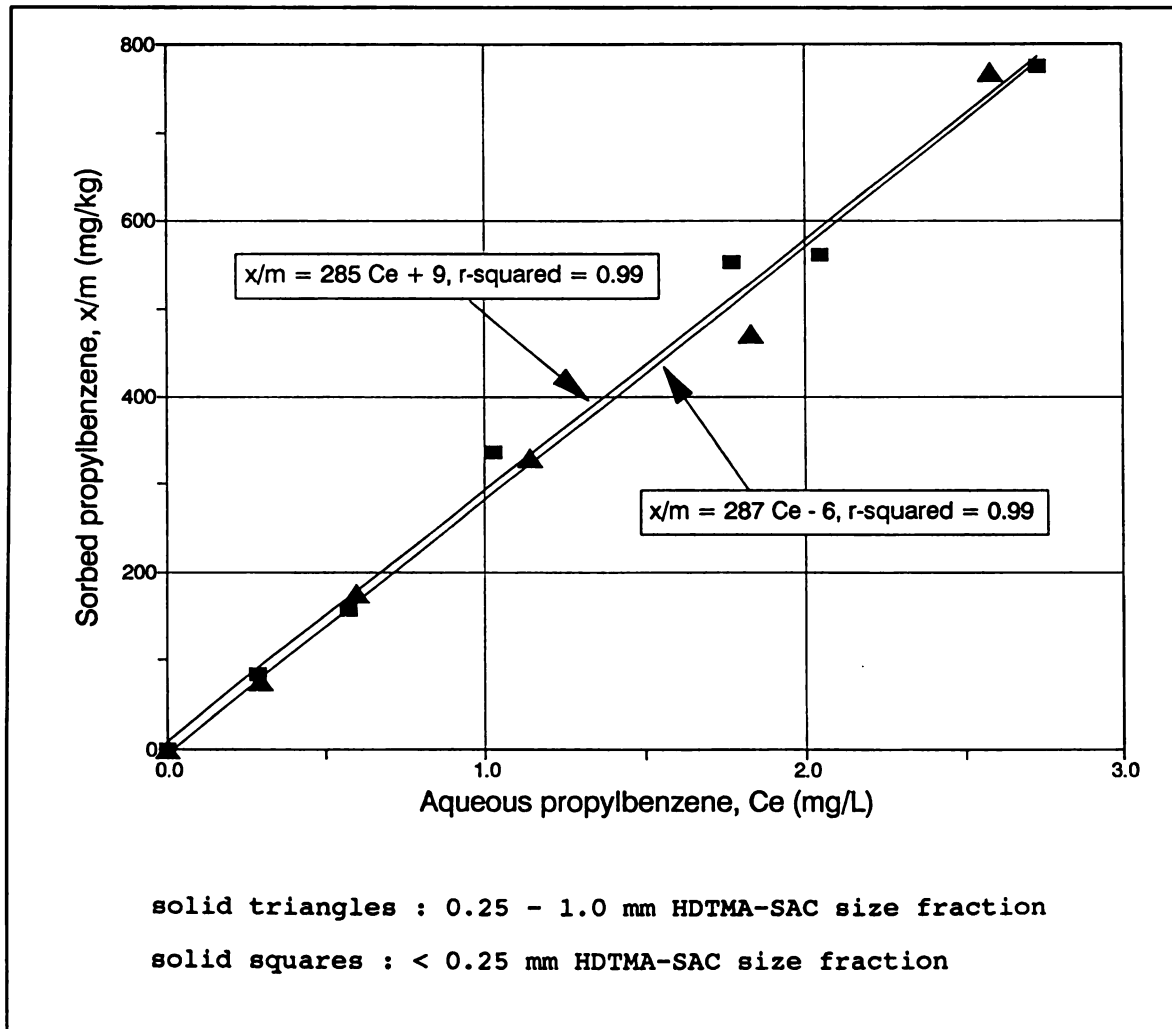


Figure 16: Propylbenzene Isotherms on HDTMA-SAC Aggregates

Table XIII: Sorptive Strength of HDTMA Phase in Organoclay

<u>Compound</u>	<u>log K_{ow}</u>	<u>clay (ag)</u>	<u>log K_{om} clay (fd)</u>	<u>soil</u>
HDTMA-SAC:				
toluene	2.73	2.32	2.50	1.94
ethylbenzene	3.15	2.67	2.78	1.98
propylbenzene	3.69	3.15	3.24	--
HDTMA-SAz:				
toluene	2.73	3.16, 3.32'	3.05	1.94
propylbenzene	3.69	3.99, 4.04	3.69	--
' Both size fractions are reported (<0.25 mm, 0.25-1.0 mm) ag = aggregate, fd = freeze-dried				

the structure of the interlamellar region. A paraffin-type complex is produced in the SAz, whereas a pseudotrimolecular arrangement occurs in SAC (49).

Table XIV: Sorptive Strength of OM Fractions

	log K _{om}	
	<u>toluene</u>	<u>propylbenzene</u>
Colwood A horizon (whole)	1.55	2.32
53-125 um SOM fraction	1.62	2.47
250-500 um SOM fraction	1.69	2.52

The log K_{om} for HDTMA-modified soils is intermediate between the log K_{om} of the natural soils and the log K_{om} for the organoclays (Table XV). As discussed earlier, the sorptive phase in the modified soils includes HDTMA-organic matter and HDTMA-natural clay complexes. Both of these types of phases (and, most likely, an intimate mixture of these complexes) enhance the solvating power of the sorptive medium. The presence of natural organic matter dilutes the HDTMA phase so that it is not as strong as the pure HDTMA phase in organoclays.

The organic matter fractions that were isolated from Colwood A horizon exhibit higher K_ds than the original soil. The K_ds were

Table XV: Sorptive Strength of Three Sorbent Types

	<u>toluene</u>	<u>log K_{om}</u> <u>ethylbenzene</u>	<u>propylbenzene</u>
Soils:			
Capac A	1.29	1.68	2.20
Colwood A	1.55	1.91	2.32
HDTMA-Soils:			
Capac A	1.73	1.97	2.45
Colwood A	1.75	2.25	2.52
HDTMA-Clays:			
<0.25 mm	2.33	2.67	3.15
0.25-1.0 mm	2.31	2.68	3.15

normalized to organic matter content to evaluate the sorptive strength of the organic matter in the size fractions relative to the whole soil (Table XV). The resultant log K_{om}s have been used to interpret the quality of the organic matter (80). The magnitudes of log K_{om} for both toluene and propylbenzene follow the order; 250-500 um fraction > 53-125 um fraction > whole soil. Since alkylbenzenes are nonpolar and, therefore, are expected to sorb most strongly in nonpolar sorbents, this trend suggests an inverse trend in SOM polarity. The implied trend in polarity is as follows; whole soil > 53-125 um fraction > 250-500 um fraction.

IV. Conclusions

In conclusion, HDTMA-modified soils and clays have been prepared and characterized. Two surface soils have proven to be stable and nonfoaming when modified with HDTMA at 40% of their CEC. Aggregates of an organoclay prepared from bentonite are stable in water. Even when subjected to prolonged stirring and shaking, recoveries of the aggregates exceed 90%.

The equilibrium sorptive behavior of these materials has been quantified. Isotherm experiments have shown that the HDTMA modification of soil surface horizons and clays enhances their sorptive strength. When normalized for organic matter content, organoclays are more

strongly sorptive than soils. The sorptive strength of modified soils is intermediate. The K_d s determined in these experiments will be used in modelling the behavior of these sorbents under kinetic conditions.



Endnotes - Chapters 1-3

1. Bailey, G.W. and J.L. White. 1970. Factors Influencing the Adsorption, Desorption, and Movement of Pesticides in Soil. *Residue Reviews*. 32: 29-92.
2. Schwarzenbach, R.P. and J. Westall. 1981. Transport of Nonpolar Organic Compounds from Surface Water to Groundwater. Laboratory Sorption Studies. *Environ. Sci. Technol.* 15(11): 1360-1367.
3. Valocchi, A.J. 1985. Validity of the Local Equilibrium Assumption for Modeling Sorbing Solute Transport Through Homogeneous Soils. *Water Resources Res.* 21(6): 808-820.
4. Steinberg, S.M., J.J. Pignatello and B.L. Sawhney. 1987. Persistence of 1,2-Dibromoethane in Soils: Entrapment in Intraparticle Micropores. *Environ. Sci. Technol.* 21: 1201-1208.
5. Scribner, S.L., T.R. Benzing, S. Sun and S.A. Boyd. 1992. Desorption and Bioavailability of Aged Simazine Residues from a Continuous Corn Field. *J. Environ. Qual.* 21(1): 115-120.
6. Karickhoff, S.W. 1980. Sorption Kinetics of Hydrophobic Pollutants in Natural Sediments. Ch. 11 in Contaminants and Sediments, vol. 2; Baker, R.A., Ed.; Ann Arbor Press: Ann Arbor, MI.
7. Pignatello, J.J. 1989. Sorption Dynamics of Organic Compounds in Soils and Sediments. Ch. 3 in Reactions and Movement of Organic Chemicals in Soils. Sawhney, B.L. and K. Brown, Eds. SSSA Special Publication 22. pp. 45-80.
8. Gschwend, P.M. and S. Wu. 1985. On the Constancy of Sediment-Water Partition Coefficients of Hydrophobic Organic Pollutants. *Environ. Sci. Technol.* 19(1): 90-96.
9. Hsu, T. and R. Bartha. 1974. Interaction of Pesticide-Derived Chloroaniline Residues with Soil Organic Matter. *Soil Sci.* 116(6): 444-452.
10. Parris, G.E. 1980. Covalent Binding of Aromatic Amines to Humates. 1. Reactions with Carbonyls and Quinones. *Environ. Sci. Technol.* 14(9): 1099-1106.
11. Saxena, A. and R. Bartha. 1983. Modeling of the Covalent Attachment of Chloroaniline Residues to Quinoidal Sites of Soil Humus. *Bull. Environ. Contam. Toxicol.* 30: 485-491.
12. Bollag, J., R.D. Minard, and S. Liu. 1983. Cross-Linkage between Anilines and Phenolic Humus Constituents. *Environ. Sci. Technol.* 17(2): 72-80.
13. Horzempa, L.M. and D.M. DiToro. 1983. The Extent of Reversibility of Polychlorinated Biphenyl Adsorption. *Water Res.* 17(8): 851-859.

14. Rao, P.S.C. and J.M. Davidson. 1980. In Environmental Impact of Nonpoint Source Pollution; Overcash, M.R. and J.M. Davidson, Eds. Ann Arbor Science: Ann Arbor, MI. pp. 23-67.
15. Brusseau, M.L., R.E. Jessup and P.S.C. Rao. 1991. Nonequilibrium Sorption of Organic Chemicals: Elucidation of Rate-Limiting Processes. *Environ. Sci. Technol.* 25(1): 134-142.
16. Brusseau, M.L. and P.S.C. Rao. 1990. Modelling Solute Transport in Structured Soils: A Review. *Geoderma.* 46: 169-192.
17. Brusseau, M.L. and P.S.C. Rao. 1989. Sorption Nonideality during Organic Contaminant Transport in Porous Media. *Crit. Rev. Env. Control.* 19(1): 33-99.
18. Tanford, C. 1980. The Hydrophobic Effect: Formation of Micelles and Biological Membranes, 2nd Ed. Wiley-Interscience.
19. Chiou, C.T., L.J. Peters, and V.H. Freed. 1979. A Physical Concept of Soil-Water Equilibria for Nonionic Organic Compounds. *Science.* 206: 831-832.
20. Karickhoff, S.W. 1984. Organic Pollutant Sorption in Aquatic Systems. *J. Hydraul. Eng.* 110(6): 707-735.
21. Roberts, P.V., M.N. Goltz and D.M. Mackay. 1986. A Natural Gradient Experiment on Solute Transport in a Sand Aquifer 3. Retardation Estimates and Mass Balances for Organic Solutes. *Water Resources Res.* 22(13): 2047-2058.
22. Steen, W.C., D.F. Paris, and G.L. Baughman. 1980. Effects of Sediment Sorption on Microbial Degradation of Toxic Substances. Ch. 23 in Contaminants and Sediments, vol. 1. R.A. Baker, Ed. Ann Arbor Science. Ann Arbor, MI.
23. Ogram, A.V., R.E. Jessup, L.T. Lou, and P.S.C. Rao. 1985. Effects of Sorption on Biological Degradation Rates of (2,4-Dichlorophenoxy)acetic Acid in Soils. *Appl. Environ. Microbiol.* 49: 582-587.
24. Shimp, R.J. and R.L. Young. 1988. Availability of Organic Chemicals for Biodegradation in Settled Bottom Sediments. *Ecotoxicol. Environ. Safety.* 15: 31-45.
25. Racke, K.D. and E.P. Lichtenstein. 1985. Effects of Soil Microorganisms on the Release of Bound ¹⁴C Residues from Soils Previously Treated with [¹⁴C]Parathion. *J. Agric. Food Chem.* 33: 938-943.
26. Guerin, W.F. and S.A. Boyd. 1992. Differential Bioavailability of Soil-Sorbed Naphthalene to Two Bacterial Species. *App. Env. Microbiology.* 58(4): 1142-1152.
27. Fischer, H.B., E.J. List, R.C.Y. Koh, J. Imberger, and N.H. Brooks. 1979. Shear Flow Dispersion, Chapter 4 in Mixing in Inland and Coastal Waters. Academic Press, Inc.: New York. pp. 80-87.
28. Leenheer, J.A. and J.L. Ahlrichs. 1971. A Kinetic and Equilibrium Study of the Adsorption of Carbaryl and Parathion upon Soil Organic Matter Surfaces. *Soil Sci. Soc. Amer. Proc.* 35: 700-705.

29. Wu, S. and P.M. Gschwend. 1986. Sorption Kinetics of Hydrophobic Organic Compounds to Natural Sediments and Soils. *Environ. Sci. Technol.* 20(7): 717-725.
30. Ball, W.P. and P.V. Roberts. 1991. Long-Term Sorption of Halogenated Organic Chemicals by Aquifer Material. 2. Intraparticle Diffusion. *Environ. Sci. Technol.* 25: 1237-1249.
31. Freeman, D.H. and L.S. Cheung. 1981. A Gel Partition Model for Organic Desorption from a Pond Sediment. *Science.* 214: 790-792.
32. Conversations with P.S.C. Rao. 1990.
33. Brusseau, M.L. and P.S.C. Rao. 1989. The Influence of Sorbate-Organic Matter Interactions on Sorption Equilibrium. *Chemosphere.* 18: 1691-1706.
34. Bailey, G.W. and J.L. White. 1964. Review of Adsorption and Desorption of Organic Pesticides by Soil Colloids, with Implications Concerning Pesticide Bioactivity. *J. Agr. Food Chem.* 12: 324-332.
35. Lambert, S.M. 1968. Omega, a useful index of soil sorption equilibria. *J. Agr. Food Chem.* 16: 340-343.
36. Briggs, G.G. 1969. Molecular structure of herbicides and their sorption by soils. *Nature.* 223: 1288.
37. Chiou, C.T., L.J. Peter, and V.H. Freed. 1979. A Physical Concept of Soil-Water Equilibria for Nonionic Organic Compounds. *Science.* 206: 831-832.
38. Hansch, C., J.E. Quinlan, and G.L. Lawrence. 1968. The Linear Free-Energy Relationship between Partition Coefficients and the Aqueous Solubility of Organic Liquids. *J. Org. Chem.* 33: 347-350.
39. Chiou, C.T., P.E. Porter, and D.W. Schmedding. 1983. Partition Equilibria of Nonionic Organic Compounds between Soil Organic Matter and Water. *Environ. Sci. Technol.* 17: 227-231.
40. Karickhoff, S.W., D.S. Brown, and T.A. Scott. 1979. Sorption of Hydrophobic Pollutants on Natural Sediments. *Water Res.* 12: 241-248.
41. Boyd, S.A., J. Lee, and M. Mortland. 1988. Attenuating Organic Compound Mobility by Soil Modification. *Nature.* 333: 345-347.
42. Lee, J.F., J. Crum, and S.A. Boyd. 1989. Enhanced Retention of Organic Contaminants by Soils Exchanged with Organic Cations. *Environ. Sci. Technol.* 23: 1365-1372.
43. Mortland, M.M., S. Shaobai, and S.A. Boyd. 1986. Clay-Organic Complexes as Adsorbents for Phenol and Chlorophenols. *Clays and Clay Minerals.* 34: 581-585.
44. Boyd, S.A., S. Shaobai, J.F. Lee, and M.M. Mortland. 1988. Pentachlorophenol Sorption by Organo-Clays. *Clays and Clay Minerals.* 36: 125-130.
45. Boyd, S.A., M.M. Mortland, and C.T. Chiou. 1988. Sorption Characteristics of Organic Compounds on Hexadecyltrimethylammonium Smectite. *Soil Sci. Soc. Amer. J.* 52: 652-657.

46. Lee, J.F., M.M. Mortland, C.T. Chiou, and S.A. Boyd. 1989. Shape Selective Adsorption of Aromatic Molecules from Water by Tetramethylammonium-Smectite. *J. Chem. Soc. Faraday Trans. I.* 85: 2953-2962.
47. Lee, J.F., M.M. Mortland, C.T. Chiou, D.E. Kile, and S.A. Boyd. 1990. Adsorption of Benzene, Toluene, and Xylene by Two Tetramethylammonium Smectites of Different Charge Densities. *Clays and Clay Minerals.* 38: 113-120.
48. Jaynes, W.F. and S.A. Boyd. 1990. Trimethylphenylammonium-Smectite as an Effective Adsorbent of Water-Soluble Aromatic Hydrocarbons. *J. Air Waste Manage. Assoc.* 40: 1649-1653.
49. Jaynes, W.F. and S.A. Boyd. 1991. Clay Mineral Type and Organic Compound Sorption by Hexadecyltrimethylammonium-Exchanged Clays. *Soil Sci. Soc. Amer. J.* 55(1): 43-48.
50. Jaynes, W.F. and S.A. Boyd. 1991. Hydrophobicity of Siloxane Surfaces in Smectites as Revealed by Hydrocarbon Adsorption from Water. *Clays and Clay Minerals.* 39(4): 428-436.
51. Boyd, S.A., W.F. Jaynes, and B.S. Ross. 1991. Immobilization of Organic Contaminants by Organo-Clays: Application to Soil Restoration and Hazardous Waste Containment. Ch. 11 in Organic Substances and Sediments in Water. CRC Press. Boca Raton, FL.
52. Burris, D.R. and C.P. Antworth. 1992. In situ Modification of an Aquifer by a Cationic Surfactant to Enhance Retardation of Organic Contaminants. *J. Contam. Hydrol.* 10: 325-337.
53. Khan, S.U. 1973. Equilibrium and Kinetic Studies of the Adsorption of 2,4-D and Picloram on Humic Acid. *Can J. Soil Sci.* 53: 429-434.
54. McCall, P.J. and G.L. Agin. 1985. Desorption Kinetics of Picloram as Affected by Residence Time in Soil. *Environ. Toxicol. Chem.* 4: 37-44.
55. Walters, R.E. and A. Guiseppi-Elie. 1988. Sorption of 2,3,7,8-Tetrachlorodibenzo-p-dioxin to Soils from Water/Methanol Mixtures. *Environ. Sci. Technol.* 20: 717-725.
56. Rao, P.S.C., J.M. Davidson, R.E. Jessup and H.M. Selim. 1979. Evaluation of Conceptual Models for Describing Nonequilibrium Adsorption-Desorption of Pesticides During Steady-flow in Soils. *Soil Sci. Soc. Amer. Proc.* 43: 22-28.
57. Miller, C.T. and W.J. Weber. 1986. Sorption of Hydrophobic Organic Pollutants in Saturated Soil Systems. *J. Contam. Hydrol.* 1: 243-261.
58. Southworth, G.R., K.W. Watson, and J.L. Keller. 1987. Comparison of Models that Describe the Transport of Organic Compounds in Macroporous Soil. *Environ. Toxicol. Chem.* 6: 251-257.
59. Lee, L.S., P.S.C. Rao, M.L. Brusseau, and R.A. Ogwada. 1988. Nonequilibrium Sorption of Organic Contaminants during Flow through Columns of Aquifer Materials. *Environ. Toxicol. Chem.* 7: 779-793.
60. Karickhoff, S.W. 1980. Sorption Kinetics of Hydrophobic Pollutants in Natural Sediments. in Contaminants and Sediments, vol. 2, Baker, R.A., Ed.; Ann Arbor Press: Ann Arbor, MI, 193-205.

61. Karickhoff, S.W. and K.R. Morris. 1985. Sorption Dynamics of Hydrophobic Pollutants in Sediment Suspensions. *Environ. Toxicol. Chem.* 4: 469-479.
62. Oliver, B.G. 1985. Desorption of Chlorinated Hydrocarbons from Spiked and Anthropogenically Contaminated Sediments. *Chemosphere.* 14: 1087-1106.
63. Coates, J.T. and A.W. Elzerman. 1986. Desorption Kinetics for Selected PCB Congeners from River Sediments. *J. Contamin. Hydrol.* 1: 191-210.
64. Brusseau, M.L., R.E. Jessup, and P.S.C. Rao. 1990. Sorption Kinetics of Organic Chemicals: Evaluation of Gas-Purge and Miscible Displacement Techniques. *Environ. Sci. Technol.* 24(5): 727-735.
65. Lee, L.S., P.S.C. Rao, and M.L. Brusseau. 1991. Nonequilibrium Sorption and Transport of Neutral and Ionized Chlorophenols. *Environ. Sci. Technol.* 25: 722-729.
66. Brusseau, M.L., A.L. Wood, and P.S.C. Rao. 1991. Influence of Organic Cosolvents on the Sorption Kinetics of Hydrophobic Organic Chemicals. *Environ. Sci. Technol.* 25: 903-910.
67. Mackay, D. and W.Y. Shiu. 1981. A Critical Review of Henry's Law Constants for Chemicals of Environmental Interest. *J. Phys. Chem. Ref. Data.* 10(4): 1175-1199.
68. Hwang, Y., J.D. Olson, and G.E. Keller II. 1992. Steam Stripping for Removal of Organic Pollutants from Water. 2. Vapor-Liquid Equilibrium Data. *Ind. Eng. Chem. Res.* 31(7): 1759-1768.
69. Lyman, W.J., W.F. Reehl, and D.H. Rosenblatt. 1990. Handbook of Chemical Property Estimation Methods. American Chemical Society, Washington, DC; p. 15-11.
70. Verschueren, K. 1983. Handbook of Environmental Data on Organic Chemicals, 2nd Ed. Van Nostrand Reinhold Co. New York.
71. Mackay, D., W.Y. Shiu and R.P. Sutherland. 1979. Determination of Air-Water Henry's Law Constants for Hydrophobic Pollutants. *E,S&T.* 13(3): 333-337.
72. Perlinger, J.A., S.J. Eisenreich, and P.D. Capel. 1993. Application of Headspace Analysis to the Study of Sorption of Hydrophobic Organic Chemicals to Al₂O₃. *Environ. Sci. Tech.* 27: 928-937.
73. Straszewski, M. 1993. Colwood A Horizon Organic Fractionation and Isotherm Experiments. CSS 490 Independent Study.
74. Steelink, C. 1985. Implications of Elemental Characteristics of Humic Substances. Ch. 18 in Humic Substances in Soil, Sediment and Water: Geochemistry, Isolation, and Characterization, Aiken, G.R., D.M. McKnight, R.L. Wershaw and P. MacCarthy, Eds. Wiley-Interscience.
75. Xu, Shihe and S.A. Boyd. 199 . Adsorption and Desorption of Hexadecyltrimethylammonium in Subsoils Containing Vermiculite. 2. Hydrophobic Bonding. in press.
76. Lagaly, G. 1992. Layer Charge Determination by Alkylammonium Ions. p. 19. as part of Clay Mineral Society Workshop: Layer Charge Characteristics of Clays (Minneapolis, MN).

77. Laird, D.A., A.D. Scott, and T.E. Fenton. 1987. Interpretation of Alkylammonium Characterization of Soil Clays. *Soil Sci. Soc. Amer. J.* 51: 1659-1663.
78. Chiou, C.T., D.E. Kile and R.L. Malcolm. 1988. Sorption of Vapors of Some Organic Liquids on Soil Humic Acid and Its Relation to Partitioning of Organic Compounds in Soil Organic Matter. *Environ. Sci. Technol.* 22: 298-303.
79. Stevenson, F.J. 1982. Humus Chemistry. John Wiley & Sons. New York.
80. Rutherford, D.W., C.T. Chiou, and D.E. Kile. 1992. Influence of Soil Organic Matter Composition on the Partition of Organic Compounds. *Environ. Sci. Technol.* 26: 336-340.

Chapter 4: HDTMA-modified Clays and Soils - Kinetic Behavior in the Gas Purge System

I. Introduction

Modification of clays and soils with tetraalkylammonium cations has been shown to greatly increase their sorptive capacity for nonionic organic compounds through enhanced sorption (NOCs) (1,2,3,4,5,6,7, 8,9,10). The in situ modification of geological materials could reduce the transport potential of organic contaminants (11). Also, this technology might be coupled with biodegradation to remediate soils and geologic materials contaminated with organic pollutants (12).

In order to successfully couple sorption with biodegradation, a greater understanding of the bioavailability of the sorbed contaminants is necessary. Bioavailability is controlled by the degree to which a microbial community can degrade sorbed contaminants and by the kinetics of exchange between sorbed and solubilized contaminant pools.

To date, studies of organic contaminant sorption on organoclays and modified soils have focused on equilibrium behavior. The equilibrium sorption of several alkylbenzenes on phenyltrimethylammonium- and hexadecyltrimethylammonium(HDTMA)-modified clays was studied by measuring sorption isotherms (8,9). Isotherms of several NOCs were reported for soils modified with various tetraalkylammonium cations (6).

Biodegradation of sorbed contaminants and transport through soils are dynamic processes. If desorption is a prerequisite for biodegradation, sorption rates, not sorption equilibrium, may control contaminant behavior under some conditions. For this reason, sorption kinetics in soils has recently become a field of intense study. This

study seeks to describe the effect of exchanging soils and clays with HDTMA on the kinetics of interchange between sorbed and solubilized alkylbenzenes in some modified soils and clays. The sorption kinetics are studied in the absence of biodegrading organisms, using a gas purge system which has been described previously (13).

Sorption kinetics in soils have been studied by using several methods including batch experiments (14,15,16), column experiments (17,18,19,20) and gas purge experiments (21,22,23,24,25,26). When sorption coefficients are high and the solutes are volatile, gas purge experiments are most appropriate for studying the kinetics (26).

II. Materials and Methods

Soils and Clays:

Two soil A horizons and two pure clays were used in this study. Some properties of these materials are summarized in Table XVI.

Table XVI: Properties of Soils and Clays

Property	Capac A horizon	Colwood A horizon	SAC	SAz-1
% org. C	3.46	5.36	-	-
CEC (meq/100g)	12.2	21.6	88	130
% sand	44	41	-	-
% silt	36	35	-	-
% clay	20	24	100	100
clay mineralogy:				
smectite	-- \		low charge	high charge
chlorite			montmorillonite	smectite
vermiculite	XXXX			
mica	XX\			
kaolinite	XX\			
quartz	\			
source	Ingham Co., Mich.	Ingham Co., Mich.	American Colloid	Clay Mineral Society
\ = approximately 5% of clay fraction (<2 um)				
X = approximately 10% of clay fraction				
Clay mineralogy from Haile-Miriam, S. 1990. PhD thesis.				

HDTMA-Clay Preparation:

A Wyoming bentonite (SAC) was obtained from American Colloid. An Arizona smectite (SAz-1) was obtained from the Source Clay Repository (Clay Mineral Society, Columbia, MO). The clays were wet sedimented to separate the <2 um fraction. The SAC sample was used without further modification. The SAz-1 sample was Na-saturated by washing three times with 1 M NaCl, acidified to pH 4. A suspension of each clay (approx. 10 g/L) was prepared in deionized water. The concentration of the suspension was determined by evaporating a subsample to dryness.

The exchange reaction was carried out in a 2L Erlenmeyer flask containing a magnetic stirbar. Sufficient hexadecyltrimethylammonium (HDTMA) bromide to satisfy one equivalent of the clay's cation exchange capacity (CEC) was dissolved in a minimum volume of deionized water. The HDTMA solution was poured into the stirring clay suspension. The mixture was allowed to stir for 2 hours.

The flocculated HDTMA-clay was allowed to settle and the supernatant was decanted. The remaining slurry was washed several times with deionized water. After each wash, the slurry was centrifuged at 500 rpm for 20 minutes. The washed clay was stored in a 1L polyethylene bottle. Several batches of modified clay were combined at this point.

The modified clays were oven dried. To remove the majority of the water prior to drying, the clay slurry was poured onto a sheet of filter paper (Whatman #1) which sat on top of several paper towels. This dewatering step produced a thick paste which was transferred to watch glasses and dried in the oven at 100 degrees Centigrade. Upon drying, the clays cracked into thick flakes. The dried clays were ground using a mortar and pestle. The ground clays were separated into two size fractions; 0.25 - 1.0 mm and < 0.25 mm. The clays were stored in amber glass jars.



HDTMA-Soil Preparation:

The A horizon from both Colwood and Capac soil was collected, air-dried, and passed through a 1 mm sieve. Fifty grams Colwood A (or 80 grams Capac A) horizon were weighed into a 1000 mL Erlenmeyer flask. 500 mL of deionized water were added to the flask. A glass stirbar was used to mix the soil and water.

Sufficient HDTMA bromide to satisfy the desired percentage of the soil CEC was dissolved in another 500 mL of deionized water. The HDTMA solution was added to the flask and mixed with the soil for one hour.

The mixture was vacuum filtered (Whatman #1, 12 cm). Complete transfer of the solids to the filter was accomplished with a minimal amount of water (<100mL). The filter cake was placed on paper towels and allowed to air dry for several days. A spatula was used to break apart the soil during drying. Several batches of each dried soil were combined and stored in a glass jar.

Organic Carbon Purification and Fractionation:

A purification and separation of organic matter from Colwood A horizon was performed (27). Air-dried Colwood A horizon (200 g) was added to a sealable 1 L polypropylene bottle. The bottle was filled with a 5% solution of sodium hexametaphosphate in deionized water (Millipore MilliQ). The bottle was sealed and placed on a rotary shaker for 24 hours.

After shaking, the mixture was transferred to a continuous flow separation system. A density separation was performed by vortexing the solution in a column. The lightest material passed through the column into a series of sieves. The sieve trays (500 um, 250 um, 125 um, and 53 um) collected various sizes of the soil solids.

The size fractions were harvested from the trays and centrifuged to remove excess solution. The solids were freeze dried and stored in polypropylene bottles.

Organic Carbon Determinations:

Organic carbon content was determined for the soils, modified soils and modified clays by combustion (Dohrmann DC-190 with 183 Boat Sampling Module). As suggested by the instrument manufacturer, sucrose solutions acidified with phosphoric acid were used as standards (28). At least five replicate analyses of each sample were performed.

Gas Purge Experimental Procedure:

Each gas purge experiment involved three steps; the setup and equilibration, the desorption run, and the data analysis. All of the desorption experiments were carried out in 250 mL roundbottom flasks that had been fitted with an injection port (reaction flask).

Two reaction flasks were used in the setup and equilibration step; the experiment flask, containing sorbent, and a no-sorbent control flask. Sufficient sorbent (soil, modified soil, or modified clay) was added to the experiment flask to sorb 20-30% of the injected alkylbenzene. The air-dried sorbent was weighed directly into a dry reaction flask. An aqueous matrix solution (soils: 0.01 N CaCl_2 , 0.5% HgCl_2 , clays: Millipore water) was added to the flask to bring the total volume to 200 mL. A glass stirbar (Fischer Scientific 09-311-7) was placed in the bottom of the flask. At this point, the flask was fully sealed by fitting the injection port with a Teflon-lined septum and a cap with hole and placing a ground glass stopper in the neck of the flask. After sealing the flask, a measured volume of alkylbenzene stock solution was introduced through the injection port.

Stock solutions of toluene, ethylbenzene and propylbenzene were prepared by equilibrating the neat alkylbenzene with Millipore water in a 500 mL amber glass bottle for several days. Whenever the alkylbenzene-saturated aqueous solution was withdrawn from the flask, a Gastight syringe (Hamilton Series 1000) was used to penetrate the overlying organic phase. Precautions were taken to avoid capturing any

neat organic liquid in the syringe.

Except for the absence of sorbent, setup of the control flask was identical to the experiment flask. Both of these reaction flasks were placed on a rotary shaker for 48-72 hours to reach sorption equilibrium.

The next step was to run the desorption experiment. With the gas purge system (see 13 for a more detailed description of the MSU Gas Purge System) in the purge mode, baselines were established at several attenuations using a reaction flask containing only matrix solution. A coarse adjustment of flow was made using the metering valve upstream from the flask. Fine adjustment and detector flow were controlled using the two downstream metering valves.

The experiment flask was removed from the shaker and, with flow directed through flask 1, inserted into the gas purge apparatus at the flask 2 position. Stirring was initiated, the system was switched into the recirculate mode (closed) and, using the flask selection switch, flow was directed through the experiment flask. Approximately 10 minutes of constant detector signal were recorded to ensure that the system was free of leaks.

To initiate the purge portion of the experiment, the system was switched into the purge mode. Readings of flow, attenuation/range settings and chart speed were written directly on the chart. Overall flow was measured using a bubble flowmeter. Detector flow was read directly from the ball flowmeter. The water bath temperature was also recorded periodically.

Attenuation/range settings were adjusted to keep the signal on scale. When the signal had decayed to the baseline, the run was ended. Another set of baseline readings were recorded to determine if any baseline drift had occurred during the experiment.

The purge run for the control flask was collected immediately before or after the experiment flask, using the above procedure.

Between purge runs, the system was dried by running the incoming air through a Drierite drying tube. The activated carbon in the intake filter was replaced daily.



Sorption Isotherms:

Batch equilibrium sorption isotherms of alkylbenzenes on soils, modified soils and modified clays were determined by difference between initial and final aqueous phase concentrations. To minimize the error in this type of experiment, a ratio of sorbent mass, m , to solution volume, V , that resulted in a 50% reduction ($x = 0.5$) in aqueous concentration was used. To determine the mass of soil to use for a given isotherm, an approximate distribution coefficient, K_d , is necessary. For soils, an approximate K_d was estimated from literature values of the organic-matter-normalized distribution coefficient, K_{om} , and the fraction of organic matter, f_{om} (Figure 19) using Equation (24) (29). For the modified soils and clays, a range-finding experiment was performed to find an approximate K_d .

$$K_d = f_{om} * K_{om} \quad (24)$$

Range-finding experiments were performed by adding different amounts of the modified soil or clay to three centrifuge tubes (25 mL Corning Corex). 25 mL of matrix solution were pipetted into each tube. At the same time, a fourth tube was filled with 25 mL of the matrix solution, which served as a no-soil control. The matrix solution for isotherms and range-finding experiments of the soils and modified soils was the same as for the gas purge experiments. All four tubes were fitted with Teflon-lined septa (Thomas Scientific 9711D45) and caps with a 5/16" hole. A syringe was used to introduce the same volume of alkylbenzene stock solution into each tube. The tubes were placed on a shaker for 24 hours.

After the equilibration period, the tubes were centrifuged (Sorvall RC5C with Model SS34 rotor) at 8000 rpm for 20 minutes. Five scintillation vials (Research Products International 121000) containing 10 mL carbon disulfide were chilled in a freezer for several hours. A



Gastight syringe was used to withdraw 5.0 mL of the supernatant from the centrifuge tube. The supernatant was injected into the chilled CS₂ for extraction. Each scintillation vial was quickly recapped to minimize volatilization losses. The extraction vials were allowed to warm to room temperature and shaken occasionally to promote the extraction of the alkylbenzene.

Two crimp seal vials (Supelco 3-3123) were filled with the CS₂ extract from each scintillation vial. The fifth scintillation vial provided a blank. The vials were analyzed for the alkylbenzene using gas chromatography (GC). A one-point determination of the K_d for each tube can be made by using a ratio of the soil-containing and soil-free GC peak areas. This ratio is equivalent to the alkylbenzene concentration ratio and can be substituted for the quantity, $1-x$, in Equation (25).

$$m = \frac{x \cdot V}{K_d (1 - x)} \quad (25)$$

With an approximate K_d in hand, an accurate isotherm experiment can now be performed. Twelve clean, dry centrifuge tubes were placed in a tube rack. An amount of sorbent necessary to reduce the aqueous phase concentration by 50% (as calculated using Equation (25)) was weighed into six of these tubes. 25.0 mL of the matrix solution was pipetted into all twelve of the tubes. The tubes were fitted with septa and capped as above. Each tube was inverted several times to insure that the sorbent was fully wetted.

Each sorbent-containing tube was paired with a sorbent-free tube. Each tube pair represents one point on the isotherm. Different initial concentrations were produced in each tube pair by varying the amount of stock solution injected. For example, toluene isotherms were set up with 50, 100, 200, 300, 400, and 500 μ L of stock solution. The initial concentrations ranged over an order of magnitude and encompassed the initial concentration to be used in the gas purge experiments.



The tubes were placed on a rotary shaker for 24 - 48 hours, centrifuged, extracted and analyzed for final aqueous alkylbenzene concentrations as above. A linear form of the Freundlich equation (Equation (26)) was fit to the data to yield the distribution coefficient.

$$\frac{x}{m} = K_d C_e \quad (26)$$

Data Analysis:

A bicontinuum model has been used by others (17,21) to describe NOC sorption kinetics in soils. This model is appropriate when detailed information about the structure of the sorbent is not available (26).

Briefly, the bicontinuum model is a mass-transfer model that divides the sorbent into two regions, a region (S_1) in rapid equilibrium with the soil solution (C) and a region (S_2) governed by slow kinetics (Figure 17). The relative distribution of these regions is defined by F , the fraction of solute in S_1 . The kinetically controlled process, mass transfer between S_1 and S_2 , is described by first order rate constants, k_1 and k_2 .

The bicontinuum model collapses to one of two submodels at extreme values of F . When $F = 0$, there are no rapidly equilibrated sites in the sorbent. Exchange between solution and sorbent is governed by the rate constants, k_1 and k_2 , alone. This submodel of the bicontinuum model is a one-box model (Figure 18a). The rate constants are related to one another by the equilibrium constant, K_d .

When $F = 1$, all sorbent sites are rapidly equilibrated. The distribution of NOC between sorbent and solution is governed by the equilibrium constant, K_d . This submodel of the bicontinuum model is the equilibrium model (Figure 18b).



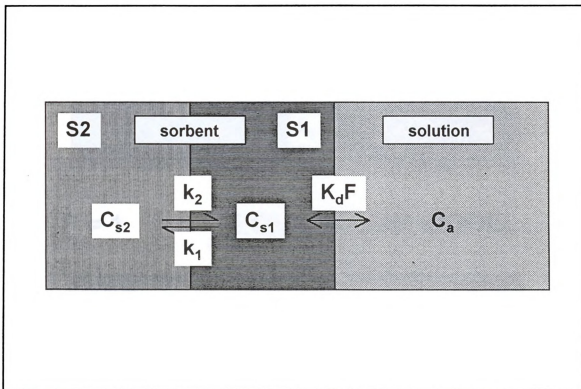


Figure 17: The Bicontinuum Model



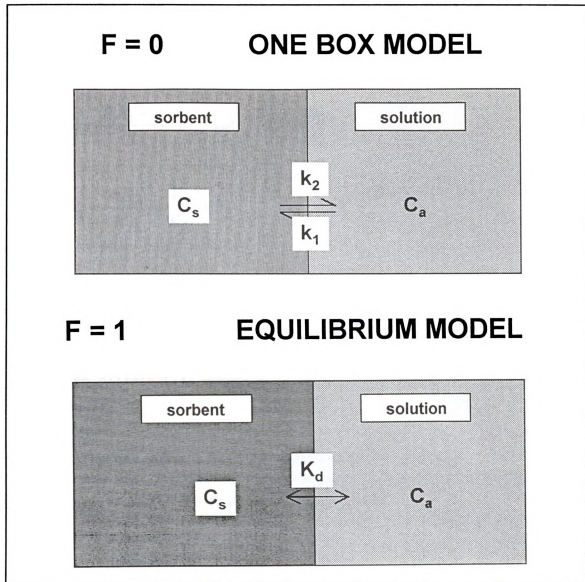
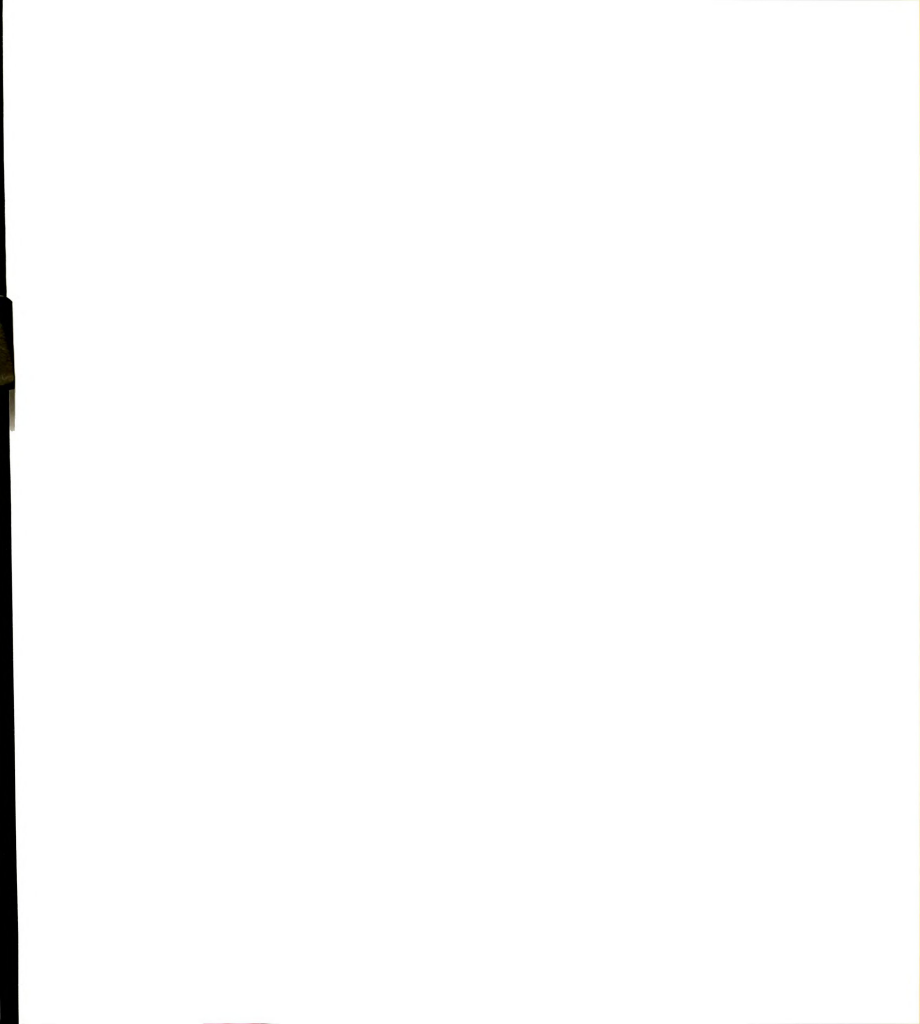


Figure 18: Submodels of the Bicontinuum Model



A solution of the bicontinuum model to be used for gas purge experiments has been derived (30) following the derivation of Brusseau (26). A second-order, linear, constant coefficient differential

$$\frac{d^2M}{dt^2} + P \frac{dM}{dt} + QM = 0$$

$$P = \frac{R_t k_2 + q}{R_i} \quad \text{and} \quad Q = \frac{q k_2}{R_i} \quad (27)$$

$$R_t = \frac{mK_d}{K_H} + \frac{V_a}{K_H} + V_g \quad \text{and} \quad R_i = \frac{FmK_d}{K_H} + \frac{V_a}{K_H} + V_g$$

equation describes the system (Equation (27)). System constants include the volume of aqueous solution, V_a , the volume of gas, V_g , the gas flow rate, q , and the Henry's Law constant, K_H . An analytical solution to the system differential equation is obtained by making the following assumptions:

1. the gas purge system is closed prior to purging,
2. the distribution of solute between aqueous and sorbed states is at equilibrium prior to purging, and
3. Henry's Law (Equation (28)) describes the distribution of solute between aqueous and gaseous states at all times during purging (Equation (29)).

$$C_g = K_H C_a \quad (28)$$

Equation (29) contains two time-dependent exponential terms. These terms express the decay of the solute concentration in the gas phase as



$$RMP = 1 + \frac{L_2 + \frac{q}{R_t}}{L_1 - L_2} e^{L_1 t} - \frac{L_1 + \frac{q}{R_t}}{L_1 - L_2} e^{L_2 t} \quad (29)$$

$$L_1 = \frac{-P + \sqrt{P^2 - 4Q}}{2} \quad \text{and} \quad L_2 = \frac{-P - \sqrt{P^2 - 4Q}}{2}$$

the purge time increases from 0 to infinity. M_c/M_T , the relative mass purged (RMP) from the system, goes from 0 to 1 during the course of the purging experiment.

Figure 19a shows an example of the raw data obtained during a purge of ethylbenzene from the control flask. The detector signal decreases curvilinearly with time as ethylbenzene is purged out of the system. Since the detector is responding linearly to concentration in the gas phase (13), the area under the curve is proportional to the mass removed from the system. To convert the raw data to M_c/M_T versus time, the area at selected time points is normalized to total area. The ratio of the area at a given time to the total area is a measure of the RMP. Using Figure 19a as an example, RMP at ten minutes is the area to the left of the dotted line divided by the total area. In this case, RMP equals 0.67. The plot of RMP versus time will be referred to as a purge curve (Figure 19b).

The gas purge data was fit to the bicontinuum model (Equation (29)) using a nonlinear curve-fitting program, SIGMAPLOT (Jandel Scientific). The control experiment was used to determine the Henry's Law constant. With all other variables independently determined, SIGMAPLOT fit values for the desorption rate constant, k_2 , and the fraction of fast sites, F , by employing the Marquardt-Levenberg algorithm to minimize the error between the data and the system of equations for the bicontinuum model. The error associated with the fitted variables was also determined by SIGMAPLOT.



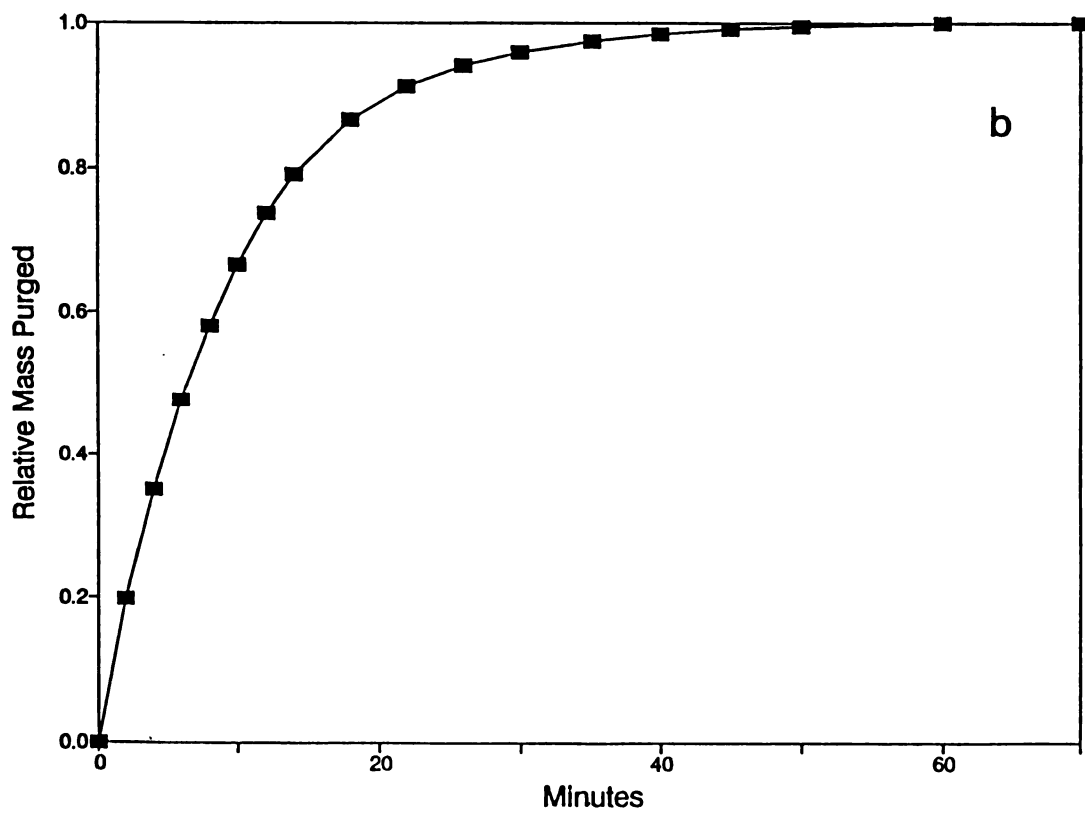
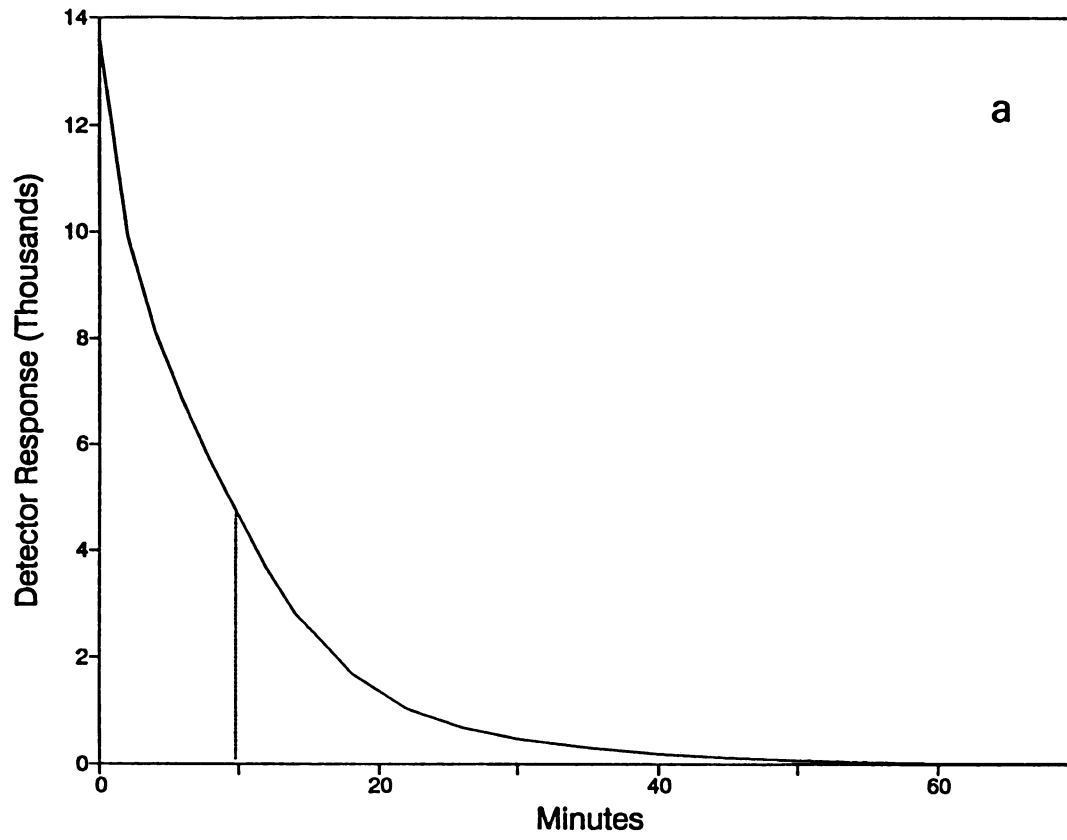
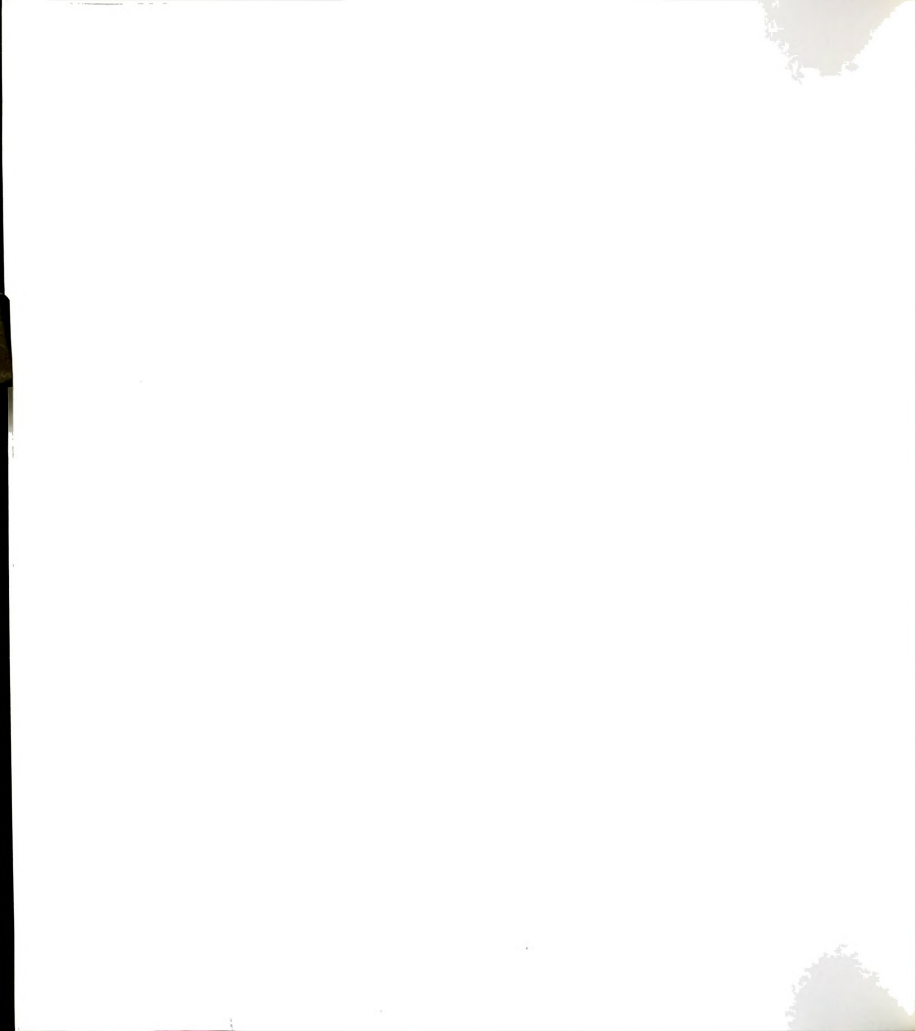




Figure 19: Raw Data and Purge Curve for Ethylbenzene



III. Results and Discussion

The results of the organic carbon analyses confirm that the added HDTMA was bound to the soils and clays (Table XVII). The organic carbon contents of the soils and clays after modification agree with the predicted carbon contents calculated using the cation exchange capacities (Table XVI).

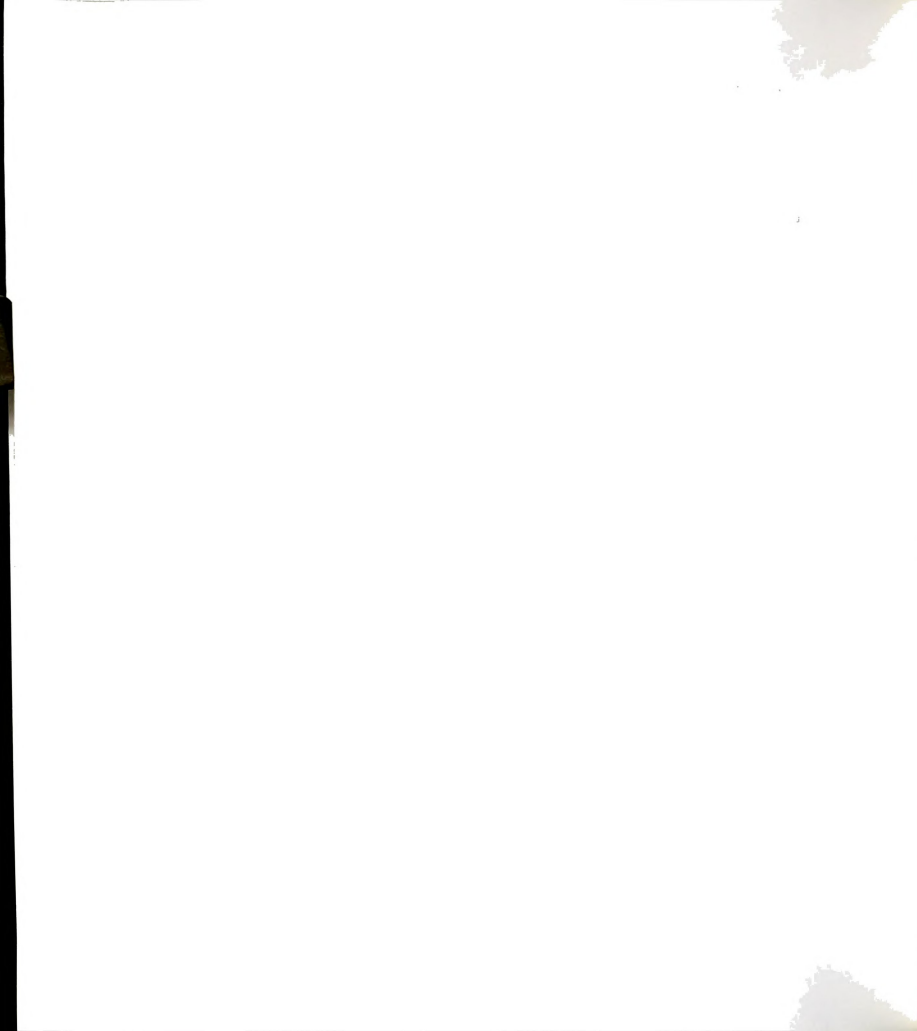
The organic carbon contents of the modified clays are the same for both size fractions. This result is expected since these size fractions are ground from the same material.

Table XVII: Organic Carbon Content for Sorbents

<u>Sample</u>	<u>%CEC Exchanged with HDTMA</u>	<u>OC Content (%)</u>	
		<u>calculated</u>	<u>measured</u>
Capac A	0	---	3.32(0.06)
	20	3.85	3.60(0.21)
	40	4.38	4.03(0.17)
	60	4.90	5.01(0.42)
	80	5.41	5.86(0.24)
	100	5.92	6.11(0.72)
Colwood A	0	---	5.19(0.13)
	40	7.00	7.41(0.36)
53-125 um	0	---	23.30(0.57)
125-250 um	0	---	24.80(0.97)
250-500 um	0	---	26.09(0.95)
SAC			
<0.25 mm	100	16.3	16.0(0.8)
0.25-1.0 mm	100	16.3	16.2(0.1)
SAz-1			
<0.25 mm	100	22.1	20.7(0.5)
0.25-1.0 mm	100	22.1	21.0(1.0)

Numbers in parentheses represent the standard deviation.

The organic matter fractions that were isolated from Colwood A horizon range from 23.3 to 26.1 % organic carbon. Since soil humic and fulvic acids range from 41 to 59 % carbon (31), these fractions still contain 36 to 60 % mineral matter. The separation and isolation procedure resulted in a 4- to 5-fold purification of the organic matter.



All of the isotherms are linear in the measured concentration range ($r^2 > 0.95$). Linear isotherms are consistent with a partitioning mechanism as suggested in previous studies of the equilibrium behavior of HDTMA-modified soils and clays (6,8,9). The HDTMA-clays, soils and HDTMA-soils all show increasing K_d with decreasing solute solubility (Table XVIII, Table XIX, and Table XX). K_d s for the alkylbenzenes are higher on the HDTMA-SAz-1 fractions than the corresponding HDTMA-SAC fractions. While the K_d s do not change significantly between the size fractions of HDTMA-SAC, they are larger on the 0.25-1.0 mm fraction of HDTMA-SAz-1 than on the <0.25 mm fraction. If the sorption mechanism were adsorptive, the size fraction with the greatest surface area would be expected to have the largest K_d . The 0.25 - 1.0 mm size fraction with the larger K_d has lower surface area so the increase in sorptive capacity must be related to partitioning. To explain the increase in sorptive strength of the larger size fraction relative to the smaller size fraction in HDTMA-SAz-1, the structure of these aggregates must be considered.

Table XVIII: Distribution Coefficients for Soils and HDTMA-Soils

<u>Soil</u>	<u>Solute</u>	<u>K_d (0% HDTMA)</u>	<u>K_d (40% HDTMA)</u>
Capac A horizon	toluene	1.11	3.59
	ethylbenzene	2.78	6.25
	propylbenzene	9.16	18.8
Colwood A horizon	toluene	3.20	6.62
	ethylbenzene	7.24	20.9
	propylbenzene	18.6	38.8

The larger size fraction may contain a more contiguous organic phase. Both size fractions are composed of many aggregated clay layers. These aggregates probably contain at least two levels of structure. At the primary level, individual clay layers stack together to form quasicrystals. These quasicrystals are highly ordered structures with the layers parallel to one another and are established while the HDTMA-



clay is still in solution. Most of the clay layers are probably involved in quasicrystal structures. The secondary level of structure in the aggregate involves the manner in which these highly ordered quasicrystal structures aggregate during the drying stage of the material preparation.

At the secondary level, the structure is probably much less ordered. Clay layers in one quasicrystal need not be aligned with layers in an adjacent quasicrystal. At the edges of each quasicrystal, the clay layers have hydroxyl groups that exchange HDTMA. The hexadecyl "tails" of HDTMA exchanged on edge hydroxyls together with HDTMA extending from edge exchange sites of the interlamellar region may fill the region between quasicrystals. Tail-to-tail interactions between edge HDTMA of adjacent quasicrystals may stabilize this type of secondary structure. Hexadecyl alkyl groups in this region form an organic phase that may have different sorptive characteristics than interlamellar HDTMA.

Table XIX: Distribution Coefficients for Organoclays

<u>Clay</u>	<u>Solute</u>	<u>$K_d (<0.25\text{mm})$</u>	<u>$K_d (0.25-1.0\text{mm})$</u>
Wyoming bentonite	toluene	42.5	41.3
	ethylbenzene	92.6	97.1
	propylbenzene	285	287
Arizona smectite	toluene	369	549
	propylbenzene	2510	2864

Grinding the aggregate into smaller particles reduces the described secondary structure. The aggregate is probably broken along lines of structural weakness. These breaks are expected to leave individual quasicrystals intact, but to separate these regions from one another. Therefore, the different particle sizes represent sorbents with different relative contributions to sorption by their secondary structure.



The effect of particle size on sorption is not observed for the HDTMA-SAC. HDTMA-SAC has lower organic carbon content than HDTMA-SAz-1. Lower carbon content reduces the possible interactions between HDTMA at edge sites, thereby decreasing the effect of secondary structure on sorption in HDTMA-SAC.

Table XX: Distribution Coefficients for OM Fractions

<u>Sorbent</u>	<u>Solute</u>	K_d	$\log K_{om}$
Colwood A horizon	toluene	3.20	1.56
53-125 um OM	toluene	16.6	1.62
250-500 um OM	toluene	21.8	1.69
Colwood A horizon	propylbenzene	18.6	2.32
53-125 um OM	propylbenzene	116	2.47
250-500 um OM	propylbenzene	146	2.52

The K_d s obtained in this study can be compared with K_d s obtained for freeze-dried preparations of the same materials (9). The freeze-dried HDTMA-SAC exhibited K_d s of 71, 135, and 395 for toluene, ethylbenzene, and propylbenzene, respectively. These values are higher than those exhibited by either particle size fraction. The freeze-dried HDTMA-SAz-1 exhibited K_d s of 319 for toluene and 1412 for propylbenzene. These K_d s are lower than K_d s on the particle size fractions. This evidence supports the contention that secondary structure in the aggregate increases the sorption capacity of HDTMA-SAz-1, but not HDTMA-SAC.

The distribution coefficient increased upon modification of the A horizon soils with HDTMA (Table XVIII). Although modification increased organic carbon content only 21 and 43 % for Capac A and Colwood A, respectively, K_d s increased 205 to 323 %. The disproportional increase in K_d is a reflection of the fact that the HDTMA organic phase is a more effective sorbent than natural organic matter (2,4).

The organic matter fractions that were isolated from Colwood A horizon exhibit higher K_d s than the original soil (Table XX). Sorption



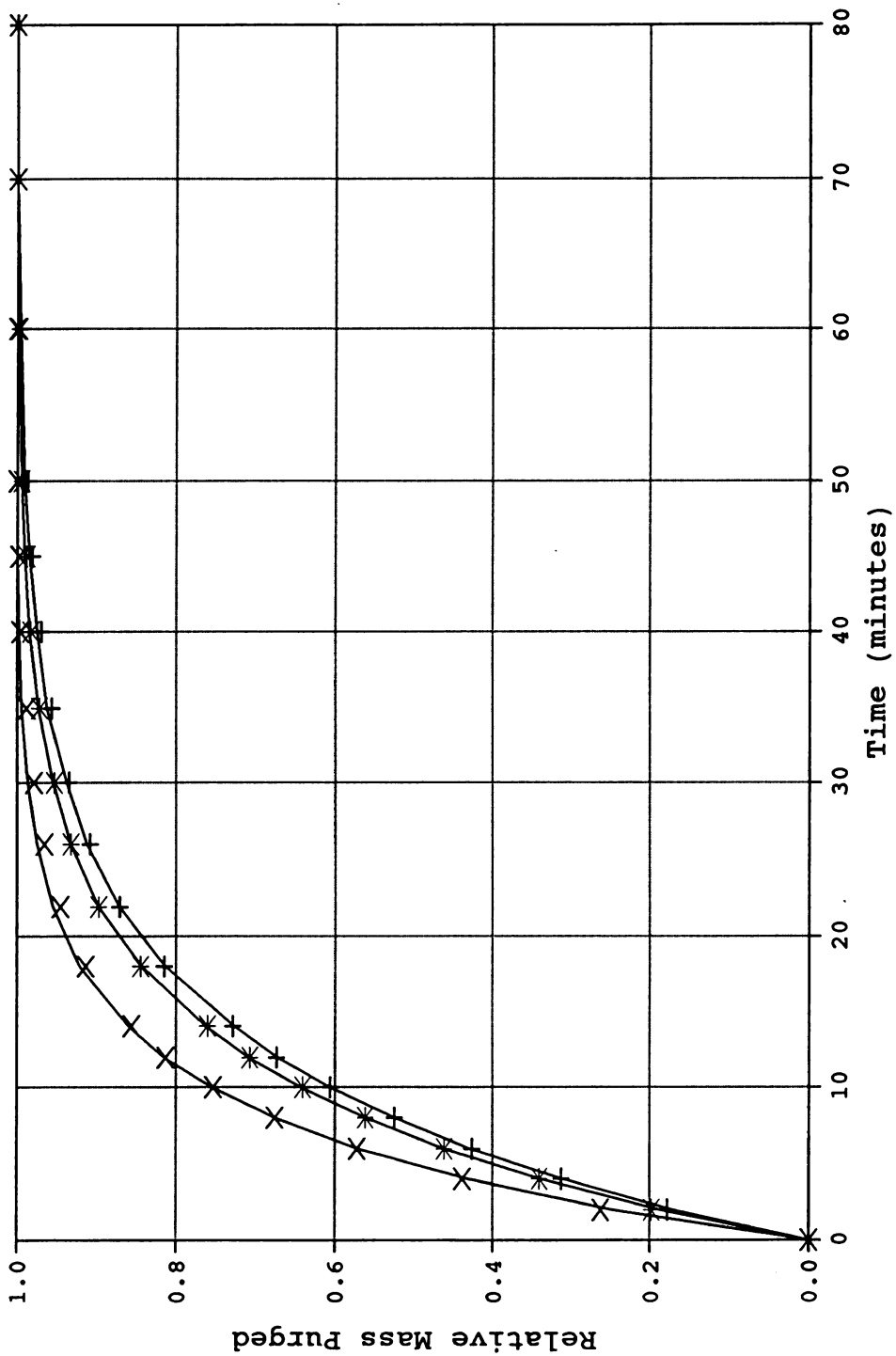
has been shown to be a function of organic carbon content on soils with greater than 0.1 % carbon (32). The K_{ds} were normalized to organic matter content. The resultant log K_{om} s reflect the solvency of the organic matter (33). The magnitude of log K_{om} for both toluene and propylbenzene follows the order; 250-500 μ m fraction > 53-125 μ m fraction > whole soil. Since alkylbenzenes are nonpolar, the trend in log K_{om} implies an inverse trend in polarity of the organic matter. The larger size fraction probably contains organic material which is younger and, therefore, is less oxidized. Oxidation of organic matter increases its polarity by introducing carboxylate and hydroxylate moieties into its structure.

The control experiments in the gas purge system were used to determine the Henry's Law constants for the volatile alkylbenzenes. Fitted gas-water exchange rate constants closely follow the data (Figure 20) and the Henry's Law constants determined in this system are in good agreement with literature values (13). The experimentally determined values of K_H were used in modelling the purge curves obtained from the experiment flasks. The gas-water exchange rate constants are assumed to be the same in the presence of the sorbent (34).

The presence of a sorbent affects the shape of the purge curve. Both natural and modified Colwood A horizon increase the time required for complete removal of propylbenzene from the flask (Figure 21). The shape of the purge curve from natural soil differs from the purge curve from the modified soil. Neither curve is fit by assuming the sorption process is at equilibrium (Figure 22a and b) suggesting that desorption kinetics become the limiting step in removal of propylbenzene from either flask.

The values of k_2 and F that were determined by fitting the purge curves from soils and modified soils appear in Table XXI. The desorption rate constants range from 0.026 to 0.183 min^{-1} . In all cases, the modification increased the desorption rate constants. For toluene, the purge curve from both modified A horizons was best fit by an equilibrium model. This result implies that the desorption rate is





+ toluene * ethylbenzene x propylbenzene

Figure 20: Purge Curves for Control Experiments

Fitted K_H curves appear as solid lines.



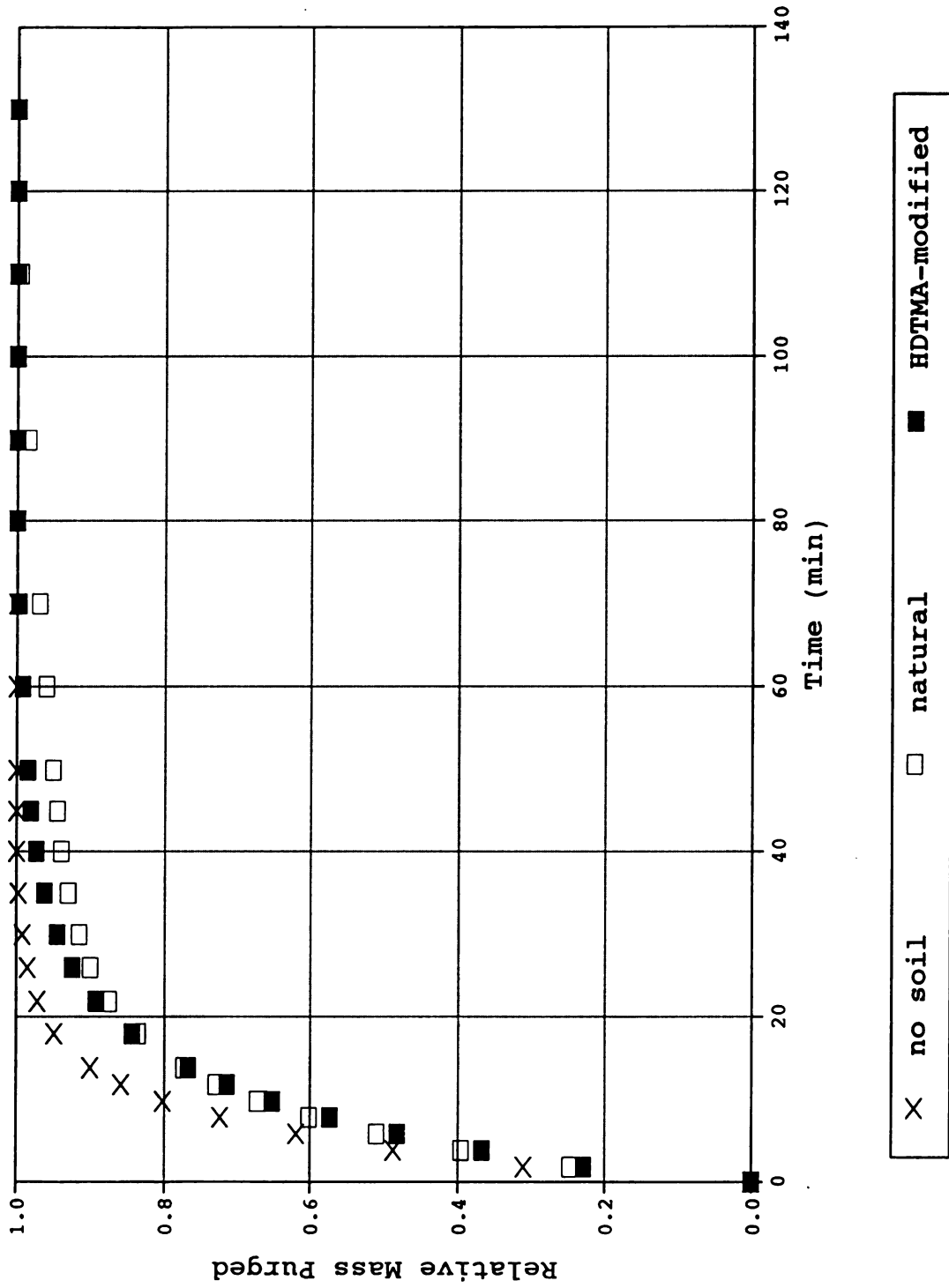
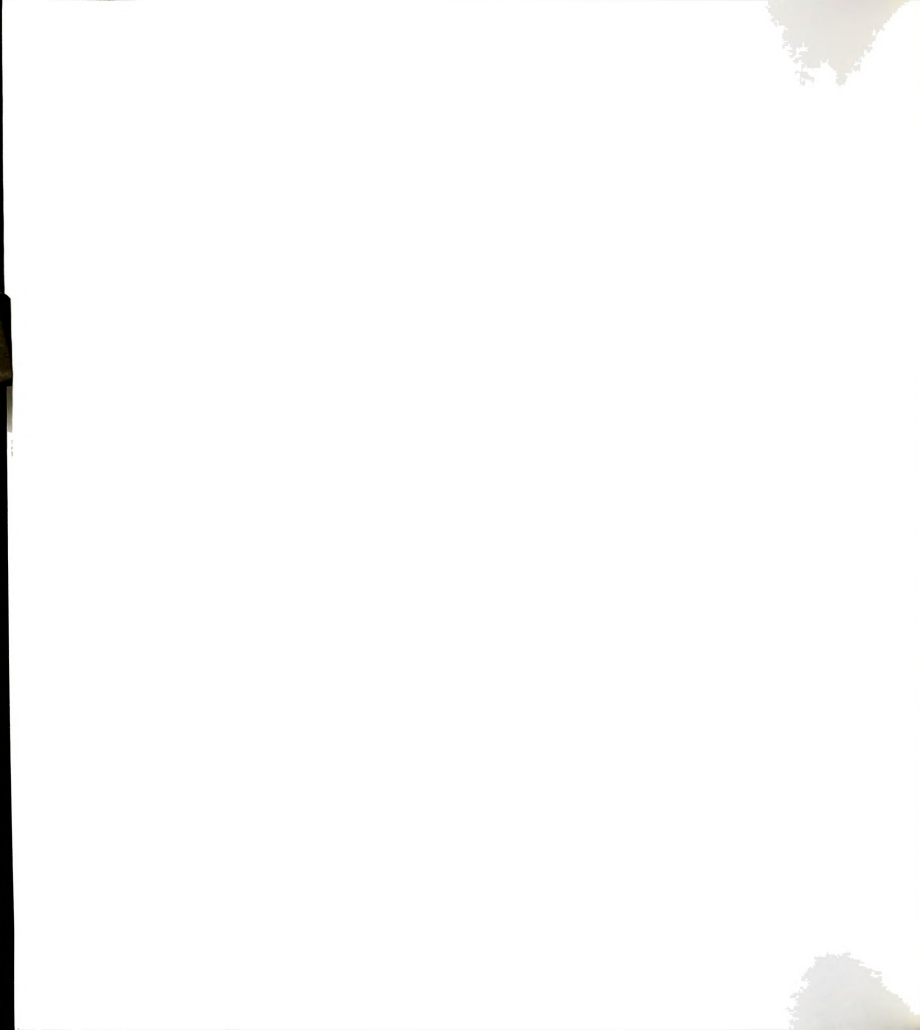


Figure 21: Purge Curves of Propylbenzene from Natural and Modified Colwood A Horizon



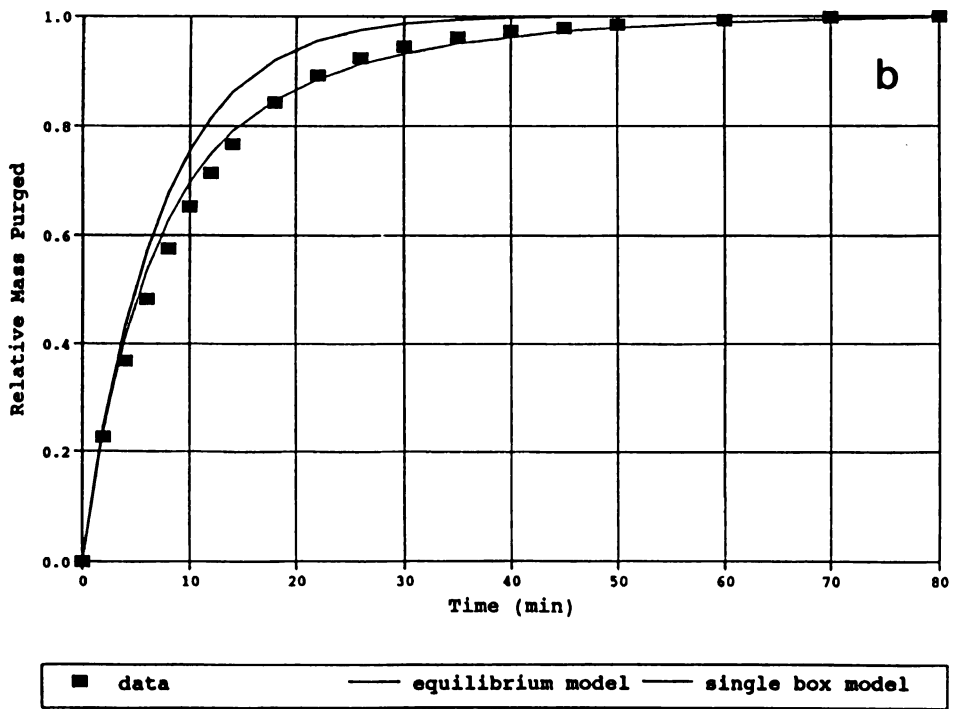
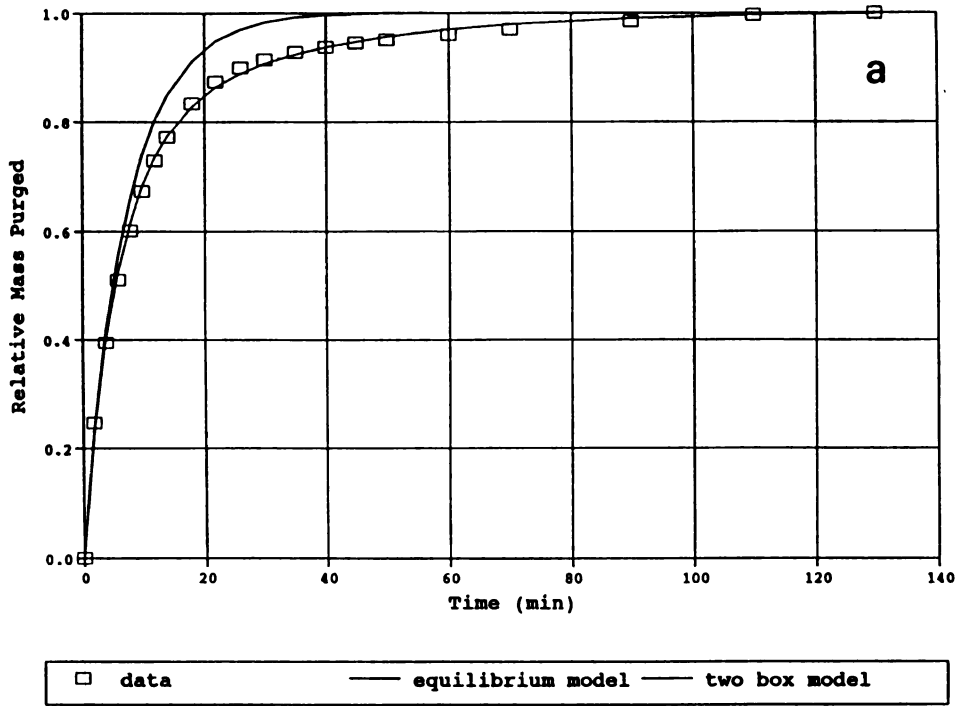




Figure 22: Model Fits for Propylbenzene/Colwood A Purge Curves

- a. Propylbenzene from Colwood A horizon.
- b. Propylbenzene from HDTMA-modified Colwood A horizon.

Table XXI: Fitted Parameters for Soils and Modified Soils

<u>Soil</u>	<u>Solute</u>	<u>k_2 (min⁻¹)</u>	<u>F</u>
Capac A horizon (0% HDTMA)	toluene	0.049 (0.059)	0.00 (0.82)
	ethylbenzene	0.026 (0.012)	0.00 (0.29)
	propylbenzene	0.045 (0.017)	0.00 (0.24)
Capac A horizon (40% HDTMA)	toluene		1.00
	ethylbenzene	0.073 (0.023)	0.00 (0.23)
	propylbenzene	0.183 (0.026)	0.45 (0.07)
Colwood A horizon (0% HDTMA)	toluene	0.031 (0.024)	0.00 (0.44)
	ethylbenzene	0.046 (0.017)	0.00 (0.25)
	propylbenzene	0.037 (0.004)	0.12 (0.05)
Colwood A horizon (40% HDTMA)	toluene		1.00
	ethylbenzene	0.098 (0.007)	0.04 (0.05)
	propylbenzene	0.064 (0.023)	0.00 (0.25)

Numbers in parentheses represent the standard deviation.

rapid enough so that it is no longer rate-limiting. In other words, the desorption rate constant is large enough to exceed the sensitive range of the purge system. The desorption rate constant for propylbenzene from modified Capac A horizon, 0.183 min^{-1} , is the largest of all rate constants determined in this study and may represent the upper limit of system sensitivity.

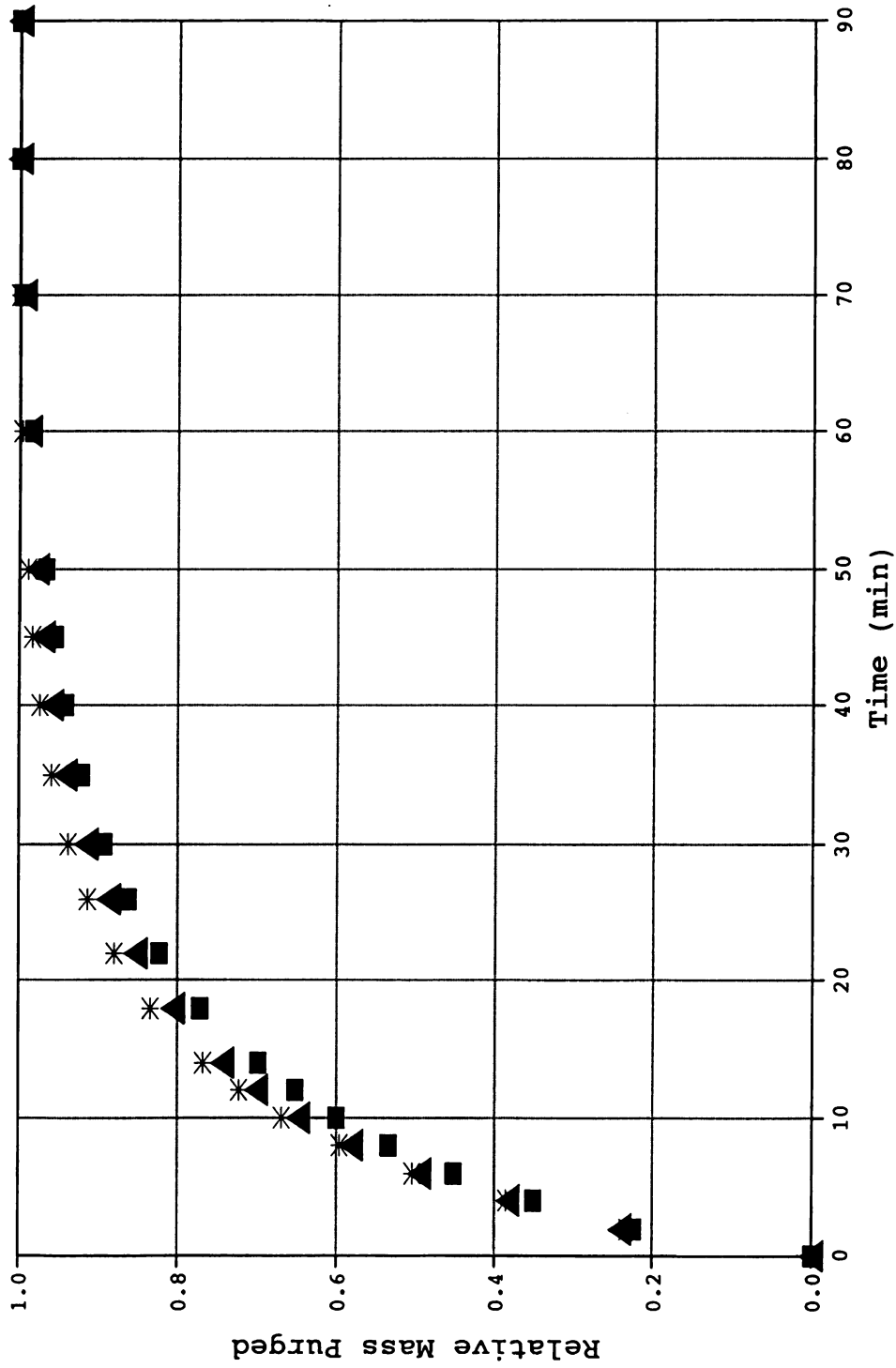
The bicontinuum model collapses to the one box model in many cases. The fitted F value is zero. Large standard deviations in the fitted F values suggest that the system is less sensitive to the behavior of solute in S_1 , the equilibrium domain. In the three cases where a good fit of the bicontinuum model is obtained (propylbenzene from modified Capac A, propylbenzene from Colwood A, and ethylbenzene from modified Colwood A), F values are lower than observed in previous studies (22,35).

Two explanations of the increase in desorption rate constant upon modification are possible. The HDTMA may modify either the soil clays or the soil organic matter. Both contribute to the cation exchange

capacity of the soil. When the HDTMA modifies soil clays it creates a sorptive phase in addition to the natural sorptive phase, the humic substances. When the HDTMA modifies natural organic matter, it probably alters the structure of this existing sorptive phase. Although the structure of natural organic matter is not known (36), its chemical composition includes humic and fulvic acids which are polymeric in nature. Carboxylate and phenolate groups in the humic and fulvic acids provide cation exchange sites that are able to complex HDTMA. Modification of these polymeric materials may expand their structure and increase diffusion rates in the polymer. In either case, the HDTMA creates a sorptive phase whose release of solute to solution is more rapid than the natural sorptive materials.

The purge curves of ethylbenzene from the two HDTMA-SAC size fractions are shown in Figure 23. Ethylbenzene removal from the system is retarded by the presence of the clay. However, the difference between the purge curve for the sorbent-containing flasks and the control flask is not as prominent as with the soils. The bicontinuum model collapses to the equilibrium model for the <0.25 mm clay size fraction (Figure 24a). This result implies that desorption is sufficiently rapid so as to maintain the sorption equilibrium throughout the purge. The larger size fraction, 0.25-1.0 mm, did show evidence of kinetic limitation to the attainment of sorption equilibrium. The bicontinuum model achieves a better fit of the data than the equilibrium model (Figure 24b).

The values of k_2 and F that were determined by fitting the purge curves from all of the modified clays appear in Table XXII. For the HDTMA-SAC size fractions, the desorption rate constants decrease with increasing particle size. For example, the replicate propylbenzene k_2 s for the small HDTMA-SAC fraction, 0.130 min^{-1} and 0.146 min^{-1} , are more than ten times larger than k_2 s for the large size fraction, 0.011 (or 0.019) min^{-1} . Larger k_2 s on the smaller size fraction are consistent with a mechanism whose rate-limiting step is solute diffusion within the particle. The desorption rate constant, k_2 , is inversely related to the



* no clay ▲ size: $0.25-1.0\text{mm}$ ■ size: <math><0.25\text{mm}</math>



Figure 23: Purge Curves of Ethylbenzene from HDTMA-SAC



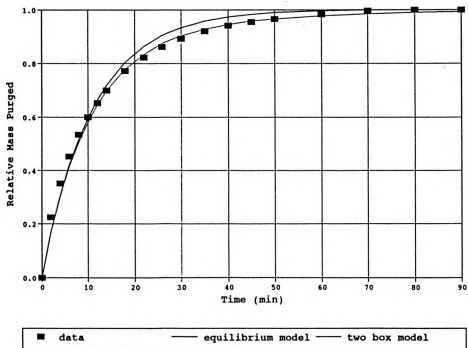
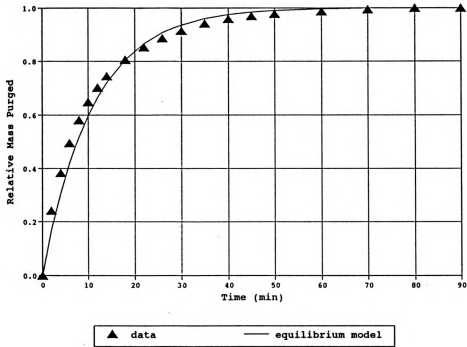


Figure 24: Model Fits for Ethylbenzene/HDTMA-SAC Purge Curves

- a. Ethylbenzene from <0.25 mm HDTMA-SAC size fraction.
- b. Ethylbenzene from 0.25-1.0 mm HDTMA-SAC size fraction.

characteristic diffusion length (35). The diffusion length, often approximated by the particle diameter, is shorter in the small size fraction and, therefore, the desorption rate constant is higher.

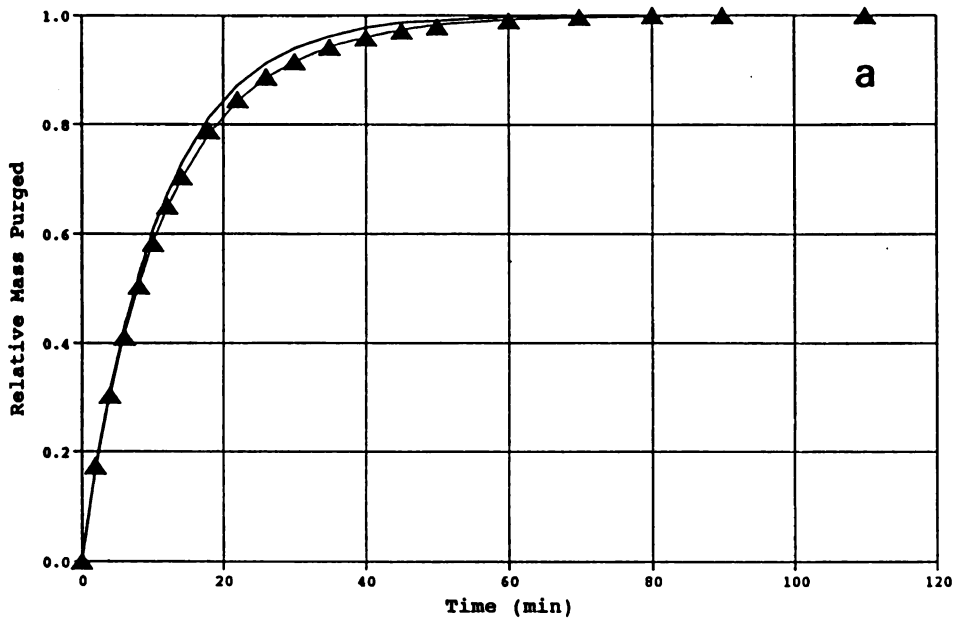
Most of the purge curve fits for the modified clays collapsed to the equilibrium model. In these cases, no k_2 is reported. However, the result implies that k_2 is large. In practical terms, desorption kinetics are less likely to influence transport or bioavailability in these cases.

Table XXII: Fitted Parameters for Modified Clays

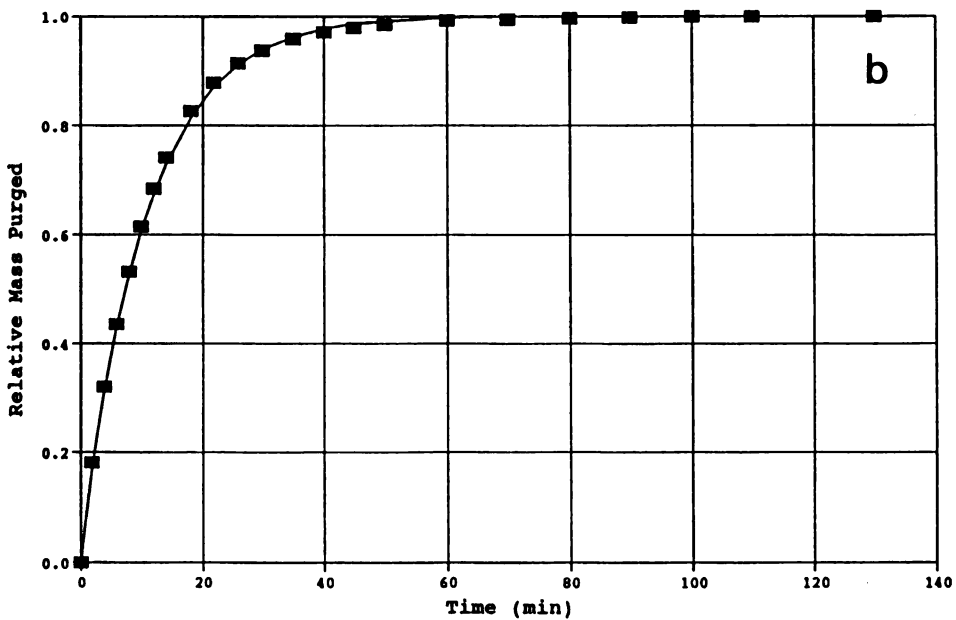
<u>Clay</u>	<u>Solute</u>	<u>k_2 (min⁻¹)</u>	<u>F</u>
Wyoming bentonite (<0.25 mm)	toluene		1.00
	ethylbenzene		1.00
	propylbenzene	0.130 (0.063) [*] 0.146 (0.039)	0.42 (0.23) 0.00 (0.24)
Wyoming bentonite (0.25-1.0 mm)	toluene		1.00
	ethylbenzene	0.035 (0.026)	0.63 (0.18)
	propylbenzene	0.011 (0.033) 0.019 (0.010)	0.82 (0.17) 0.75 (0.07)
Arizona smectite (<0.25 mm)	toluene	0.116 (0.013)	0.30 (0.66)
	propylbenzene		1.00
Arizona smectite (0.25-1.0 mm)	toluene		1.00
	propylbenzene		1.00

^{*}Standard deviation appears in parentheses.

The kinetics of alkylbenzene desorption are also dependent on clay type. The modified high charge smectite, SAz-1, exhibited more rapid desorption kinetics than the modified low charge smectite, SAC. Three of the four fits of the purge curves from HDTMA-SAz-1 collapse to the equilibrium model. Toluene purge curves from both HDTMA-SAz-1 size fractions are closely approximated by the equilibrium model (Figure 25a and b). A bicontinuum model fit is obtained for toluene from the small HDTMA-SAz-1 fraction. However, the large standard deviation in F may not make this fit significantly different from that predicted by the



▲ data — equilibrium model - - - two box model



■ data — equilibrium model

Figure 25: Model Fits for Toluene/HDTMA-SAz-1 Purge Curves

- a. Toluene from <0.25 mm HDTMA-SAz-1 size fraction.
- b. Toluene from 0.25-1.0 mm HDTMA-SAz-1 size fraction.

equilibrium model.

The difference in kinetic behavior of the modified clays is most likely related to differences in d-spacing. The modified SAC is a bilayer complex with a d-spacing of 1.84 nm, whereas the modified SAz-1 is a pseudotrimolecular or paraffin complex with a d-spacing of 2.29 nm (9). Since solute sorption occurs in the interlamellar region, the alkylbenzene must diffuse in and out between the layers. Diffusion between the layers will be faster in clays when the d-spacing is large.

In the cases where k_2 s are reported, k_2 decreases with increasing substituent chain length of the solute. On the large HDTMA-SAC size fraction, the k_2 is lowest for propylbenzene, intermediate for ethylbenzene, and largest for toluene (so large, in fact, that it is not measurable). This trend is not discernible on the other modified clay fractions since k_2 s were too large to be measured.

The purge curves of toluene from the OM fractions that were isolated from Colwood A soil are shown in Figure 25. Although they both differ from the control experiment, the purge curves of both size fractions are quite similar to one another. The purge curves are not predicted by assuming the sorption process to be at equilibrium (Figure 26a and b).

The values of k_2 and F that were determined by fitting the purge curves from the organic matter (OM) fractions appear in Table XXIII. For comparison, the values for the whole soil are repeated in this table. The toluene k_2 values on the OM fractions are not significantly different from one another or from the whole soil k_2 . The propylbenzene k_2 s are lower on the OM fractions than on the whole soil. However, the propylbenzene k_2 s are not distinguishable between the 53-125 μm and 250-500 μm size fractions. The difference in diffusion length for the two size fractions does not distinguish the dynamic behavior of toluene or propylbenzene sorption on these organic matter isolates. However, a significant difference in the F values for propylbenzene exists. Nearly 60% of the propylbenzene is rapidly equilibrated on the smaller fraction, whereas, essentially no rapidly equilibrated domain exists in

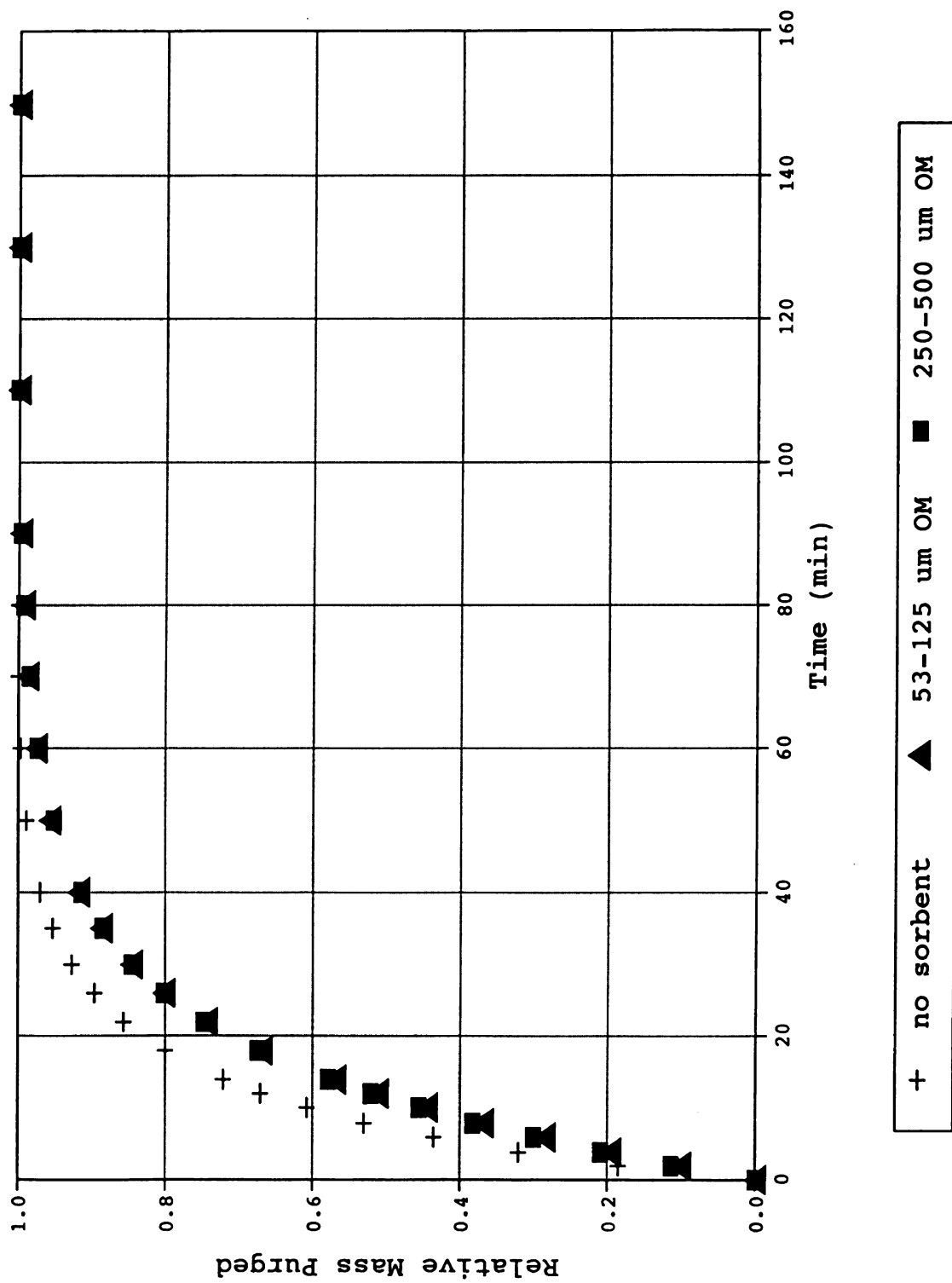


Figure 26: Purge Curves of Toluene from OM Fractions

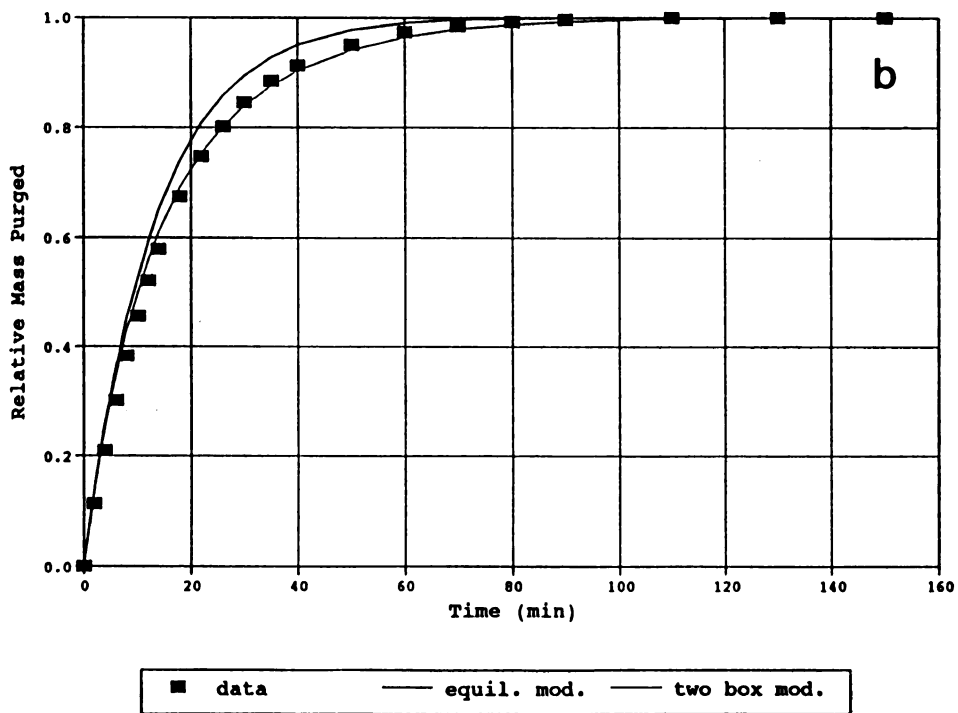
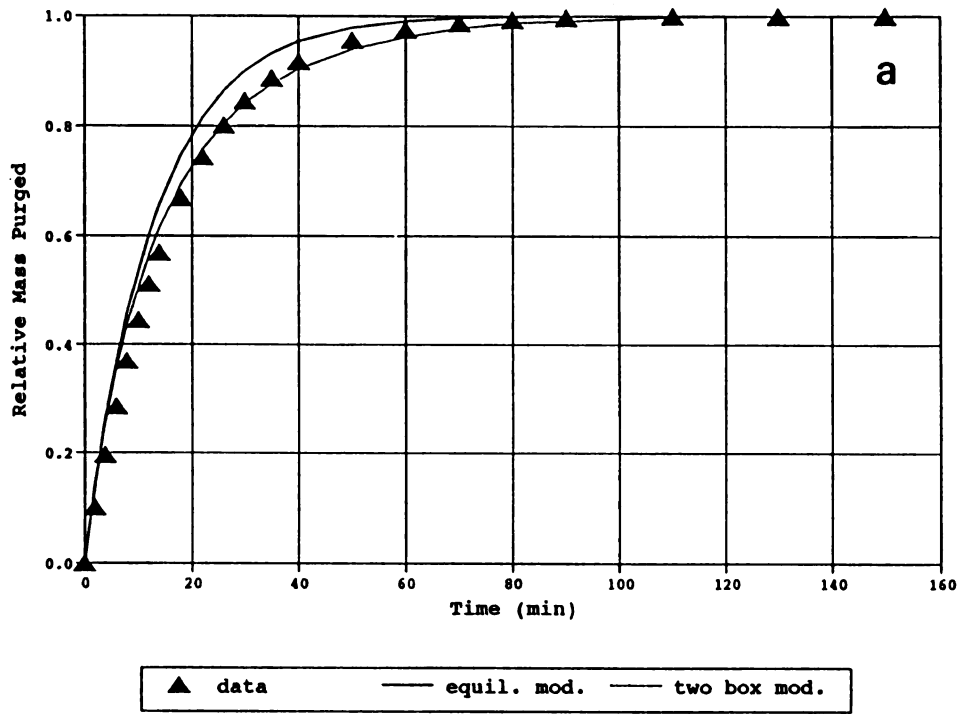


Figure 27: Model Fits for Toluene/OM Fraction Purge Curves

- a. Toluene from 53-125 um organic matter isolate.
- b. Toluene from 250-500 um organic matter isolate.

the larger fraction. Any trend in F is obscured by the larger standard deviations in the toluene fits.

Table XXIII: Fitted Parameters for OM Fractions

<u>Sorbent</u>	<u>Solute</u>	<u>k_2 (min⁻¹)</u>	<u>F</u>
Colwood A horizon	toluene	0.031 (0.024)*	0.00 (0.44)
53-125 um OM	toluene	0.059 (0.036)	0.00 (0.44)
250-500 um OM	toluene	0.064 (0.030)	0.00 (0.34)
Colwood A horizon	propylbenzene	0.037 (0.004)	0.12 (0.05)
53-125 um OM	propylbenzene	0.024 (0.006)	0.59 (0.06)
250-500 um OM	propylbenzene	0.018 (0.005)	0.00 (0.14)

*Standard deviation appears in parentheses.

IV. Summary and Conclusions

When modified with HDTMA, natural soils and clays are strong sorbents of alkylbenzenes. Under conditions where the alkylbenzene is rapidly purged from slurries containing these sorbents, the influence of the desorption kinetics are apparent. The purge curves can be fit to a bicontinuum model to extract desorption rate constants. In several instances the bicontinuum model collapses to one of two simpler models, the one box model or the equilibrium model.

Rate constants for desorption of alkylbenzenes increase upon modification of two A horizon soils. Since bioavailability may be related to desorption rate, this result suggests that alkylbenzenes sorbed to modified soils are more bioavailable than those sorbed to natural soils. Higher rate constants on modified materials suggest that transport through these media is less likely to be affected by slow kinetics. These results are consistent with the high desorption rates for tetrachloroethene and naphthalene that were found in transport experiments through HDTMA-modified aquifer material (37). The exact

mechanism whereby the rate constants are increased is still speculative. The increase may be related to formation of a second phase, modified clays, in the soil, to alteration of the native organic matter, or to a combination of both of these mechanisms. If alteration of the organic matter is involved, the modification probably acts to increase diffusion rates by swelling the structure of this polymeric material.

The kinetic behavior of sorption to modified pure clays was studied separately. The desorption rate constants are higher in these materials. Increased d-spacing in the HDTMA-SAz-1 relative to the HDTMA-SAC may be responsible for differences in the desorption rates for toluene and propylbenzene. The desorption rates for all HDTMA-SAz-1 experiments were very rapid; nearly all exceeded the sensitivity of the gas purge system.

Clay particle size affects desorption rate constants measured for HDTMA-SAC fractions. An order of magnitude difference between desorption rate constants for propylbenzene was observed in going from a <0.25 mm to a 0.25-1.0 mm size fraction.

Some studies have shown that there is an inverse relationship between k_2 and K_d (22,38). The results from all experiments in which a k_2 value was obtained appear in Figure 28 together with the regression line obtained by Brusseau et al (38). The natural soil results fall close to the regression line. The modified soils exhibit both higher equilibrium constants and desorption rate constants than the natural soils. The modified clay results show the dependence on particle size; the smaller particles exhibit higher rate constants for the same equilibrium constant.

In situations where alkylbenzene sorption is coupled with the dynamic processes of transport through porous media or biological degradation, the desorption kinetics may significantly influence the system behavior. The results of this study rank the importance of desorption kinetics in the order: soils > modified soils > modified clays.

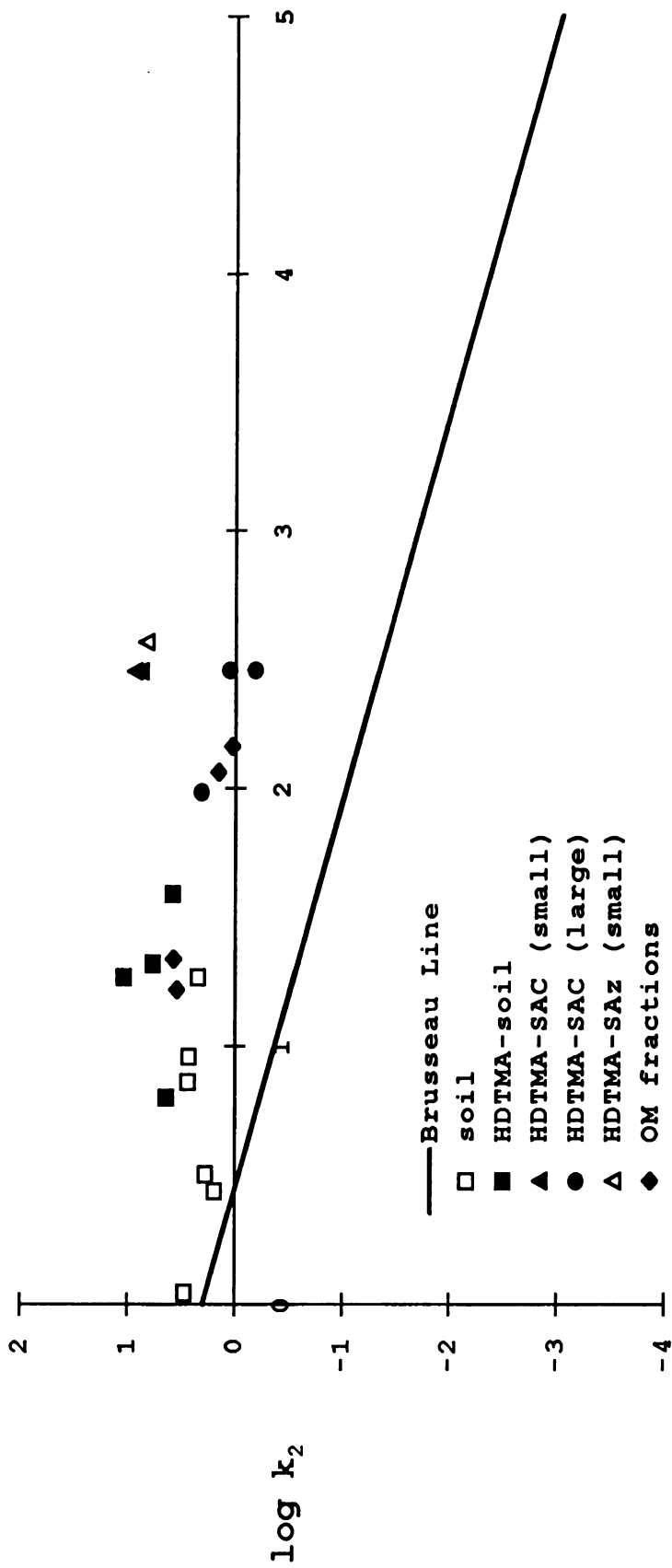


Figure 28: $\text{Log}(K_d)$ versus $\text{log}(k_2)$ and Brusseau Line



V. Acknowledgements

The authors would like to acknowledge the USDA Cooperative State Research Service (Food and Agricultural Sciences National Needs Graduate Fellowship Program) for support under grant number 88-38420-3834.

Michael Straszewski isolated the organic matter fractions and performed the toluene and propylbenzene isotherms.

REFERENCES

1. Mortland, M.M., S. Shaobai, and S.A. Boyd. 1986. Clay-Organic Complexes as Adsorbents for Phenol and Chlorophenols. *Clays and Clay Minerals*. 34(5): 581-585.
2. Boyd, S.A., S. Shaobai, J.F. Lee, and M.M. Mortland. 1988. Pentachlorophenol Sorption by Organo-clays. *Clays and Clay Minerals*. 36: 125-130.
3. Boyd, S.A., M.M. Mortland, and C.T. Chiou. 1988. Sorption Characteristics of Organic Compounds on Hexadecyltrimethylammonium Smectite. *Soil Sci. Soc. Amer. J.* 52: 652-657.
4. Boyd, S.A., J.F. Lee, and M.M. Mortland. 1988. Attenuating Organic Contaminant Mobility by Soil Modification. *Nature*. 333: 345-347.
5. Lee, J.F., M.M. Mortland, C.T. Chiou, and S.A. Boyd. 1989. Shape Selective Adsorption of Aromatic Molecules from Water by Tetramethylammonium-Smectite. *J. Chem. Soc. Faraday Trans.* 85: 2953-2962.
6. Lee, J.F., J. Crum, and S.A. Boyd. 1989. Enhanced Retention of Organic Contaminants by Soils Exchanged with Organic Cations. *Environ. Sci. Technol.* 23: 1365-1372.
7. Lee, J.F., M.M. Mortland, C.T. Chiou, D.E. Kile, and S.A. Boyd. 1990. Adsorption of Benzene, Toluene and Xylene by Two Tetramethylammonium Smectites of Different Charge Densities. *Clays and Clay Minerals*. 38: 113-120.
8. Jaynes, W.F. and S.A. Boyd. 1990. Trimethylphenylammonium-Smectite as an Effective Adsorbent of Water Soluble Aromatic Hydrocarbons. *J. Air Waste Manage. Assoc.* 40: 1649-1653.
9. Jaynes, W.F. and S.A. Boyd. 1991. Clay Mineral Type and Organic Compound Sorption by Hexadecyltrimethylammonium-Exchanged Clays. *Soil Sci. Soc. Amer. J.* 55(1): 43-48.
10. Boyd, S.A., W.F. Jaynes and B.S. Ross. 1991. Immobilization of Organic Contaminants by Organoclays: Application to Soil Restoration and Hazardous Waste Containment, Ch. 11 in Organic Substances and Sediments in Water. CRC Press. Boca Raton, FL.
11. Burris, D.R. and C.P. Antworth. 1991. In situ modification of an aquifer material by a cationic surfactant to enhance retardation of organic contaminants. *J. Contamin. Hydrol.* 10: 325-33.
12. Crocker, F.H., J.V. Nye, S.A. Mueller, W.F. Guerin and S.A. Boyd. 1992. "The Effects of Quaternary Ammonium Compounds (QUATs) on Microbial Metabolic Activity and the Biostability of QUATs in Soil". SSSA meeting, Minneapolis, MN.

13. Benzing, T.R. 1993. PhD Thesis. Michigan State University. Chapter 2: Construction and Behavior of the Gas Purge System.
14. Khan, S.U. 1973. Equilibrium and Kinetic Studies of the Adsorption of 2,4-D and Picloram on Humic Acid. *Can. J. Soil Sci.* 53: 429-434.
15. McCall, P.J. and G.L. Agin. 1985. Desorption Kinetics of Picloram as affected by Residence Time in the Soil. *Environ. Tox. Chem.* 4: 37-44.
16. Walters, R.W. and A. Guiseppi-Elie. 1988. Sorption of 2,3,7,8-Tetrachlorodibenzo-p-dioxin to Soils from Water/Methanol Mixtures. *Environ. Sci. Technol.* 22(7): 819-825.
17. Rao, P.S.C., J.M. Davidson, R.E. Jessup, and H.M. Selim. 1979. Evaluation of Conceptual Models for Describing Nonequilibrium Adsorption-Desorption of Pesticides During Steady-flow in Soils. *Soil Sci. Soc. Amer. J.* 43: 22-28.
18. Miller, C.T. and W.J. Weber. 1986. Sorption of Hydrophobic Organic Pollutants in Saturated Soil Systems. *J. Contamin. Hydrol.* 1: 243-261.
19. Southworth, G.R., K.W. Watson, and J.L. Keller. 1987. Comparison of Models that Describe the Transport of Organic Compounds in Macroporous Soil. *Environ. Tox. Chem.* 6: 251-257.
20. Lee, L.S., P.S.C. Rao, M.L. Brusseau, and R.A. Ogwada. 1988. Nonequilibrium Sorption of Organic Contaminants during Flow through Columns of Aquifer Materials. *Environ. Tox. Chem.* 7: 779-793.
21. Karickhoff, S.W. 1980. Sorption Kinetics of Hydrophobic Pollutants in Natural Sediments. Ch. 11 in Contaminants and Sediments, vol. 2, Baker, R.A., Ed. Ann Arbor Press: Ann Arbor, MI.
22. Karickhoff, S.W. and K.R. Morris. 1985. Sorption Dynamics of Hydrophobic Pollutants in Sediment Suspensions. *Environ. Tox. Chem.* 4: 469-479.
23. Oliver, B.G. 1985. Desorption of Chlorinated Hydrocarbons from Spiked and Anthropogenically Contaminated Sediments. *Chemosphere.* 14(8): 1087-1106.
24. Coates, J.T. and A.W. Elzerman. 1986. Desorption Kinetics for Selected PCB Congeners from River Sediments. *J. Contamin. Hydrol.* 1: 191-210.
25. Wu, S. and P.M. Gschwend. 1986. Sorption Kinetics of Hydrophobic Organic Compounds to Natural Sediments and Soils. *Environ. Sci. Technol.* 20: 717-725.
26. Brusseau, M.L., R.E. Jessup and P.S.C. Rao. 1990. Sorption Kinetics of Organic Chemicals: Evaluation of Gas Purge and Miscible Displacement Techniques. *Environ. Sci. Technol.* 24: 727-735.
27. Straszewski, M. 1993. Colwood A Horizon Organic Fractionation and Isotherm Experiments. CSS 490 Independent Study.
28. DC-190 High-Temperature TOC Analyzer Operation Manual. 1991. Rosemount Analytical, Inc. Dohrmann Division. Santa Clara, CA.
29. Chiou, C.T., P.E. Porter, and D.W. Schmedding. 1983. Partition Equilibria of Nonionic Organic Compounds between Soil Organic Matter and Water. *Environ. Sci. Technol.* 17(4): 227-231.

30. Sun, S. 1992. Sorption of Nonionic Organic Compounds by Anthropogenic Organic Phases in Soil-Water Systems. PhD Thesis, Michigan State University.
31. Steelink, C. 1985. Implications of Elemental Characteristics of Humic Substances. Ch. 18 in Humic Substances in Soil, Sediment and Water: Geochemistry, Isolation, and Characterization, Aiken, G.R., D.M. McKnight, R.L. Wershaw and P. MacCarthy, Eds. Wiley-Interscience.
32. Schwarzenbach, R.P. and J. Westall. 1981. Transport of Nonpolar Organic Compounds from Surface Water to Groundwater. Laboratory Sorption Studies. *Environ. Sci. Technol.* 15(11): 1360-1367.
33. Rutherford, D.W., C.T. Chiou, and D.E. Kile. 1992. Influence of Soil Organic Matter Composition on the Partition of Organic Compounds. *Environ. Sci. Technol.* 26: 336-340.
34. Hassett, J.P. and E. Milicic. Determination of Equilibrium and Rate Constants for Binding of a Polychlorinated Biphenyl Congener by Dissolved Humic Substances. *Environ. Sci. Technol.* 19: 638-643.
35. Brusseau, M.L., R.E. Jessup, and P.S.C. Rao. 1991. Nonequilibrium Sorption of Organic Chemicals: Elucidation of Rate-Limiting Processes. *Environ. Sci. Technol.* 25: 134-142.
36. MacCarthy, P., P.R. Bloom, C.E. Clapp, and R.L. Malcolm. 1990. Humic Substances in Soil and Crop Sciences: An Overview. Ch. 11 in Humic Substances in Soil and Crop Sciences: Selected Readings, MacCarthy, P., C.E. Clapp, R.L. Malcolm, and P.R. Bloom, Eds. American Society of Agronomy, Inc.
37. Burris, D.R. and C.P. Antworth. 1992. In situ modification of an aquifer material by a cationic surfactant to enhance retardation of organic contaminants. *J. Contamin. Hydrol.* 10: 325-337.
38. Brusseau, M.L., R.E. Jessup, and P.S.C. Rao. 1989. The Influence of Sorbate-Organic Matter Interactions on Sorption Nonequilibrium. *Chemosphere.* 18: 1691-1706.

MICHIGAN STATE UNIV. LIBRARIES



31293009087861